

ADSORPTION AND POROSITY: A MULTIPLE EQUILIBRIUM ANALYSIS

By

WILLIAM SCOTT KASSEL

A DISSERTATION PRESENTED TO THE GRADUATE SCHOOL
OF THE UNIVERSITY OF FLORIDA IN PARTIAL FULFILLMENT
OF THE REQUIREMENTS FOR THE DEGREE OF
DOCTOR OF PHILOSOPHY

UNIVERSITY OF FLORIDA

1998

This work is dedicated to my friend and mentor Russell S. Drago.

ACKNOWLEDGMENTS

When I think back about my graduate career, and it has been a career, it has been the people that I have met along the way that have meant the most to me. I came to UF to gain a knowledge of chemistry to take me to the level I needed to be a successful educator and scientist, what I come away with is so much more.

I would like to thank the past and present members of my group for many fond memories and insightful discussions involving our research. I would especially like to thank Mike McGilvray for putting up with my moods for the three years we shared a lab, and Andrew Cottone for our many discussions about people and “culture”. I am also grateful to Ed Webster and Ben Gordon for listening to my ramblings and giving their honest opinions and help as I moved forward with my research.

I don't want to go without thanking Nick Kob who helped me get established quickly in the group and for the many “Kob” stories that I acquired during my two years living with him. Thanks to David Kage for being a great friend and roommate for the last four years. I thought that I put up with a lot, but David lived with *both* Nick and me! I would like to thank Bennett Novak for the many evenings spent contemplating and venting at the *rotator*. It is remarkable to think that two intelligent adults

could spend so much time, and enjoy, sitting at a bar that rotates, drinking beer. I guess stranger things have happened. I wish to express my gratitude to Tracie Williams, especially for her often motivating words: “aren’t you done with your dissertation yet?” and “u-huh, I told you!” I would like to thank her for her friendship and for always being honest and open with me.

I am very grateful to Jim House from Illinois State University. He found something in me that I had yet to discover and gave me the opportunity to explore many new and exciting avenues in science and in my life. I would also like to thank Jim for all of his help and advice that he has given, especially after Russ passed away. Special thanks go to Dave Richardson for all that he has done for me and the members of my group after Russ’s passing. I do not know anyone who could have handled that situation any better than Dave has. I thank you for your advice, and for being there when I needed to ask for help. I would also like to thank Dan Talham, Russ Bowers, Mike Scott, and Jon Martin for their helpful advice and guidance.

Of course, I thank my parents. They have always been supportive of my decisions, both good and bad. I cannot thank them enough for instilling in me the feeling that I could do anything that I set my mind to. I love them both very much. And I thank my brother Jeff for his always kind words: “do you have a job yet?”

I thank my friend and mentor, Russ Drago. I know that he will never get to see this, and I cannot begin to thank him enough for all that he has done

for me, both in and out of the lab. I regret that I will never again get the chance to “discuss” research problems with him or “argue” over his calls from his baseline about shots on my baseline during our weekly tennis matches. Finally, thanks to Russ’s wife Ruth for treating me as one of her own. I thank them both.

TABLE OF CONTENTS

	<u>page</u>
ACKNOWLEDGMENTS.....	iii
ABSTRACT.....	viii
CHAPTERS	
1 A BRIEF INTRODUCTION TO ADSORPTION AND POROSITY.....	1
Porosity	1
Structure.....	1
Heterogeneity	2
Adsorption	6
Molecular Interactions	6
Chemical versus Physical Adsorption	7
Adsorbents and Porous Materials.....	9
Applications of Porous Solids.....	10
Synthesis	12
Characterization	13
Modeling Adsorption	18
Henry's Law.....	18
The Langmuir Isotherm.....	19
The BET Isotherm.....	20
The Freundlich Isotherm	21
The Harkins and Jura Method	21
The Dubinin-Radushkevich Equation	23
Concluding Remarks	24
2 A MULTIPLE EQUILIBRIUM ANALYSIS (MEA) OF ADSORPTION AND POROSITY IN CARBONS.....	25
The Langmuir Model.....	25
The Multiple Equilibrium Analysis	28
Definition of the MEA.....	31
Information Provided by the MEA	36
Experimental Isotherms.....	37

Adsorbents and Adsorptives	37
Adsorption Measurements	38
Data Analysis	39
The MEA Parameters	41
The Meaning of the MEA Parameters	53
Simulated Adsorption Isotherms	54
Monte Carlo Simulation and Sensitivity Analysis	56
The MEA Surface Area and Pore Volume	66
The Enthalpy of Adsorption	70
Prediction of Adsorption Isotherms	77
Concluding Remarks	82
3 THE MEA PORE SIZE DISTRIBUTION (MEA-PSD)	83
Heterogeneity and PSDs	83
Determining PSDs	84
The Horvath - Kawazoe Model	85
Derivation	86
Mariwala and Foley	88
The MEA-PSD	89
MEA Extension of the Horvath - Kawazoe Model	90
MEA - PSD of Selected Carbons	93
Predicting n_i 's from the MEA-PSD	100
Concluding Remarks	100
4 A MEA DESCRIPTION OF MULTILAYER FORMATION	102
Multilayer Formation on a Homogeneous Surface	102
Pore Filling and Cooperative Adsorption	104
MEA Multilayers	107
Concluding Remarks	115
5 SUMMARY AND CONCLUDING REMARKS	117
APPENDICES	
A ADSORPTION DATA	121
B FITTING ROUTINE AND INPUT FORMAT	157
LIST OF REFERENCES	179
BIOGRAPHICAL SKETCH	185

Abstract of Thesis Presented to the Graduate School
of the University of Florida in Partial Fulfillment of the
Requirements for the Degree of Doctor of Philosophy

ADSORPTION AND POROSITY: A MULTIPLE EQUILIBRIUM ANALYSIS

By

William Scott Kassel

August 1998

Chairman: David E. Richardson
Major Department: Chemistry

The goal of the research presented in this dissertation is to gain a fundamental understanding of adsorptive-adsorbent interactions in the hope that the information obtained may be applied to the rational design of new adsorbents tailored to specific adsorptives. A multiple equilibrium analysis model (MEA) has been developed to interpret adsorption isotherms and to show that the parameters obtained are meaningful within the context of the model. Adsorptives have been selected that vary in size and polarizability, to permit adsorbent characterization in terms of these physical properties. The equilibrium constants (K_i 's), capacities (n_i 's), and enthalpies ($-\Delta H_i$'s) obtained from the analysis of the varied adsorptives are then used to directly compare

activated carbon adsorbents to identify the variables that will be the most important in novel adsorbent synthesis.

The pore size distribution (PSD) for a porous material is an essential piece of information for selecting a material for a specific application. With crystalline materials such as zeolites, the width of the distribution is narrow and an idea of the average pore size(s) can be determined from crystallography. The determination of pore sizes is a little more difficult for amorphous materials, for example, carbons, silicas, and aluminas, which usually have a wide distribution of pore sizes. The research presented examines a few of the current methods used for determining PSDs and introduces a method that takes advantage of the information provided by the MEA.

The MEA has been applied to the transition from the filling of the small micropores to the filling of the larger micropores (> 2 molecular dimensions) where multilayer formation is possible. The purpose of this study is not to necessarily gather information about the larger pores using MEA, although that may be a result, but to gain insight into adsorption from the liquid phase. To this end, the adsorption of ethane and sulfur hexafluoride at subcritical temperatures is examined using MEA.

CHAPTER 1

A BRIEF INTRODUCTION TO ADSORPTION AND POROSITY

One of the more important problems a scientist faces is the characterization of the materials they create. Single molecules, crystals, and bulk materials all require different methods for determining identity, structure, reactivity, or any of a myriad of physical properties. The methods used in characterization must be reliable, accurate, and, probably most importantly, accessible. Thus, when one is developing a characterization methodology, these considerations must be taken into account.

Porosity

A typical household sponge with its interconnecting series of channels and holes is an example of a porous solid. The number, type, and size of the pores and the way that they are arranged in the sponge refer to its overall porosity. Porosity is a broad term used to describe the porous structure of a solid and is usually described by the quantities surface area, pore volume, pore size distribution, and heterogeneity [1,2]. All of these terms are used to classify and describe porous solids using macroscopic concepts.

Structure

A crystalline material such as a zeolite has a well-defined and regular structure. The zeolite H-ZSM5 is shown in Figure 1.1a. From

crystallography, the dimensions of the channels and pore openings can be determined, and it is possible to estimate the type and size of molecules that can access these structures [1]. However, for porous materials that are globally amorphous, that is, no long range ordering exists, crystallography is not possible and other techniques must be used to obtain the similar information.

Activated carbon is an example of a material that is globally amorphous and shows some short-range order on the microscale [1,2]. Usually short-range ordering consists of graphite microcrystallites that do not show a preferential orientation. A representation of graphite microcrystallite ordering is shown in Figure 1.1b. The arrangement and size of the graphite microcrystallites reflect the structure of the starting material and the specific treatments it received during synthesis. Gaps, cracks, and crevices in the pore structure of the solid result from the arrangement and size of the graphite microcrystallites and impurities in the matrix. The molecular scale pores created by the gaps, cracks, and crevices in the pore structure of the solid are referred to as micropores and range up to 20\AA in width [3,4]. Mesopores range from 20 to 500\AA , and macropores are designated as pores with widths greater than 500\AA [3,4].

Heterogeneity

A homogeneous surface can be likened to a perfectly smooth tabletop where one part of the surface is indistinguishable from another. If the

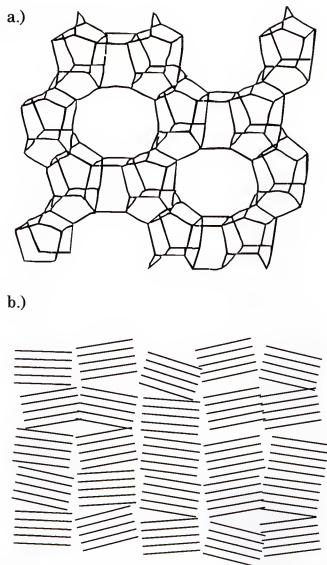


Figure 1.1: a.) The crystal structure of the zeolite H-ZSM5 and b.) a representation of the structure of an activated carbon.

surface is considered to have various and random dents, scratches, and other surface irregularities, it would be described as being heterogeneous. Some possible representations of surfaces are shown in Figure 1.2. The first case (a.) is the perfect homogeneous surface, while the other four show different heterogeneous cases: random, regular, patch-wise, island.

Most surfaces can be categorized as being heterogeneous. Notable exceptions include ideal crystallographic faces, for example, a nickel 001 face. The nickel 010 face is different from the 001 face and a mixture of the two would be considered heterogeneous. Certainly, on the atomic scale, the 001 face of a crystal is different from its 010 face, but, if examined from a different perspective, that is, using a probe molecule, they may be indistinguishable. It has been shown that a mixture of basal plane and edge plane graphite may be distinguished using CO_2 as a probe molecule [5].

Surface heterogeneity arises, as discussed above, from molecular sized flaws, cracks, different exposed crystal faces, and chemical impurities, and is usually important when discussing crystalline solids and non-crystalline macroporous, mesoporous, and nonporous solids [6]. When examining microporous solids, however, pore size and geometry become the major contributors to the observed heterogeneity and another type of heterogeneity must be considered, energetic heterogeneity [7,8,9]. Energetic heterogeneity is a result of the energy differences that exist in molecular size pores due to the additive potential from each of the pore walls [10]. This means that in

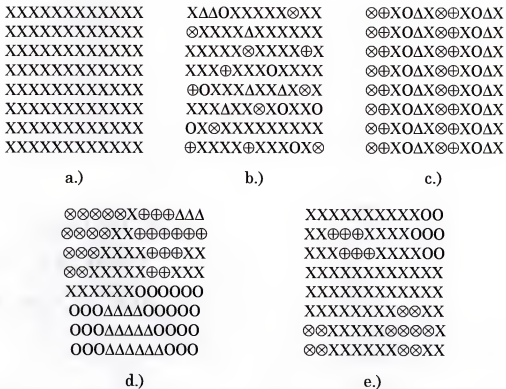


Figure 1.2: Possible representations of real surfaces: a.) a homogeneous surface, b.) a random heterogeneous surface, c.) a regular heterogeneous surface, d.) a patchwise heterogeneous surface, and e.) an island-like heterogeneous surface.

addition to basic surface heterogeneity, pore size and energetic effects must be considered, especially when considering microporous solids.

Adsorption

Adsorption is the concentration of molecules at or near a surface or interface. Adsorption should not be confused with *absorption*, which is a diffusion controlled process involving a bulk fluid entering the porous structure of a solid. Adsorption occurs because the forces binding the bulk of the solid together are unbalanced at the surface. The unbalanced surface forces create a resultant potential field perpendicular to the plane of the surface that can attract a molecule coming within proximity.

Molecular Interactions

The attractive potential between an adsorbing molecule and the atoms that make up the surface is a function of the distance from the molecule to the surface. The potential is due to the attractive London dispersion forces that are present in any system involving more than one atom or molecule. In one simple model, the strength of the dispersion forces is dependent on the polarizability of the molecules, the molecular masses, and the distance between the molecules, r . In the Lennard-Jones model, Equation 1.1, the attraction is a function of r^{-6} and becomes greater at smaller values of r , Figure 1.3. However, at a certain value of r , the overlap of the electron densities leads to repulsive forces proportional to r^{-12} . r_{12} is the distance that maximizes the interaction energy, E_{12} , which is the minimum in the function

shown in Figure 1.3, while σ is distance between the molecules at the zero-point energy, $E(r) = 0$. Modeling the interaction between two isolated molecules therefore takes into account both the attractive and repulsive forces.

$$E(r) = 4 \cdot E_{12} \cdot \left[\left(\frac{\sigma}{r} \right)^{12} - \left(\frac{\sigma}{r} \right)^6 \right] \quad (1.1)$$

If a non-polar adsorptive molecule is considered, the strength of the interaction will depend on the polarizability of both the adsorbing molecule and the atoms of the surface and on the orientation that the molecule takes when adsorbed [1,11,12,13]. If we further consider that the molecule is oriented in a way that maximizes the dispersion interaction with the surface, the resultant energy approximates the free energy of adsorption (ΔG_{ads}). For adsorption to be a spontaneous process, ΔG_{ads} must necessarily be negative. The loss of translational, rotational, and vibrational degrees of freedom by a molecule upon adsorption requires that ΔS_{ads} be negative, meaning that ΔH_{ads} must therefore be negative also. Some physisorption processes may only occur at low temperatures because then ΔG is favorable. Experiments run at a series of temperatures then allows the determination of the enthalpy (ΔH_{ads}) and entropy (ΔS_{ads}) of adsorption.

Chemical versus Physical Adsorption

The strength of the interaction between a molecule and a surface depends on the nature of the interaction. Chemical adsorption (chemisorption) is

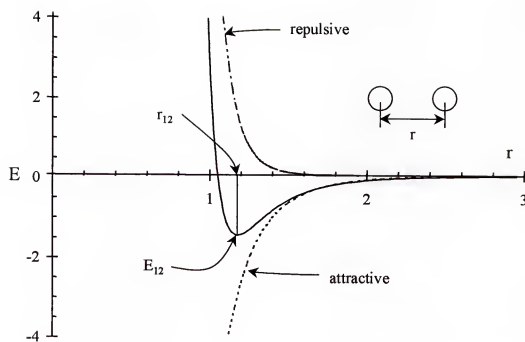


Figure 1.3: The Lennard-Jones potential function describing the interaction between two molecules.

characterized by a large negative enthalpy of adsorption, usually greater than $20 \text{ kcal-mole}^{-1}$ [1]. However, a large $-\Delta H_{\text{ads}}$ does not necessarily mean chemical adsorption. Chemisorption also requires is the formation of a chemical bond between the adsorbing species and the surface. An example of a chemisorption process is the adsorption of H_2 gas on platinum metal. Other characteristics of chemisorption are site specificity (localized adsorption), irreversibility, and that adsorption is limited to a monolayer [1].

In contrast, physical adsorption (physisorption) is dominated by intermolecular forces such as dipole - dipole and dispersion forces [1]. The interacting species retain their individuality on adsorption and adsorbate molecules are free to move about the surface, that is, no localized adsorption exists. This means that there is no localized adsorption or that it is not site specific. Physical adsorption is also fully reversible. Attempts to model both chemical and physical adsorption have required necessary simplifying assumptions such as site specific adsorption that will be discussed later.

Adsorbents and Porous Materials

The materials of interest in this research are adsorbents, catalysts, and catalyst supports. It should be mentioned that although protein clusters and other small clusters undergo similar interactions, they belong to another class of materials and will not be discussed here. A knowledge of the behavior of adsorption and adsorptive materials [14] and an understanding of the workings of these behaviors may allow the improvement of existing

materials [15] and the synthesis of novel materials for applications yet to be discovered [16-19].

Applications of Porous Solids

Adsorbents. Perhaps the largest use of porous materials is as adsorbents. The function of an adsorbent is the selective removal of one or more substances from the bulk of another. Water treatment plants use adsorbents to remove harmful waste products from water supplies [20]. The simple water filter at home uses a similar type of material. Chemists use carbon adsorbents to clarify solutions and aquarists use these same carbons to remove colors and toxic waste products from their tropical aquariums. The chemist also uses silica to purify the compounds that they make. The same silica is also used as a desiccant to keep moisture sensitive products viable.

Catalysis. Another area that takes advantage of the many properties of porous materials is catalysis [21-24]. Catalysts are used for many varied processes from oil refining to drug synthesis. Heterogeneous catalysts are solids that consist of discrete sites responsible for the observed chemistry. The way the active sites interact with reactants and products depends on adsorption.

In addition to understanding the interaction of the reactants and the products with a catalyst's active sites, the interaction of these molecules with the remainder of the solid surface is critical. In a zeolite, for example, a strong interaction between a reactant and the zeolite may prevent the

reactant from reaching the catalyst's active site, thus preventing or at least slowing the reaction [25]. Conversely, interactions that are too weak may not allow a sufficient concentration to build up around the active site, again restricting the efficiency of the reaction. On the other hand, a strong interaction between the support and reaction products could result in the catalyst becoming saturated with product and prevent reactants from reaching the active site, or result in a reaction between product and the active site [26].

Gas separation. The last major use of porous materials is in the area of separations. It was briefly mentioned above that porous silica is used in chromatographic separations, but other materials such as alumina, aluminosilicates, carbon molecular sieves, and zeolites also perform separations [16,25-29]. One industrially important application is in the area of gas separation, particularly pressure swing adsorption. Pressure-swing adsorption is a process used for the removal from one gas from another that could otherwise be accomplished using cryogenic distillation. The method is based on the selective adsorption of one component followed by a release of the adsorbed component by reducing the pressure and heating. A common use is the separation of air. The nitrogen molecule is slightly larger than the oxygen molecule and this slight difference in size is exploited to effect their separation [30].

Synthesis

Many methods exist for the synthesis of porous materials, the activity of which greatly depends on the starting materials and the specific treatments they receive. Extensive reviews covering synthetic techniques for making zeolites and zeolite-like materials, amorphous silicas, aluminas, aluminosilicates and activated carbons may be found in the literature [31,32]. Since the work to be presented involves only carbon derived materials a brief discussion of their synthesis follows.

Ultimately, precursor materials and activation procedures determine the properties of an activated carbon or a carbon molecular sieve [33]. Activated carbon materials have been made from a variety of starting materials including coal, coconut shells, peat, wood, graphite, nut shells, fruit pits, and synthetic polymers and resins; basically anything that can be converted to a char can become an activated carbon [2,20,31,32,34-36]. First, the precursor material is heated under vacuum or in the presence of a controlled amount of gas for a certain amount of time. This is called pyrolysis and involves the carbonization of the compounds that make up the starting material. Carbonization is a complex series of reactions where the compounds making up the precursor are decomposed to mostly carbon containing products. Temperature, the nature of the pyrolysis atmosphere, and time are the most important variables during this stage of the synthesis and affect the degree of carbonization attained in the final product [37,38]. The decomposition of the

precursor affects the formation of small gas pockets and a shifting and collapse of other regions of the solid. It is the collapse and rearrangement of the carbon structure during carbonization that gives the resulting material its unique pore structure [37,39].

After carbonization, the material is activated using steam, air, or CO_2 to oxidize remnants of the carbonization process [40]. Activation opens pores that may be blocked by residual ash and other compounds. This is also the stage where the size of the pores may be altered either by further oxidation (to increase pore size) or by the controlled decomposition of additives (to decrease pore size) [40,41]. Additional activation may include: washing with water to remove ash, again opening blocked pores; acid washing, to remove residual impurities and ash; and neutralization with Na_2CO_3 to neutralize any residual acidity either from acid washing or an oxidation step. Impurities remaining within the structure of the material, mostly sulfur, phosphorous, and iron, can greatly affect the final properties of the activated carbon. In any case, it is in the activation process that an activated carbon's properties are altered for specific applications [20].

Characterization

Activated carbons are difficult to characterize because common techniques, for example, normal spectroscopy, are useless due to the extreme complexity of the spectra obtained. However, NMR studies of probe molecules such as xenon have been used to examine the pore structures of

activated carbons [42,43]. Advances in microscopy have allowed direct observation of the pore structures within activated carbon materials [30,33]. Several other physical techniques have been used to examine the structure of activated carbons [44-48]. The usual characterization of microporous solids relies on adsorption experiments to determine the specific surface area (the area with respect to a certain molecule), the micro-, meso-, macropore, and total pore volumes, and, possibly, the distribution of the micropores [3,4,49-51].

The adsorption experiment. Probably the most used and useful technique for examining the porosity of porous materials is gas adsorption [49,52-58]. In a typical experiment, a solid material is exposed to a known pressure of a gas. The pressure of the gas drops proportionally to the amount of gas that is adsorbed by the material. Another known amount of gas is then introduced to raise the external gas pressure to its previous value followed by exposure to the solid. The dosing of known amounts of gas, followed by an equilibration period, is repeated until the pressure ceases to change within a specified time interval, that is, equilibrium is established at the applied pressure. The amount of gas adsorbed is recorded at each equilibrium pressure, which is varied to cover a range of pressure. When collected at a single temperature, isothermally, a plot of the amount adsorbed versus pressure is called an adsorption isotherm. In a similar manner the pressure can be reduced by a controlled amount with the amount of gas desorbed being

measured. This is the desorption isotherm. Differences between the adsorption and desorption isotherms yields information about the pore structure of the solid, but analysis of the adsorption or desorption isotherm alone can also yield a great deal of information about the structure of the solid. The analysis of the isotherm data often varies and the interpretation of the data sometimes yields conflicting results.

Surface area. The idea of surface area is really a macroscopic one. The surface area of a tabletop has real physical meaning, it is the length of the table multiplied by the width. The result is the amount of area that is available for use for a given application. If the table was then covered with identical circles of known area, the area of the table could be estimated with respect to the number of circles needed to cover its area without overlapping (monolayer coverage). This would not be the true surface area of the tabletop, but a valid estimation based on summing the areas of the individual circles. Using smaller circles would give a better estimate of the real area, but the meaning of the area measurement becomes clear when the area necessary for a particular use is taken into account, for example, the number of books of a certain dimension that can be placed on the tabletop. The purpose of the tabletop analogy is to show that surface area is dependent on the method used to determine its value. The measured surface area of a porous solid is strongly dependent on the molecule used to measure it, the true surface area is constant [3,4,59,60]

The area of non-porous, mesoporous, and macroporous materials is not very difficult to rationalize and the macroscopic view of the tabletop can be used. Only the size of the molecule used to measure the surface area and its orientation on the surface need be considered. The meaning of surface area as a property of a microporous solid is not as clear. In pores with widths on the order of the size of the adsorptive molecule, the adsorptive may interact with both of the pore walls effectively doubling the effective surface area, if using the macroscopic view. The idea of surface area in microporous solids is further complicated by heterogeneous surfaces and pore distributions.

The most widely used method for determining surface area is the BET method using the nitrogen adsorption isotherm collected at 77K [59]. Although BET is useful for comparing porous materials, it tends to greatly exaggerate surface areas for microporous solids [1]. Other methods have been suggested for the determination of surface area [11,46,60], but BET is still widely used even with its limitations.

Pore volume. In addition to surface area, it is useful to know the fluid volume capacity of a porous solid [3,4]. The macroscopic equivalent is the amount of fluid that can be held in a specific volume, for example, the amount of water that can be held in a glass. The total pore volume is usually taken as the amount of fluid adsorbed at ~ 1 atmosphere of pressure, which is usually a valid estimation since the adsorptive gas is usually liquefied at the experimental temperature at one atmosphere. The total pore volume

includes the contribution from the macro-, meso-, and micropores with the micropores being the largest contributor in many cases involving microporous carbons. As the micropores are responsible for most of the activity observed for porous solids, it is useful to know their contribution to the total volume.

Several t-plot methods have been used for determining micropore volumes based on a statistical thickness parameter (t) that corresponds to the formation of multiple layers of adsorbate on a reference material. The choice of reference material, and thus, parameters, determines the validity of the resulting volumes. Other methods have used micropore capacities derived from model parameters and determined micropore volumes by assuming the adsorbed fluid is similar to its liquid state and using the liquid density. Again, meaning comes into play when considering the small micropores, < 2 molecular diameters, where only the possibility of monolayer adsorption exists.

Pore size distribution. The pore size distribution (PSD) is a useful piece of information for selecting a material for a specific application [3,4]. For example, the separation of nitrogen from oxygen is possible because of a slight difference in size between the two molecules. For the separation to be efficient, the material used should have a large number of pores that will allow the adsorption of oxygen while excluding nitrogen. Accurate PSDs [61-64] for a range of materials allows quick screening for suitable candidates for testing.

Modeling Adsorption

Methods used for characterizing porous solids usually rely on an underlying theory of adsorption and an associated equation to describe the theory [65,66]. The equations used are usually a simple way to explain the adsorptive behavior observed for different gas/solid systems [67-69]. Further, the observed behavior must be described in terms that attach physical significance to the parameters used to describe the model [70,71]. Usually, several simplifying assumptions concerning a real system are made to get a model to work. Sometimes the assumptions are invalid but the reasoning behind the assumptions may lead to a modification of the model. Brief descriptions of the most used and influential models for adsorption follow.

Henry's Law

Generally, at very low pressures (dilute concentrations), the amount of adsorbate per gram of solid (N) is directly proportional to the equilibrium pressure (P_{eq}) of the adsorptive over the solid, Equation 1.2. Equation 1.2 is known as Henry's Law [1,2,72]. K_H is a proportionality constant and is

$$N = K_H \cdot P_{eq} \quad (1.2)$$

referred to as the Henry constant. Equation 1.2 is usually valid only in regions of low pressure where the surface coverage is very low and neighbor interactions are virtually nonexistent as the solid effectively "solvates" the adsorbate molecules. Most isotherm equations are considered valid only if they reduce to Henry's Law in the low-pressure range [1,72].

The Langmuir Isotherm

The nature of the Langmuir adsorption isotherm will be addressed in detail in Chapter 2 and will only be briefly introduced here. The original construction of Langmuir's theory of adsorption considered the chemical adsorption of gases and the formation of monomolecular layers on plane solid surfaces [11]. The assumptions of the model are that molecules are adsorbed by a localized, specific site on the surface, sites can contain a single molecule only, all of the sites on the surface are equivalent, and lateral interactions between adsorbed molecules are ignored. The kinetic derivation of the Langmuir model leads to Equation 1.3, where b is taken as the adsorption

$$\theta = \frac{b \cdot P_{eq}}{1 + b \cdot P_{eq}} \quad (1.3)$$

equilibrium constant, P_{eq} is the equilibrium pressure of the adsorptive over the solid, and θ is the surface coverage [1]. If χ is taken to be the amount adsorbed at pressure P_{eq} and χ_M is the amount of gas needed to complete a monolayer on the surface, θ can be represented by Equation 1.4

$$\theta = \frac{\chi}{\chi_M} \quad (1.4)$$

and (1.3) becomes

$$\chi = \frac{\chi_M \cdot b \cdot P_{eq}}{1 + b \cdot P_{eq}} \quad (1.5)$$

A plot of P_{eq} / χ versus P_{eq} allows the determination of the monolayer capacity χ_M and, given adsorbate dimensions, the specific surface area of the

monolayer. Deviations from linearity are observed for heterogeneous materials, however, at low coverage Equation 1.5 reduces to Henry's Law (Equation 1.2) [72].

The BET Isotherm

A modification of Langmuir's theory for monolayer adsorption was made by Brunauer, Emmett, and Teller (BET) to include the formation of multilayers [1,59]. The assumptions made in the BET model are:

1. each adsorbed molecule serves as an adsorption site for the next layer of molecules
2. adsorption is localized (sites) and lateral interactions between adsorbed molecules are ignored
3. the enthalpy of adsorption for the second and subsequent layers is assumed to be equal to the enthalpy of liquefaction, ΔH_L , and different from the enthalpy of adsorption for the first layer, ΔH_1 .

The result is the BET Equation, (Equation 1.6), where V is the volume

$$V = \frac{V_M \cdot C \cdot P}{(P_0 - P) + \left[1 + (C - 1) \cdot \frac{P}{P_0} \right]} \quad (1.6)$$

adsorbed at an equilibrium pressure P , V_M is the volume of the monolayer, P_0 is the saturation pressure of the adsorptive at the temperature of the experiment, and C is referred to as the BET C constant. C is related to ΔH_1

$$C = e^{(\Delta H_1 - \Delta H_L)/RT} \quad (1.7)$$

and ΔH_L by Equation 1.7. Thus, the enthalpy of adsorption for the monolayer can be determined from C . The surface area of the monolayer can be found

by determining χ_M (the amount of gas needed to complete the monolayer) from Equation 1.8 by plotting $P / V(P_0 - P)$ versus P/P_0 , Equation 1.8. The slope is equal to $(C-1)/V_M C$ and the intercept is $1/V_M C$. The

$$\frac{P}{V \cdot (P_0 - P)} = \frac{1}{V_M \cdot C} + \frac{(C-1)}{V_M \cdot C} \cdot \frac{P}{P_0} \quad (1.8)$$

limitations of the BET method are well documented [1,2] and attempts have been made to improve its meaning by including a correction for lateral interactions between adsorbed molecules [73,74], but it remains as the most used method for estimating surface areas.

The Freundlich Isotherm

Another adsorption isotherm equation that has been widely used and modified is the Freundlich isotherm, Equation 1.9 [1,75]. χ is the amount adsorbed per gram of solid, P_{eq} is the equilibrium pressure of the adsorptive over the solid, and K and $1/n$ are constants characteristic to the

$$\chi = K \cdot P_{eq}^{1/n} \quad (1.9)$$

solid / adsorptive system being studied. The Freundlich isotherm takes into account the heterogeneity of the solid and the distribution of the adsorption sites and their energies.

The Harkins and Jura Method

In 1944, Harkins and Jura developed a method for determining surface area derived from thermodynamics as an alternative to BET, which is derived from kinetics [60]. The most notable difference between the two

methods comes from H-J not requiring an estimate of the molecular size of the adsorptive used, which BET requires. BET uses molecular areas calculated from assumed packing arrangements for the molecules in the liquid or solid state, each of which gives a different result [59]. H-J on the other hand, assumes that surface area (Σ) is an intrinsic property of the solid that can be directly solved for using an adsorption isotherm.

Harkins and Jura found that a plot of $\ln(p/p_0)$ (p is the equilibrium pressure and p_0 is the saturation pressure of the gas at the temperature of the experiment) versus the reciprocal of the square of the amount adsorbed (N^2) yields a straight line. The square root of the slope (s) of this line is proportional (k) to the surface area of the solid, Equation 1.10. The examination of many isotherms involving different gases and solids led to the

$$\Sigma = ks^{1/2} \quad (1.10)$$

determination of a value for k for each gas studied. When Equation 1.10 was used with data from Brunauer and Emmett there was close agreement with the BET surface area values, but with less range in their values, that is, the H-J areas were closer to one another than the BET values were [60]. Although the Harkins-Jura method appears to be better than BET, it finds little use today.

The Dubinin-Radushkevich Equation

The empirical Dubinin-Radushkevich isotherm (D-R) is based on a Gaussian distribution function for describing micropore filling, θ , Equation 1.11 [72,76]. E_0 is the characteristic energy of adsorption for a reference

$$\theta = \exp \left[- \left(\frac{A}{E_0 \beta} \right)^2 \right] \quad (1.11)$$

gas and β is the similarity coefficient. A is the free energy change on adsorption and is given by Equation 1.12 where R is the gas constant,

$$A = -RT \ln(P/P_0) \quad (1.12)$$

T is the experimental temperature, P is the equilibrium pressure of the gas, and P_0 is the saturation pressure of the gas at the experimental temperature. The D-R equation has been used extensively for describing physical adsorption processes for many gas / solid systems including microporous solids. To take into account the energetic heterogeneity that exists due to the distribution of micropore sizes, Equation 1.11 takes the form

$$\theta = \int_0^{\infty} \exp \left[- \left(\frac{A}{E} \right)^2 \right] \cdot g(E) \cdot dE \quad (1.13)$$

where $g(E)$ is an assumed energy distribution function describing the micropores. Although this isotherm equation has been remarkably successful for describing a variety of gas/solid systems, little progress has been made to elevate it from its empirical foundations to a sound theoretical level [76].

Concluding Remarks

The purpose of this introductory chapter has been to briefly describe the important and noteworthy concepts necessary for discussing gas / solid equilibria involving porous solids. In no way should it be taken as a comprehensive compilation of the accomplishments in this area. Rather, the methods and theories that have had the greatest influence on current research have been summarized to introduce the methodologies that exist and their origins. It should also be noted that all common methods are, however, limited in their description of the adsorption process and restrict the meaning of the associated surface area and pore volume determinations in addition to any model derived parameters.

The remainder of this work will be devoted to a theoretical description of micropore filling using a new adsorption model and the evaluation of the model parameters to quantify specific properties of the gas / solid adsorption system. Chapter 2 describes the basis of the Multiple Equilibrium Analysis (MEA) and uses MEA derived quantities to compare and contrast five activated carbon adsorbents. Chapter 3 involves the use of MEA derived quantities to present pore size distributions (PSDs) for the solids studied and suggests the role of MEA-PSDs in the prediction of adsorption isotherms. In Chapter 4, multilayer formation is addressed in a manner consistent with the MEA, and Chapter 5 contains a brief review of the research presented.

CHAPTER 2

A MULTIPLE EQUILIBRIUM ANALYSIS (MEA) OF ADSORPTION AND POROSITY IN CARBONS

The ultimate goal of the research presented here is to gain a fundamental understanding of adsorptive-adsorbent interactions and apply the information obtained to the rational design of new adsorbents tailored to specific adsorptives of interest. A multiple equilibrium analysis model (MEA) has been developed to interpret adsorption isotherms and to define the adsorptive effects and porosity of porous materials. Adsorptives have been selected that vary in size and polarizability to permit adsorbent characterization in terms of these physical properties. The equilibrium constants (K_i 's), capacities (n_i 's), and enthalpies ($-\Delta H_i$'s) obtained from the analysis of the varied adsorptives are then used to directly compare activated carbon adsorbents to provide insight into the variables that may be important in novel adsorbent synthesis.

The Langmuir Model

In his original work, Langmuir described monolayer adsorption on an energetically homogeneous surface, specifically glass, mica, and platinum [11]. The interactions on these surfaces are chemical in nature (chemisorption). The basic assumptions of the model are: [1,11]

1. molecules are adsorbed by a localized site
2. an adsorption site may contain only one molecule
3. all adsorption sites are energetically equivalent
4. lateral interactions between adsorbed molecules are ignored.

Given the assumptions above, an expression describing the observed interactions can be derived using kinetic, thermodynamic, or statistical mechanics arguments [1]. The simple kinetic model, Figure 2.1, requires that the rate of adsorption depend on the fraction of the surface that is bare and that the rate of evaporation depend on the fraction of the surface that is covered. At equilibrium, these rates are equal leading to Equation 2.1. Here N_A is Avogadro's number, N_0 is the number of adsorption sites on the surface

$$\frac{N_A}{N_0} n = \frac{\sigma \mu}{1 + \sigma \mu} \quad (2.1)$$

of the solid, n is the amount adsorbed, σ is related to the fraction of the gas molecules adsorbed and to the evaporation rate, and μ is proportional to the equilibrium pressure of the adsorptive and to the temperature. The Langmuir model holds for systems such as the chemisorption of carbon monoxide on platinum.

What if there is more than one type of adsorption site on a single surface or there are different active surfaces in a given system, that is, heterogeneity? In the case of heterogeneity, the different types of surface sites contribute differently to the total observed equilibrium. If B_i is the

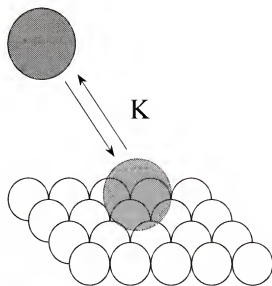


Figure 2.1: A kinetic description of adsorption.

$$\frac{N_A}{N_0} n = \sum_i \frac{B_i \sigma_i \mu}{1 + \sigma_i \mu} \quad (2.2)$$

fraction of the total adsorption attributed to site type i and there are i different types of sites, Equation 2.1 becomes 2.2 [11]. For the i types of sites to be differentiated, the interactions involved must be significantly different, that is, the chemical equilibrium describing adsorption at site type A must differ from that for B, etc. If the chemical processes are similar, however, resolution of the different sites will not be possible.

The Multiple Equilibrium Analysis

An activated carbon material (carbon) can be described in a manner similar to that used to describe the different types of chemisorption sites given above. The dominate interaction in carbons is physical adsorption (physisorption) compared to chemisorption [52,77-80]. When a molecule enters the pore structure of an activated carbon it can interact within a specific distribution of pores that differ mostly with respect to size. The size of a pore depends on its shape and the literature support is the view that the pores in activated carbons and carbon molecular sieves are slit-shaped [10,75,81,82]. A slit-shaped model for pores means that the greatest difference between pores in a given material will be in the width of their openings and the distance between the opposing walls that make up the pores [18,83]. If a molecule interacts with the surface of a pore with a width much greater than the diameter of the molecule, the observed interaction will

be similar in magnitude to that of the same molecule interacting with a single graphitic plane [10]. In pores greater than two molecular diameters in width, the opposite wall of the pore is far enough away from the adsorbed molecule that it does not contribute significantly to the observed interaction [10,82].

If the molecule interacts with the internal surface of a pore with a width similar to or slightly larger than the diameter of the molecule, both walls contribute and the interaction is significantly increased over the single wall case [10,82]. Using the equations developed by Everett and Powl, the variance of the interaction with pore width is shown in Figures 2.2 and 2.3. The scale of the y-axis (E_2/E_1) is the ratio of the interaction for two pore walls (E_2) to that observed for the one wall case (E_1), that is, the single graphitic surface. The maximum value of 2 is reached when the pore width is equal to the diameter of the adsorbing molecule ($d = r_0$). Figure 2.3 shows the calculated adsorption potential wells for three molecular diameter to pore width ratios (z/r_0). The value of z/r_0 is relative to the position (z) of the molecule between the pore walls and the radius of the molecule (r_0). The value of d/r_0 relates the width of the pore (d) to the radius of the molecule (r_0). Figure 2.3a shows the case for a z/r_0 of 1.6. Two distinct minima are observed, one associated with each wall of the pore. As the width of the pore decreases, Figure 2.3b, the two minima begin to coalesce, showing the addition of the potentials from each of the pore walls ($z/r_0 = 1.2$). The final

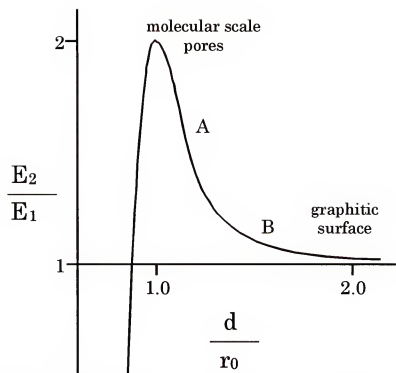


Figure 2.2: The variance of adsorption potential with respect to pore width and adsorptive radius. E_2 is the potential energy for two parallel single graphitic planes, E_1 is the energy for a single graphitic plane, d is $\frac{1}{2}$ the distance between the graphitic planes, and r_0 is the radius of the adsorptive.

case, Figure 2.3c, occurs when the pore width corresponds to the diameter of the adsorptive molecule. The minimum of the resulting potential well indicates the maximum addition of the two individual potentials. These values roughly correspond to the assignment of the three Processes for the MEA shown in Figure 2.4.

Definition of the MEA

Further examination of Figure 2.2 shows two regions with distinct slopes, points A and B, and a transition region of a gradually changing slope in between. Each of these regions represents a group of pores with similar adsorption characteristics, which is attributed to pore width. Adsorption into these regions is defined in the MEA as a *Process*. A formal definition of a Process is adsorption within a group of pores that are so similar in character that the group cannot be divided into smaller groups. In the MEA, each Process is described by an equilibrium constant for adsorption (K) and an associated specific capacity (n). The capacity is an intrinsic property of the solid and is a measure of the number of molecules that can be adsorbed into the pores describing a given Process. The mathematical form of the model is given in Equation 2.3. Again, the capacity for each Process i , is described by

$$N_{tot} = \sum_i \frac{n_i K_i P_{eq}}{1 + K_i P_{eq}} \quad (2.3)$$

n_i , K_i is the associated equilibrium constant, P_{eq} is the equilibrium pressure of the adsorptive over the solid given in atmospheres, and N_{tot} is the total amount, in moles·g⁻¹ solid, of adsorptive adsorbed (adsorbate) at P_{eq} . The

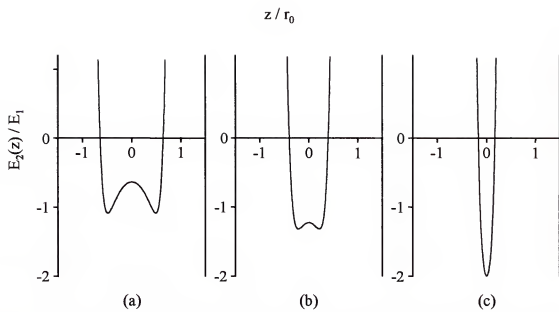


Figure 2.3: Potential wells corresponding to d/r_0 values of 1.6, 1.2, and 1.0, respectively.

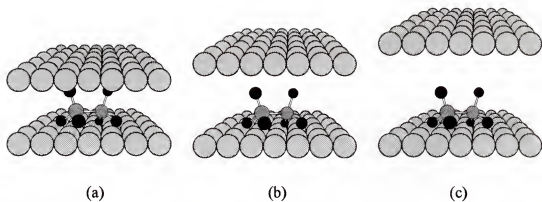


Figure 2.4: Representations of the adsorption Processes described in the text: a.) Process I, b.) Process II, and c.) Process III.

number of Processes, i , is the minimum number necessary to fit the data to within experimental error. For all of the carbons and adsorptives studied to date, an $i = 3$ has been found to fit the data. The equilibrium constants effectively describe the extent to which a particular pore size fills at a given temperature. Thus, raising the temperature of the adsorption experiment results in less of the adsorptive being adsorbed. The n_i 's, however, should not vary significantly with temperature as they represent the adsorption maximum for the individual adsorption Processes.

Equation 2.3 is similar in form to the Langmuir equation but is conceptually very different [84-87]. Adsorption sites, as defined by Langmuir, are replaced by the accessible pore volumes for each of the individual Processes. With this in mind, the equilibrium constants for physisorption are, in effect, distribution coefficients involving the gaseous adsorptive in equilibrium with adsorbed molecules within the pores of the solid. The pores with molecular dimensions are filled first (they have the largest K 's), but all Processes occur simultaneously. Additional neighbor interactions are expected as the capacity for each Process is reached and contribute to the total interaction observed for each Process. From this point forward the term *Process* will be used to describe adsorption occurring within a specific pore size regime as opposed to adsorption by a specific type of surface site.

The question arises “what are resolvable Processes?” For the resolution of two Processes, the K 's must be approximately an order of magnitude different [87]. For the carbons used in this study, and in the two previous studies, three Processes were found in all cases. Process I has been defined as adsorption in pores ~ 1 to 1.2 molecular diameters in width, Figure 2.4a. Process II occurs in pores ~ 1.2 to 1.5 molecular diameters while Process III is defined as adsorption into pores from ~ 1.5 to 2 molecular diameters in width, Figures 2.4b and c, respectively. These assignments reflect the regions where the slope changes rapidly in Figure 2.2, points A and B (Process I from $d/r_0 = 1$ to A, Process II from A to B, and Process III from B to $d/r_0 = 2$).

In the case of a three Process system, that is, three average pore size regimes for a given adsorptive/solid system, solving for the six unknowns, three K 's and three n 's, in Equation 2.3 using a single experimental isotherm leads to a shallow minimum in the data fit and uncertainty in the parameters [88,89]. A better minimum is reached using isotherms collected at a series of different temperatures and solving all of the data sets simultaneously. The only new unknowns added to the system at each new temperature are the new K 's. In the MEA, it is assumed that the n values, like solid and liquid densities, are for practical purposes temperature independent as they represent a solid's maximum capacity (saturation limit) for each Process and, as such, the same set applies to a given adsorptive/solid system at each different temperature. Using the three Process example again, the 6:1 ratio

of unknowns to isotherms becomes 9:2 for two isotherms, 12:3 for three, 15:4 for four, etc. The smaller ratio of unknowns to experimental isotherms leads to a better definition of the minimum in the analysis of the combined data set.

As with all of the current methods available for the analysis of adsorption data, the multiple equilibrium analysis relies on, and produces, an excellent empirical fit of the experimental data. However, a new model will be significant only if the parameters obtained from the fit of data involving different adsorptives and adsorbents have meaning within the context of the model and offer new insights concerning adsorption. The direct thermodynamic basis for the parameters of the MEA suggests these advantages if it can be demonstrated that the data fit provides meaningful results, which will be addressed later in this chapter.

Information Provided by the MEA

Of course, the adsorption of a single type of molecule cannot effectively describe the porosity of a solid. Multiple adsorptive molecules, differing in size, polarizability, and polarity, should be used. The differently sized adsorptives will utilize different pores in each solid and allow the definition of the Processes relative to the size of the adsorptive used.

The Process capacities (n_i 's) are used with each adsorptive's molar volume to provide an estimate of the accessible pore volume for different adsorptives that can be compared to the those determined from conventional N_2

porosimetry techniques. Additionally, these capacities and the adsorptives' cross-sectional areas can be used to calculate accessible surface areas for different size adsorptives for each resolved Process. These areas are compared and contrasted to the N_2 BET areas which are known to be unrealistic for microporous solids [1].

The temperature dependence of K can be exploited to determine thermodynamic quantities for each adsorption Process, namely the enthalpy and entropy of adsorption. The $-\Delta G$ and $-\Delta H$ values for adsorption will be shown to correlate to molecular properties of the adsorptives, which leads to a characterization of the dispersion characteristics of the adsorbents. The success of these correlations indicates that the parameters obtained from the data fits have the thermodynamic meaning implied by the model employed. A long range goal of isotherm modeling is the prediction of adsorption isotherms from fundamental properties and the potential use of the MEA model to predict isotherms is discussed. Finally, the information offered by MEA allows the direct comparison of different carbon materials in terms of their porosity and allows one to draw conclusions as to what makes these materials different and what is significant about those differences.

Experimental Isotherms

Adsorbents and Adsorptives

Five commercially available carbonaceous adsorbents were chosen for this study. The adsorbents A563, A572, and A600 are made via the controlled

pyrolysis of a polysulfonated polystyrene resin and were obtained from Rohm and Haas Co. BPL 4x10 and Filtrasorb 300 8x30 are coal derived materials donated by Calgon Carbon Co. The N_2 (99.99%) was obtained from Liquid Air, Inc., while CO , CH_4 , and C_2H_6 were purchased from Matheson Gas Co. SF_6 was purchased from Aldrich. All gases were used as received. Physical characteristics of the adsorptives and carbons are given in Tables 2.1 and 2.2, respectively.

Adsorption Measurements

All of the reported adsorption data was collected using a Micromeritics® ASAP 2000 system with both chemisorption and physisorption capabilities. Pressure measurements were made using 1000 and 10 torr pressure transducers with resolutions of 0.052 and 0.0005 torr, respectively. All measurements were taken with the instrument operating in the chemisorption mode except for N_2 porosimetry measurements at 77K, which were taken in the physisorption mode. The differences between these two modes lies in the data collection software.

Approximately 0.3g of sample were used for each experiment. The sample was degassed at 200°C under vacuum, $<10^{-3}$ torr, for at least 8 hours prior to the adsorption experiment. Each experiment consisted of the collection of 36-50 adsorption points covering the pressure range from 1 to 760 torr with the majority of the points taken below 100 torr. An example of a typical pressure table can be found in Appendix A. To prevent the possibility of capillary

condensation, all experiments were run at temperatures above the critical temperature of the given adsorptive. Temperatures below ambient were maintained using an appropriate solvent- liquid nitrogen slurry. Temperatures above ambient were maintained using the heating mantle and thermocouple provided with the ASAP instrument. All temperatures were held to within 1°C of the reported values. All of the adsorption data used in this dissertation may be found in Appendix A.

Data Analysis

Fitting the collected data with the MEA is accomplished through a series of steps. The raw adsorption data is in the form of volume adsorbed in $\text{cc}\cdot\text{g}^{-1}$ at STP and equilibrium pressure in torr. The data is converted to moles adsorbed per gram assuming an ideal gas at STP, by dividing the volume adsorbed by $22,414\text{-cc}\cdot\text{mole}^{-1}$ gas. The equilibrium pressure is converted to atmospheres by dividing by 760 torr. A plot of $P_{\text{eq}}\cdot\text{moles adsorbed}^{-1}$ versus P_{eq} is constructed for each temperature set (the Langmuir Isotherm). Each Langmuir Isotherm is then divided into several straight-line regions, generally 3 for carbons and 2 for zeolites and porous silicas. An initial estimate of n is calculated from the slope of the line with K taken from the intercept in each region. The slope and intercept are determined from a linear regression of the points in each region. The lowest pressure region is associated with Process I, the next with Process II, continuing until the minimum number of straight-line regions is used to fit the entire isotherm.

Only one set of n -values is needed for the fit since the n 's are temperature independent. The initial value of n_3 is taken from the temperature set closest to the critical temperature of the adsorptive. The value for n_2 is taken from either the same temperature set as n_3 or the next highest, and n_1 from the highest temperature set. It is at these temperatures that each quantity is the best defined. The initial parameter set then contains one set of n -values and a set of K -values for each temperature. For the initial fit, each parameter is given a 10% bound and all of the temperature sets for a specific adsorptive/solid system are fit simultaneously. In successive fits, the bound is reduced to 1% of the parameter. The parameters obtained from the initial fit are then entered as the initial parameters for the next fit. The parameters from the second fit are then entered into the third fit and each successive fit is done accordingly. This procedure is used since several local minima are found during the first few fits and, therefore, the fitting Process is not assumed to be complete until all of the parameters cease to vary from fit to fit.

The MEA fitting program produces a nonlinear least-squares regression of the data using a modified simplex algorithm [92-94]. The advantage of the MEA program is that multiple data sets that share parameters (the n_i 's) may be fit simultaneously. The Fortran code for the fitting program and an example input file are included in Appendix B.

The enthalpy and entropy of adsorption are calculated from the slope and intercept, respectively, obtained from the weighted least-squares regression of $\ln K_i$ versus T^{-1} plots of the best-fit parameters. A typical plot is shown in Figure 2.5. A weighting factor of K^2/σ_K^2 is typical for a weighted regression involving a natural logarithm function.

The MEA Parameters

The results of the MEA for the adsorptives and solids studied, listed in Tables 2.1 and 2.2, respectively, are presented in Table 2.3. All references to MEA parameters are to this table. The uncertainties are determined by the regression program used to fit the model to the data. Figure 2.6 shows examples of experimental adsorption isotherms along with the isotherms calculated using the associated MEA parameters and Equation 2.3. All analyses produce excellent fits of the experimental data.

The temperature dependence of typical adsorption isotherms is shown in Figure 2.7 for SF_6 adsorption by A572. Again, in the MEA, the temperature dependence is directly attributed to the K_i 's describing the adsorption. Using the MEA parameters it is possible to calculate the Process resolved isotherms. Shown in Figure 2.8 is methane adsorption by A572 at -43°C . Plots such as this show the contribution of each Process to the total adsorption as a function of pressure and may be useful for predicting breakthrough pressures for specific separations

Table 2.1: Summary of Gases and Physical Properties. ^a

Adsorptive	N ₂	CO	CH ₄	C ₂ H ₆	SF ₆
MW g·mole ⁻¹	28.01	28.01	16.04	30.07	146.05
van der Waals a ^b	1.95	1.453	2.27	5.503	7.775
α Å ³	1.74	1.95	2.59	4.47	6.54
Molar Volume ml·mole ⁻¹ ^c	25.02	28.28	29.74	47.21	77.04
T _{nbp} °C	-195.8	-191.5	-161.5	-88.65	-63.8
T _c °C	-146.9	-140.2	-82.6	32.3	45.6
ΔH_v kcal·mole ⁻¹	1.33	1.44	1.95	3.52	1.44
ΔS_v cal·mole ⁻¹ ·K ⁻¹	17.22	17.67	17.6	19	19.5
ΔH_{np} ^d kcal·mole ⁻¹	2.39	2.5	3.11	4.78	5.67
Molecular Area Å ² ^c	15.27	15.77	16.26	24.01	31.17

a. All data is from Lange's Handbook of Chemistry, 13th ed.; Dean, J.A, Ed.; McGraw-Hill: New York, 1985 unless otherwise specified.

b. Calculated from the critical constants of the adsorptives [91].

c. Reference [90].

d. ΔH for adsorption on a nonporous carbon [58]. The SF₆ value is calculated from a plot of ΔH_{np} versus $a^{1/2}$.

Table 2.2: Physical Properties of the Adsorbents. ^a

Solid	BET surface area (m ² ·g ⁻¹) ^b	Micropore Area (m ² ·g ⁻¹) ^c	Total Pore Volume (mL·g ⁻¹) ^d	Micropore Volume (mL·g ⁻¹) ^c	% V _m /V _T	Ave. Pore Diameter (Å)
A563	625	563	0.6515	0.2266	34.78	41.72
A572	1180	1095	0.9656	0.4346	45.01	32.73
A600	623	564	0.6015	0.2268	37.71	38.61
BPL	1080	1066	0.4998	0.4656	93.16	18.51
F300	953	905	0.4948	0.3939	79.61	20.76

- a. Calculations based on the N₂ adsorption isotherm collected at 77K.
b. Surface area is based on a 5-point BET calculation
c. Calculated using the Harkins-Jura t-plot
d. Total pore volume at the highest measured pressure.

Table 2.3: MEA Adsorption Parameters (n -values are in mmole·g⁻¹).

<i>Nitrogen</i>		K value for Process		
	T(°C)	I	II	III
A563	-93	70±1	11.7±0.2	1.1±0.1
	-62	10.64±0.05	1.96±0.01	0.258±0.007
	-43	4.21±0.02	0.881±0.004	0.128±0.003
	<i>n</i>	0.316±0.003	1.36±0.02	2.3±0.2
A572	-93	88.22±0.02	8.631±0.005	0.752±0.002
	-43	4.54±0.01	0.72±0.02	0.118±0.008
	0	0.922±0.002	0.1381±0.0005	0.0456±0.0002
	<i>n</i>	0.463±0.003	1.79±0.04	5.3±0.2
A600	-93	90.2±0.02	11.88±0.06	1.12±0.04
	-62	10.92±0.07	1.92±0.01	0.23±0.01
	-43	4.51±0.06	0.85±0.01	0.118±0.008
	<i>n</i>	0.349±0.003	1.39±0.02	2.3±0.1
BPL	-93	115.6±0.4	12.56±0.09	0.92±0.02
	-62	13.34±0.06	1.93±0.01	0.209±0.003
	-43	5.44±0.03	0.905±0.006	0.119±0.001
	<i>n</i>	0.209±0.001	0.990±0.007	4.92±0.08
F300	-93	128.6±0.5	13.9±0.1	1.07±0.03
	-62	16.4±0.1	2.31±0.03	0.286±0.007
	-43	6.51±0.05	1.08±0.01	0.162±0.003
	<i>n</i>	0.231±0.002	0.97±0.01	3.73±0.09

Table 2.3: MEA Adsorption Parameters (cont.).

Carbon Monoxide		K value for Process		
T(°C)		I	II	III
A563	-93	310±4	29±1	1.7±0.5
	-62	20.6±0.5	4.9±0.2	0.61±0.07
	-43	7.91±0.04	1.96±0.01	0.287±0.006
	<i>n</i>	<i>0.342±0.007</i>	<i>1.06±0.03</i>	<i>2.5±0.5</i>
A572	-93	219.1±0.9	18.0±0.3	1.3±0.1
	-62	24.0±0.6	2.9±0.2	0.33±0.08
	-43	8.9±0.1	1.26±0.04	0.16±0.01
	<i>n</i>	<i>0.58±0.01</i>	<i>1.92±0.08</i>	<i>4.9±0.7</i>
A600	-93	189±1	20.0±0.6	1.7±0.4
	-62	17.5±0.4	3.1±0.2	0.42±0.09
	-43	6.35±0.03	1.26±0.04	0.193±0.007
	<i>n</i>	<i>0.537±0.008</i>	<i>1.28±0.05</i>	<i>2.2±0.4</i>
BPL	-93	189.4±0.8	13.8±0.2	0.93±0.05
	-62	22.1±0.5	3.9±0.1	0.24±0.04
	-43	8.42±0.08	1.09±0.02	0.128±0.006
	<i>n</i>	<i>0.334±0.006</i>	<i>1.25±0.05</i>	<i>5.0±0.5</i>
F300	-93	305.2±0.9	30.8±0.2	1.88±0.06
	-62	32.1±0.5	4.2±0.1	0.45±0.03
	-43	12.3±0.2	1.91±0.05	0.24±0.01
	<i>n</i>	<i>0.252±0.005</i>	<i>0.96±0.02</i>	<i>3.8±0.2</i>

Table 2.3: MEA Adsorption Parameters (cont.).

<i>Methane</i>		K value for Process		
	T(°C)	I	II	III
A563	-62	150.6±0.9	17.1±0.3	1.4±0.2
	-43	47.4±0.5	6.2±0.1	0.6±0.1
	-16	10.8±0.1	1.69±0.04	0.17±0.03
	<i>n</i>	0.514±0.006	1.68±0.04	2.1±0.4
A572	-62	125.2±0.9	10.5±0.3	1.1±0.1
	-43	28.0±0.3	3.2±0.1	0.38±0.05
	0	4.63±0.02	0.679±0.006	0.117±0.002
	<i>n</i>	0.775±0.009	2.20±0.07	5.4±0.6
A600	-62	170.6±0.6	17.5±0.2	1.3±0.1
	-43	56.5±0.7	5.5±0.2	0.5±0.2
	-16	11.8±0.1	1.75±0.04	0.16±0.03
	<i>n</i>	0.499±0.006	1.71±0.04	2.0±0.5
BPL	-62	142±1	13.0±0.3	0.95±0.07
	-43	50.7±0.7	5.0±0.2	0.51±0.04
	-16	11.8±0.3	1.48±0.08	0.20±0.02
	<i>n</i>	0.348±0.007	1.29±0.05	5.7±0.5
F300	-62	188.7±0.3	16.04±0.08	1.13±0.02
	-43	60.3±0.8	6.1±0.2	0.52±0.06
	-16	14.2±0.3	1.76±0.07	0.20±0.02
	<i>n</i>	0.332±0.005	1.27±0.04	4.5±0.4

Table 2.3: MEA Adsorption Parameters (cont.).

<i>Ethane</i>		K value for Process		
T(°C)		I	II	III
A563	40	78.3±0.2	11.04±0.06	1.13±0.05
	55	37.9±0.4	6.0±0.1	0.7±0.1
	70	19.2±0.8	3.5±0.2	0.4±0.2
	100	8.80±0.06	1.54±0.02	0.17±0.02
	<i>n</i>	0.329±0.008	1.08±0.04	1.3±0.4
A572	40	176.9±0.6	15.0±0.1	1.35±0.05
	55	74.1±1	7.6±0.2	0.75±0.09
	70	42.0±0.4	4.82±0.09	0.53±0.03
	100	13.9±0.3	1.88±0.07	0.23±0.03
	<i>n</i>	0.318±0.005	1.42±0.04	3.7±0.3
A600	40	117.2±0.6	13.7±0.1	1.2±0.1
	55	56.8±0.4	7.8±0.1	0.70±0.08
	70	30.7±0.2	4.63±0.06	0.44±0.05
	100	11.1±0.1	1.76±0.03	0.17±0.02
	<i>n</i>	0.272±0.003	1.10±0.01	1.3±0.1
BPL	40	92.4±0.9	9.7±0.2	0.72±0.04
	55	50.3±0.5	5.8±0.1	0.49±0.2
	70	28.2±0.3	3.10±0.08	0.33±0.02
	100	13.4±0.1	1.86±0.03	0.244±0.007
	<i>n</i>	0.193±0.003	0.84±0.02	4.0±0.2
F300	40	141.8±0.4	13.3±0.1	1.01±0.03
	55	72.6±0.2	7.41±0.05	0.66±0.01
	70	40.1±0.5	4.6±0.1	0.43±0.03
	100	15.4±0.3	2.05±0.07	0.22±0.02
	<i>n</i>	0.199±0.003	0.87±0.02	3.3±0.2

Table 2.3: MEA Adsorption Parameters (cont.).

Sulfur Hexafluoride		K value for Process		
T(°C)		I	II	III
A563	50	97±1	11.6±0.2	1.0±0.2
	65	54.2±0.5	7.24±0.09	0.63±0.08
	80	28.8±0.4	4.43±0.06	0.39±0.06
	95	16.6±0.2	2.77±0.03	0.24±0.02
	<i>n</i>	0.109±0.002	0.63±0.008	0.66±0.09
A572	50	173.0±0.8	14.6±0.1	1.47±0.05
	65	102.9±0.4	9.32±0.06	1.11±0.03
	80	54.0±0.7	6.1±0.1	0.67±0.05
	95	31.1±0.3	3.76±0.06	0.39±0.02
	<i>n</i>	0.165±0.003	1.00±0.01	2.5±0.1
A600	50	161±2	13.4±0.2	1.1±0.1
	65	65±1	6.8±0.1	0.77±0.08
	80	44.9±0.5	5.91±0.06	0.53±0.04
	95	29.7±0.3	3.82±0.03	0.37±0.02
	<i>n</i>	0.055±0.002	0.529±0.006	0.71±0.07
BPL	50	149.0±0.3	12.4±0.04	0.963±0.009
	65	71.1±0.5	6.68±0.08	0.62±0.02
	80	38.7±0.9	4.6±0.1	0.41±0.03
	95	24.0±0.5	3.26±0.07	0.29±0.02
	<i>n</i>	0.110±0.002	0.73±0.01	3.2±0.2
F300	50	138.7±0.3	11.58±0.06	1.05±0.02
	65	68.5±0.8	7.0±0.1	0.63±0.04
	80	41.3±0.3	4.30±0.05	0.49±0.01
	95	23.1±0.7	3.1±0.1	0.33±0.04
	<i>n</i>	0.128±0.003	0.69±0.02	2.4±0.2

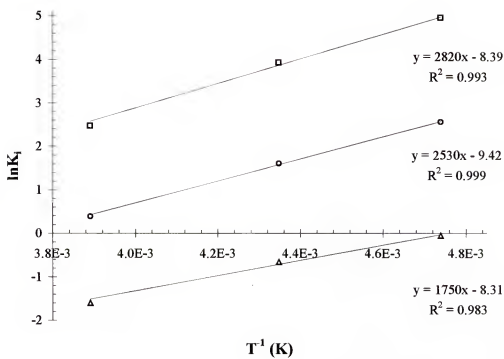


Figure 2.5: $\ln K_i$ versus T^{-1} (K) for methane adsorption by BPL.

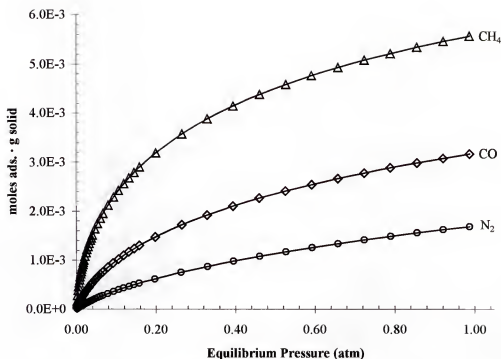


Figure 2.6: Isotherms for the adsorption of N_2 , CO , and CH_4 by A572 at -62°C . Points represent experimental adsorption values, \circ for N_2 adsorption, \square for CO adsorption, and Δ for CH_4 adsorption, while the solid and dashed lines represent the calculated isotherms using the n and K values in Table 2.3 with Equation 2.3.

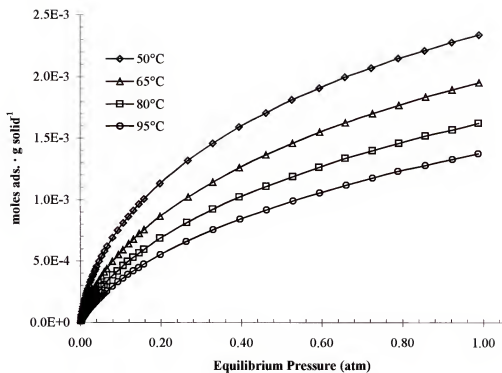


Figure 2.7: SF_6 adsorption by A572.

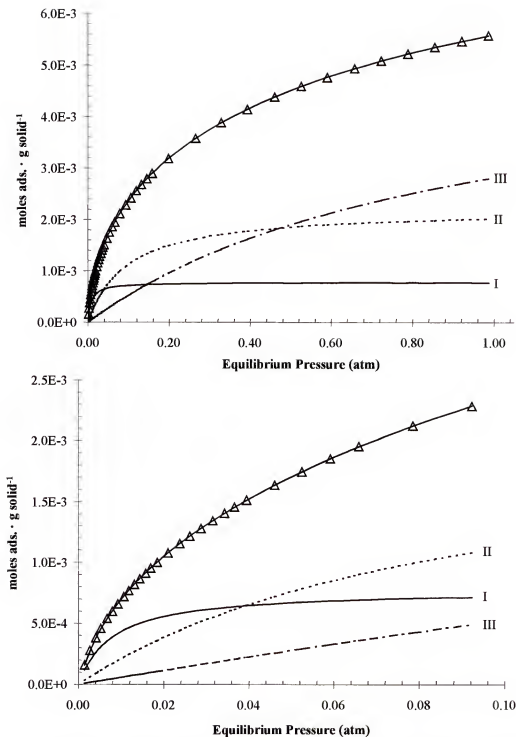


Figure 2.8: Process resolved adsorption for CH_4 by A572 at -43°C . The points represent the experimental adsorption values and the solid line calculated values. The component isotherms, labeled I, II, and III for Processes I-III, are calculated using the n_i and K_i values from Table 2.3 with Equation 2.3.

The Meaning of the MEA Parameters

As mentioned previously, an adsorption model will be significant only if the parameters obtained have meaning within the context of the model and if the model offers new insights concerning adsorption. In the case of the MEA, questions concerning the meaning of the parameters (n_i and K_i) have been raised. Specifically, the concern is that the parameters are merely empirical fitting parameters without physical meaning [88]. Although the MEA relies on an empirical fit of experimental adsorption data, the parameters have been patterned after those of the Langmuir equation, which are true thermodynamic parameters [1]. The sensitivity of n_i and K_i will be addressed using Monte Carlo Simulations.

Another serious question raised concerning the MEA is that it artificially divides a given pore size distribution (PSD) into smaller, unrealistic regions. An argument such as this may be valid if a continuous PSD was concerned, however, most activated carbons and carbon molecular sieves have varied distributions that depend on the precursor material and its successive treatments [31,32]. To show that the MEA does not result in the creation of unrealistic pore size regions, simulated adsorption data based on a model microporous solid with a continuous distribution of pore sizes were analyzed using the MEA.

Simulated Adsorption Isotherms

Simulated adsorption data. Adsorption data were generated by using a series of n_i and K_i values with a set of equilibrium pressures and Equation 2.3. The worst-case scenario, with respect to the MEA, would be an even distribution of pore sizes consisting of an equal number of pores in each pore size region, that is, all n_i values are equal. In this case, the n_i values were arbitrarily set to 1 millimole. Since $-\Delta H_i$ and $-\Delta S_i$ should not vary significantly over the temperature ranges studied, it is possible to calculate K_i values using Equation 2.4. A continuum was estimated by setting i equal

$$\ln K_i = \frac{-\Delta H_i}{RT} + \frac{\Delta S_i}{R} \quad (2.4)$$

to 10. The slope in Equation 2.4 ($-\Delta H_i / R$) was varied such that the difference between $-\Delta H_i$ and $-\Delta H_{i+1}$ was 0.5 Kcal·mole⁻¹ starting with a value of 6.46 Kcal·mole⁻¹ for $-\Delta H_1$. In the analysis of methane adsorption by BPL, it was observed that $-\Delta S_i$ decreased linearly with i so the ΔS_i used followed this trend. The value used for ΔS_1 was -18.42 cal·mole⁻¹·K⁻¹ with the remaining values incremented by +0.40 cal·mole⁻¹·K⁻¹. The choice of starting values determines the “width” between successive pore size regimes. A difference between $-\Delta H_i$ values of less than 0.5 Kcal·mole⁻¹ and an i greater than ~10 would require more computing power than available and should not yield, for the purpose of this study, significantly different results.

Analysis of simulated data. To reiterate, each Process obtained from the MEA refers to a distribution of pore sizes with K_i 's so close in magnitude

that the accuracy of the experimental measurements preclude further resolution. The concern is that the MEA arbitrarily breaks-up a continuous pore size distribution (PSD) with varying binding affinities into two or three groups of pores. When the simulated adsorption data was arbitrarily split into larger regions (fit to a smaller number of Processes than were used to generate the data) errors resulted in the n_i 's of the latter Processes that were greater than the actual value of the parameter. Large errors resulted even when eight Processes were used to fit the data generated from the ten Process assumption.

Large errors were also encountered in the data points, especially the low-pressure points in the higher temperature data sets resulting in unacceptable standard deviations in the Process I parameters. Since similar behavior is not observed in the fits of the experimental data, it suggests that these solids do not have continuous PSDs, but instead consist of discrete regions separated by gaps that are resolvable by the MEA. The gaps in the distribution could consist of a very small number of intermediate pore sizes. A solid with a true continuous PSD would require a large number of Processes to obtain a satisfactory fit of the experimental data, which has not been observed in any of our studies to date.

A conclusion that may be drawn from the analysis of the simulated adsorption data is that the MEA does not arbitrarily divide a continuous PSD. In fact, for a heterogeneous distribution as is observed in most

activated carbon materials, it is possible to resolve discontinuities in the distribution.

Monte Carlo Simulation and Sensitivity Analysis

Also of concern was the sensitivity of the calculated moles adsorbed to the errors in the parameters used to calculate these values. The following discussion is based on the results of several Monte Carlo simulations involving the MEA.

Simulations. All simulations were run using Crystal Ball® version 4.0c (Decisioneering, Inc., Denver, CO), a forecasting and risk analysis plug-in for Microsoft Excel. Each simulation was run by first creating an appropriate model in an Excel worksheet (each model will be described in the appropriate section). It was assumed that the variable parameters used in the models had errors that were normally distributed. The error limits used were either those from an associated MEA or a fixed percentage of the parameter values used. The limits in computational speed and available computer memory, required that simulations be limited to 100,000 individual calculations, which should be sufficient for the purpose of the following discussion.

Sensitivity of K . The first set of simulations involved the sensitivity of $\ln K_i$ (or ΔG_i) to changes in ΔH_i and ΔS_i , Table 2.4. The spreadsheet model calculated $\ln K_i$ values from given values of ΔH_i and ΔS_i , in $\text{cal}\cdot\text{mole}^{-1}$ and $\text{cal}\cdot\text{mole}^{-1}\cdot\text{K}^{-1}$, respectively, and temperatures in K. Simulations were run using the values for ΔH_i and ΔS_i (and their associated errors) obtained from

Table 2.4: Sensitivity Analysis for Methane Adsorption by F300 measured as percent (%) contribution to the variance in the free energy (ΔG) using the experimental errors in ΔH_i and ΔS_i .

Process (°C)	Parameter Error							
	experimental		5%		10%		25%	
	ΔH	ΔS	ΔH	ΔS	ΔH	ΔS	ΔH	ΔS
I (-82)	52.7	47.3	76.2	23.8	76.0	24.0	76.2	23.8
(-62)	47.3	52.7	72.1	27.8	71.9	28.1	72.1	27.9
(-43)	42.8	57.2	68.4	31.6	68.2	31.8	68.3	31.7
(-16)	37.2	62.8	63.2	36.8	63.0	37.0	63.1	36.9
II (-82)	57.6	42.4	67.5	32.5	67.9	32.1	67.2	32.8
(-62)	52.3	47.7	62.7	37.3	63.0	37.0	62.4	37.6
(-43)	47.8	52.2	58.4	41.6	58.8	41.2	58.1	41.9
(-16)	42.0	58.0	52.7	47.3	53.0	46.9	52.3	47.6
III (-82)	43.0	57.0	55.4	44.6	55.4	44.6	55.3	44.7
(-62)	37.8	62.2	50.1	49.9	50.0	50.0	49.9	50.1
(-43)	33.7	66.3	45.6	54.4	45.5	54.5	45.4	54.6
(-16)	28.7	71.3	39.9	60.1	39.8	60.2	39.7	60.3

the MEA of methane adsorption by F300. Simulations were also run using 5, 10, and 25% errors for ΔH_i and ΔS_i . The temperatures used were -82.6°C (the critical temperature of methane) and -62 , -43 , and -16°C , which were experimental temperatures. As expected, the influence of ΔS_i increases with temperature and is most influential in Process III. However, increased error in the parameters does not appear to affect the total contribution to the variance of $\ln K_i$.

Sensitivity in calculation of moles adsorbed. The second set of simulations was used to investigate the sensitivity of the calculated moles adsorbed, from Equation 2.3, to changes in ΔH_i , ΔS_i , and n_i as a function of temperature and pressure. Again, the assumption was made that the errors in ΔH_i , ΔS_i , and n_i are normally distributed and their values were taken from the MEA of methane adsorption by F300. The errors from the MEA, and 5 and 10% of the parameters were used as errors in the simulations. The spreadsheet model consisted of using ΔH_i , ΔS_i , and n_i with Equation 2.3 and selected equilibrium pressure points to calculate values for moles adsorbed. The parameters and pressure points used are shown in Table 2.5.

Figures 2.10 – 2.13 show the percent contribution to the variance in the moles adsorbed at -82.6 , -62 , -43 , and -16°C , respectively, using the MEA errors for ΔH_i , ΔS_i , and n_i . At -82.6°C , the low pressure region is dominated by Process II and the contribution of n_3 increases with pressure. Moving to higher temperatures, the influence of each Process shifts to higher pressure.

Table 2.5: Parameters determined for Methane Adsorption by F300. ΔH_i , ΔS_i , and n_i (and their associated experimental errors) are used in the simulation at the given temperature at each pressure.

Parameter Values			
T:	-82.6°C		
i:	I	II	III
ΔH_i :	-6000	-5100	-4000
\pm :	200	200	100
ΔS_i :	-18	-18.8	-18.9
\pm :	1	0.9	0.6
n_i :	0.000332	0.00127	0.0045
\pm :	0.000005	0.00004	0.0004
K_i :	886.55	55.035	2.8653
Equilibrium Pressure Points			
PRESSURE	PRESSURE	CALC MOLS	
(mmHg)	(atm)	(n/g STP)	
1.00	1.31579E-3	2.81416E-4	
3.00	2.63158E-3	4.26731E-4	
3.00	3.94737E-3	5.35200E-4	
4.00	5.26316E-3	6.25501E-4	
6.00	7.89474E-3	7.74702E-4	
2.00	1.05263E-2	8.97471E-4	
10.00	1.31579E-2	1.00268E-3	
12.00	1.57895E-2	1.09512E-3	
12.00	1.84211E-2	1.17780E-3	
18.00	2.36842E-2	1.32153E-3	
22.00	2.89474E-2	1.44444E-3	
26.00	3.42105E-2	1.55258E-3	
30.00	3.94737E-2	1.64970E-3	
40.00	5.26316E-2	1.85880E-3	
50.00	6.57895E-2	2.03529E-3	
60.00	7.89474E-2	2.18986E-3	
80.00	1.05263E-1	2.45427E-3	
100.00	1.31579E-1	2.67713E-3	
120.00	1.57895E-1	2.87029E-3	
150.00	1.97368E-1	3.11860E-3	
200.00	2.63158E-1	3.45303E-3	
250.00	3.28947E-1	3.71782E-3	
300.00	3.94737E-1	3.93352E-3	
350.00	4.60526E-1	4.11294E-3	
400.00	5.26316E-1	4.26468E-3	
450.00	5.92105E-1	4.39476E-3	
500.00	6.57895E-1	4.50754E-3	
550.00	7.23684E-1	4.60628E-3	
600.00	7.89474E-1	4.69346E-3	
650.00	8.55263E-1	4.77101E-3	
700.00	9.21053E-1	4.84045E-3	
750.00	9.86842E-1	4.90299E-3	

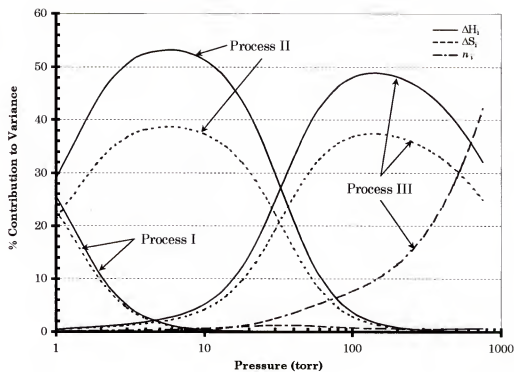


Figure 2.10: Percent Contribution to Variance in moles adsorbed versus Pressure for Methane Adsorption by F300 at -82.6°C (experimental errors are used for ΔH_i , ΔS_i , and n_i in the simulation).

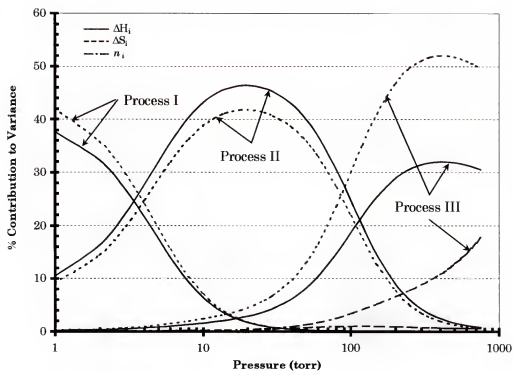


Figure 2.11: Same as 2.10 except at -62°C .

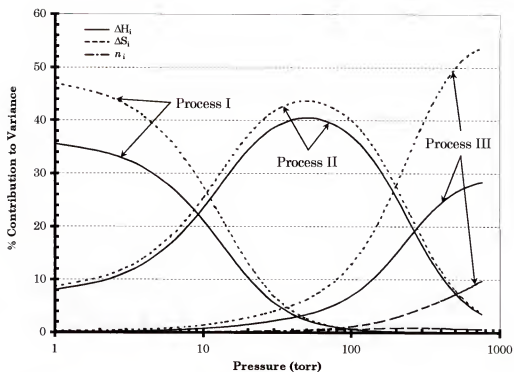


Figure 2.12: Same as 2.10 except at -43°C .

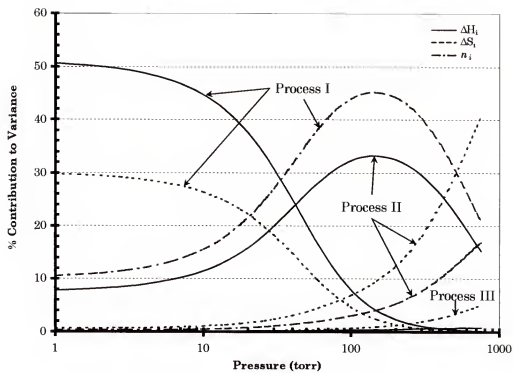


Figure 2.13: Same as 2.10 except at -16°C .

At -16°C , Process I is dominate and the influence of Process III is negligible. Process I is best defined at higher temperatures while Process III can only sufficiently defined by including adsorption data collected near the critical temperature of the adsorptive. The analysis also suggests the importance of each parameter for predicting the adsorption of a new adsorptive on a MEA characterized solid. Specifically, the quantities associated with Processes II and III are most important at temperatures approaching the critical temperature of the adsorptive. The influence of the Process I parameters is greatest at higher temperatures. Thus, an estimate of model parameters must take the temperature into account when predicting adsorption parameters.

In addition to the sensitivity data, the mean and standard deviation of the calculated moles adsorbed can be obtained from the simulations. Figure 2.9 shows the experimental and simulated adsorption isotherms for methane adsorption by F300. The error bars on the simulated isotherm reflect the standard deviation in the data point as determined from the simulation. The median values for each point are actually closer to the experimental values. The median values are closer because the distribution in moles adsorbed at each pressure is skewed by the natural logarithm function in the calculation of K . This skewness increases with temperature but decreases with increasing pressure.

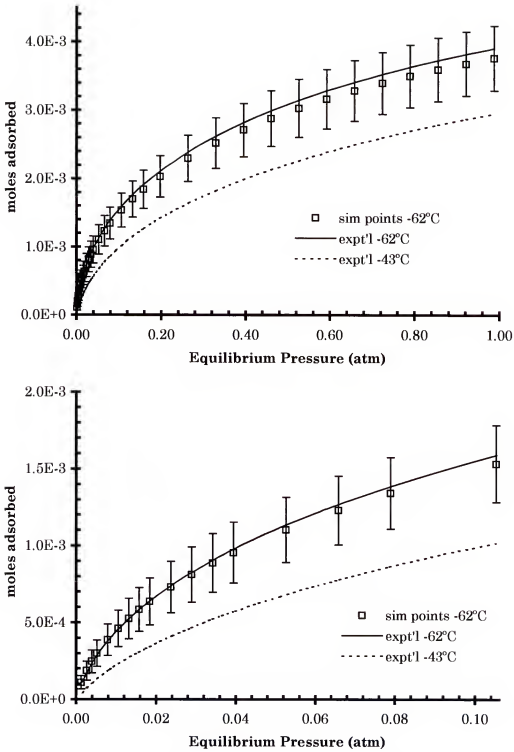


Figure 2.9: Experimental and simulated adsorption isotherms for methane adsorption by F300. Points are simulated points and lines are experimental isotherms.

The significance of the Monte Carlo simulations is that it demonstrates the importance of each of the parameter values to the calculation of an adsorption isotherm. K values were modeled using ΔH and ΔS values because they will be predicted from the correlation of adsorptive properties, namely the van der Waals a constant to $-\Delta H$.

The MEA Surface Area and Pore Volume

The meaning of surface area has been debated for some time. The widely used BET method has been the standard for determining this property of adsorbents and catalysts but its limitations and effectiveness have been questioned since its introduction [1]. A benefit of the MEA is that surface areas and pore volumes with meaningful interpretations can be established.

The n_i 's determined from the MEA are a direct measure of the capacity (total maximum occupancy) of the different pore size regimes in a given porous solid. As such, they can be manipulated to represent meaningful surface areas and pore volumes once these quantities are defined. *Surface area* is the sum of the areas occupied by a molecule such that no other molecule can occupy the same space. It is assumed that the orientation of the molecule on the surface is one that maximizes the dispersion interaction between the molecule and the surface, and the area of the surface measured is that covered by a projection of the dimensions of the adsorptive molecule on the surface. The MEA surface area represents the accessible area, which will vary with the adsorptive used as each uses a different set of pores. Since all

adsorption measurements were conducted above the critical temperature of the adsorptive, multilayer formation and capillary condensation are not involved in the MEA Processes and a monolayer condition is assumed within the pores and on the surfaces of the solid.

A problem one encounters when calculating surface areas and pore volumes is in finding realistic estimates of molecular sizes and volumes [90,95]. Conflicting or missing literature values of molecular sizes and volumes have lead to the calculation of these quantities using quantum mechanics [90]. When surface areas and pore volumes are calculated using the calculated values for molecular area and volume, Tables 2.6 and 2.7, one gains a realistic view of, at least, the minimum value of these quantities for a given solid. It should also be obvious that for a material with a distribution of pores, as with the microporous carbons studied here, the surface area is dependent on the adsorptive molecule used. In our work with zeolites with their defined pore structures, the areas determined using the different adsorptives agreed within experimental error [96].

A comparison of the five carbons studied here can be made on the basis of the MEA surface areas. Figure 2.14 shows the total MEA surface area for each solid as a function of adsorptive. Notice that while the methane MEA area is close to the BET value, the N_2 areas for the two methods do not agree. It is also apparent from Figure 2.14 that the surface area is dependent on the

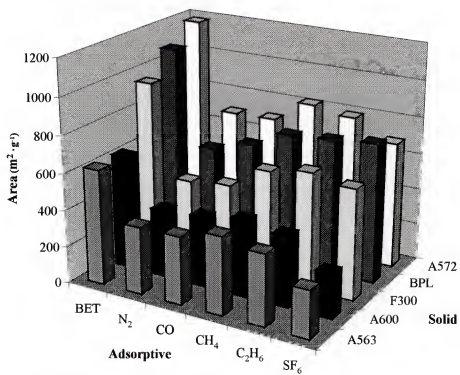


Figure 2.14: MEA surface area comparison.

adsorptive used and that an estimation of the PSD for each solid can be obtained.

Comparing A563 and A600, based on surface area, one finds that these two materials indeed have similar pore structures. The agreement extends through the Process resolved surface areas (the area that corresponds to each Process) and the total areas in Table 2.6, but the thermodynamic comparison will show slight differences in these materials. The similarity of the surface areas and the differences shown by the thermodynamic comparison gives further support for the necessity of a thermodynamic as well as physical characterization of porous materials.

Comparing BPL to A572 and F300 also reveals the differences in these materials. BPL shows a steady increase in surface area as the adsorptive size increases, indicating a rather broad distribution of pores up to $\sim 10\text{\AA}$ in width. A572, on the other hand, has larger total areas than BPL, but also shows a maximum at methane followed by a decrease in area with increasing adsorptive size. This shows a narrow distribution of pore sizes in A572. Finally, in the case of F300, the lower surface areas indicate a smaller number of pores of the appropriate size for adsorption of each adsorptive, but a maximum is reached with methane again suggesting a narrow distribution of pore sizes.

In a manner analogous to the surface area calculation, the n_i 's can be used with the adsorptive molar volume to get the accessible pore volume, Table

2.7. The MEA calculation of pore volume requires no assumption about molecular packing and results in a measure of the “usable” space within the pores. Pore volume is an important quantity when selecting a porous material for a specific application. Figure 2.15 shows the comparison of the total pore volumes for each solid as a function of adsorptive. Notice that in all instances the MEA volume is significantly less than the micropore volume determined from the H-J t-plot using the N_2 isotherm at 77K. MEA gives a more realistic view of the usable space in a solid that other methods do not provide.

The Enthalpy of Adsorption

The enthalpy of adsorption (ΔH_{ads}) determined from MEA depends on the average width of the pore size regime used by the specific Process. Additionally, the wider the distribution about the average, the greater the observed error in $-\Delta H_{ads}$. In this way, the $-\Delta H_{ads}$ and its associated error reflect the average pore size and its distribution for a given Process and adsorptive. Enthalpy and entropy data for the solids and adsorptives studied are presented in Tables 2.8 and 2.9, respectively, and will be used to compare different carbons in these terms.

An comparison of the physical properties of the adsorbents (Table 2) suggests that the synthetic adsorbents A563 and A600 are very similar, which was also supported by the analysis of MEA surface areas. Each has a BET area of about $625 \text{ m}^2\cdot\text{g}^{-1}$ and a t-plot micropore volume of $\sim 0.23 \text{ ml}\cdot\text{g}^{-1}$.

Table 2.6: MEA resolved surface areas in $\text{m}^2\cdot\text{g}^{-1}$.

N₂	A563	A572	A600	BPL	F300
I:	29.1	42.6	32.1	19.3	21.2
II:	125.2	164.6	127.5	91.0	89.6
III:	211.5	490.7	210.1	452.5	343.4
Total:	365.8	697.8	369.7	562.8	454.2
CO	A563	A572	A600	BPL	F300
I:	32.5	54.9	54.9	31.7	23.9
II:	101.0	182.1	121.4	119.1	91.1
III:	235.4	465.6	210.5	475.5	362.8
Total:	368.9	702.6	382.9	626.3	477.8
CH₄	A563	A572	A600	BPL	F300
I:	50.4	75.9	48.9	34.1	32.5
II:	164.3	215.2	167.6	125.9	124.3
III:	209.7	530.3	199.4	559.8	443.8
Total:	424.4	821.4	415.9	719.8	600.6
C₂H₆	A563	A572	A600	BPL	F300
I:	47.6	45.9	39.4	27.9	28.8
II:	156.9	205.7	159.1	121.4	125.9
III:	183.4	537.8	183.1	585.6	483.9
Total:	387.9	789.4	386.6	734.9	638.6
SF₆	A563	A572	A600	BPL	F300
I:	20.5	30.9	10.3	20.7	24.0
II:	113.1	188.6	99.2	136.5	128.8
III:	124.7	468.1	133.8	599.8	448.2
Total:	258.3	687.7	243.3	757.0	601.0

Table 2.7: MEA resolved pore volumes in mL·g⁻¹.

N₂	A563	A572	A600	BPL	F300
I:	0.0079	0.0116	0.0087	0.0052	0.0058
II:	0.0341	0.0448	0.0347	0.0248	0.0244
III:	0.0575	0.1335	0.0572	0.1231	0.0934
Total:	0.0995	0.1898	0.1006	0.1531	0.1236
CO	A563	A572	A600	BPL	F300
I:	0.0097	0.0164	0.0152	0.0094	0.0071
II:	0.0301	0.0542	0.0362	0.0355	0.0271
III:	0.0701	0.1386	0.0627	0.1416	0.1080
Total:	0.1098	0.2092	0.1140	0.1865	0.1422
CH₄	A563	A572	A600	BPL	F300
I:	0.0153	0.0231	0.0148	0.0103	0.0099
II:	0.0499	0.0653	0.0509	0.0382	0.0378
III:	0.0637	0.1610	0.0606	0.1700	0.1348
Total:	0.1289	0.2494	0.1263	0.2186	0.1824
C₂H₆	A563	A572	A600	BPL	F300
I:	0.0155	0.0152	0.0129	0.0091	0.0094
II:	0.0512	0.0671	0.0519	0.0396	0.0411
III:	0.0599	0.1756	0.0614	0.1912	0.1580
Total:	0.1266	0.2577	0.1262	0.2399	0.2085
SF₆	A563	A572	A600	BPL	F300
I:	0.0084	0.0127	0.0042	0.0085	0.0098
II:	0.0464	0.0774	0.0407	0.0560	0.0528
III:	0.0512	0.1921	0.0549	0.2461	0.1839
Total:	0.1060	0.2822	0.0999	0.3106	0.2466

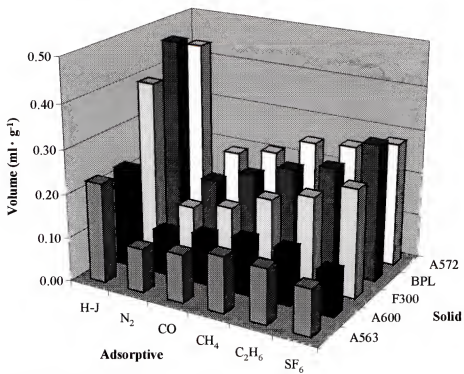


Figure 2.15: MEA pore volume comparison.

MEA, however, shows that these two materials are different. Nitrogen adsorption indicates that the Process I pores used by A600 are slightly smaller than those used by A563 (a $-\Delta H_1$ of 5.07 versus 4.66 kcal·mole⁻¹, respectively). Carbon monoxide, which is slightly larger than N₂, shows a greater ΔH_1 for A563 even though N₂ adsorption suggests a greater number of small pores in A600. This suggests the possibility of a specific interaction in A563 that would account for the difference in pore size. In terms of methane adsorption, these materials are identical.

Nitrogen, carbon monoxide, and methane have similar areas and molar volumes that limit their usefulness for providing differences in pore structure. Ethane and sulfur hexafluoride are larger than the other molecules studied and each will use a different portion of the PSD of each carbon. Continuing the comparison of A563 and A600, one finds a 0.7 and 0.5 kcal·mole⁻¹ difference in ΔH_1 for ethane and SF₆, respectively. In the case of ethane, A600 shows the larger ΔH_1 , which suggests a closer match of pore dimension to adsorptive size. However, SF₆ shows a larger ΔH_1 for A563. Clearly the deviations in the PSDs of the two materials is shown as larger adsorptives are used.

Similar observations can be made with the comparisons of BPL to F300 and A572. BPL and A572 have similar BET areas and H-J t-plot micropore volumes but differ synthetically, BPL is coal derived and A572 is made by the controlled pyrolysis of a synthetic resin. BPL and F300 are both coal derived

Table 2.8: Enthalpy of Adsorption in Kcal·mole⁻¹.

N ₂	-ΔH ₁	±	-ΔH ₂	±	-ΔH ₃	±
<i>A563</i>	4.64	0.03	4.2	0.4	3.59	0.02
<i>A572</i>	4.8	0.1	4.3	0.3	2.9	0.3
<i>A600</i>	5.0	0.2	4.38	0.08	3.8	0.4
<i>BPL</i>	5.1	0.2	4.3	0.2	3.4	0.2
<i>F300</i>	4.94	0.08	4.2	0.1	3.11	0.08
CO	-ΔH ₁	±	-ΔH ₂	±	-ΔH ₃	±
<i>A563</i>	6.0	0.4	4.48	0.07	3.4	0.4
<i>A572</i>	5.29	0.03	4.33	0.06	3.47	0.06
<i>A600</i>	5.6	0.2	4.55	0.01	3.8	0.2
<i>BPL</i>	5.14	0.08	4.19	0.01	3.26	0.02
<i>F300</i>	5.3	0.2	4.6	0.2	3.43	0.08
CH ₄	-ΔH ₁	±	-ΔH ₂	±	-ΔH ₃	±
<i>A563</i>	6.2	0.2	5.0	0.4	4.9	0.2
<i>A572</i>	6.0	0.6	4.9	0.4	3.9	0.5
<i>A600</i>	6.2	0.4	5.1	0.3	4.9	0.3
<i>BPL</i>	5.7	0.4	5.1	0.4	3.8	0.3
<i>F300</i>	6.0	0.2	5.1	0.2	4.0	0.1
C ₂ H ₆	-ΔH ₁	±	-ΔH ₂	±	-ΔH ₃	±
<i>A563</i>	8.5	0.7	7.6	0.3	7.3	0.4
<i>A572</i>	10.0	0.6	8.1	0.3	6.7	0.4
<i>A600</i>	9.2	0.2	7.6	0.1	7.5	0.1
<i>BPL</i>	7.5	0.4	6.4	0.7	4.9	0.6
<i>F300</i>	8.7	0.3	7.3	0.3	5.8	0.2
SF ₆	-ΔH ₁	±	-ΔH ₂	±	-ΔH ₃	±
<i>A563</i>	9.3	0.2	7.6	0.2	7.6	0.2
<i>A572</i>	5.0	0.5	7	0.3	7	1
<i>A600</i>	9	1	6.6	0.2	5.7	0.2
<i>BPL</i>	9.9	0.6	7.3	0.8	6.3	0.1
<i>F300</i>	9.3	0.4	7.3	0.4	5.9	0.6

Table 2.9: Entropy of Adsorption in cal·mole⁻¹·K⁻¹.

N ₂	-ΔS ₁	±	-ΔS ₂	±	-ΔS ₃	±
<i>A563</i>	17.3	0.3	18.7	0.5	19.71	0.09
<i>A572</i>	17.7	0.6	20	2	17	1
<i>A600</i>	19	1	19.4	0.4	20.7	0.7
<i>BPL</i>	18.9	0.3	19.2	0.3	18.9	0.5
<i>F300</i>	17.8	0.4	18.3	0.6	17.2	0.4
CO	-ΔS ₁	±	-ΔS ₂	±	-ΔS ₃	±
<i>A563</i>	22	2	18.2	0.3	16	2
<i>A572</i>	18.7	0.5	18.7	0.3	18.7	0.3
<i>A600</i>	20.7	0.3	19.30	0.02	18.9	0.7
<i>BPL</i>	18.1	0.4	18.02	0.07	18.9	0.4
<i>F300</i>	18.3	0.9	19	1	17.8	0.4
CH ₄	-ΔS ₁	±	-ΔS ₂	±	-ΔS ₃	±
<i>A563</i>	19.2	0.3	20.0	0.7	22.5	0.7
<i>A572</i>	19	2	19	2	19	2
<i>A600</i>	19	2	20	1	23	1
<i>BPL</i>	17	2	18.9	0.7	17	1
<i>F300</i>	18	1	18.8	0.9	18.9	0.6
C ₂ H ₆	-ΔS ₁	±	-ΔS ₂	±	-ΔS ₃	±
<i>A563</i>	18	2	19.6	0.3	23	1
<i>A572</i>	22	2	20	1	21	1
<i>A600</i>	19.8	0.6	20.0	0.3	23.7	0.4
<i>BPL</i>	19	1	16	2	14	2
<i>F300</i>	18.1	0.9	18.2	0.9	18.7	0.6
SF ₆	-ΔS ₁	±	-ΔS ₂	±	-ΔS ₃	±
<i>A563</i>	19.8	0.7	18.9	0.6	23.3	0.6
<i>A572</i>	17	1	16	1	20	3
<i>A600</i>	17	3	15.2	0.6	17.4	0.5
<i>BPL</i>	21	2	18	2	19.6	0.4
<i>F300</i>	19	1	18	1	18	2

applications, gas-phase and liquid-phase, respectively. Again, the differences in the materials is not significant for N_2 , CO , or CH_4 adsorption, but ethane and SF_6 reveal differences. The difference between ethane adsorption in BPL and A572 is $2.74 \text{ kcal}\cdot\text{mole}^{-1}$ in favor of A572 while SF_6 shows a difference of $1.47 \text{ kcal}\cdot\text{mole}^{-1}$ in favor of BPL. This shows the difference in the PSDs and, more importantly, that A572 has a more narrow distribution of pore sizes. This is also supported by the smaller difference between the SF_6 ΔH_1 and ΔH_3 values, $2.01 \text{ kcal}\cdot\text{mole}^{-1}$ for A572 versus 3.81 for BPL.

Comparing BPL and F300 shows many similarities in the two materials. In terms of N_2 , CO , and CH_4 , BPL and F300 are identical, and the $-\Delta H_i$ values for C_2H_6 and SF_6 are very similar. The similarity of the two materials suggests that they have comparable pore structures with BPL having a larger overall capacity. These simple comparisons show that small differences in molecular size can yield striking differences in PSDs.

Prediction of Adsorption Isotherms

To date, there is no model that permits even an empirical prediction of an adsorption isotherm for an adsorptive not specifically investigated using the model [97,98]. The prediction of an adsorption isotherm is one of the specific goals in the development and use of the MEA. A plot of the $-\Delta H_i$'s (or $-\Delta G_i$'s) determined using the MEA versus the square root of the van der Waals a constants ($a^{1/2}$) for the adsorptives studied yields a straight line, Figures 2.16 - 2.18. Given the a constant for an new adsorptive, which can be calculated

from the critical constants of the adsorptive [91], values for ΔH_i can be predicted. Figure 2.16 Shows a $-\Delta H_i$ versus $\alpha^{1/2}$ plot for N_2 , CO, CH_4 , C_2H_6 , and SF_6 adsorption by F300 (∇ 's). Also shown are the $-\Delta H$ values for the adsorption of the same gases on a nonporous solid [58]. First, the correlation suggests that, barring significant $-\Delta S$ contributions, $-\Delta H$ is linearly dependent on $\alpha^{1/2}$. Second, it shows that the MEA parameters have physical meaning in terms of the model. The black triangle in Figure 2.16 is the calculated $-\Delta H_{np}$ for SF_6 adsorption by a nonporous reference carbon using the best fit line of the N_2 , CO, CH_4 , and C_2H_6 values. With a reasonable estimate of ΔS_i , K_i values for the adsorption of the new adsorptive at a specific temperature can be calculated.

It may also be possible to predict K_i values from the correlation of $\ln K_i$ (or ΔG_i) to $\alpha^{1/2}$ as shown in Figures 2.17 and 2.18. This correlation requires the calculation of $\ln K_i$ values from appropriate $\ln K_i$ versus T^{-1} plots and that the entropy terms within the $\ln K_i$ values are consistent. In either case, the total adsorption isotherm can only be predicted if acceptable n_i values can be predicted. One method currently being investigated for predicting n_i values is the interpolation and extrapolation of n_i 's using adsorptive molar volumes. Another is based on using the MEA derived pore size distribution (MEA-PSD) and the critical dimensions of the adsorptives. The MEA-PSD will be introduced in the next chapter.

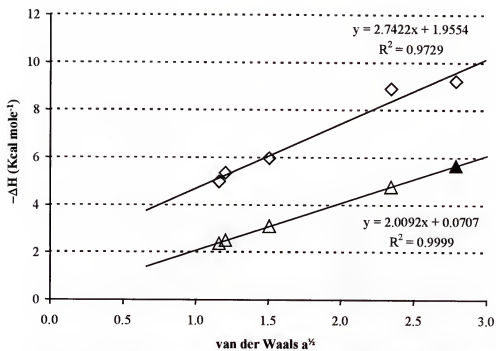


Figure 2.16: $-\Delta H_1$ versus van der Waals $a^{1/2}$ for F300. The solid triangle is the predicted value for SF_6 .

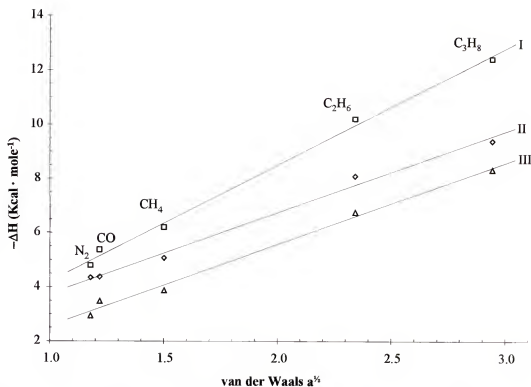


Figure 2.17: Correlation of the enthalpies of adsorption on A572 with the square root of the van der Waals a constant for the adsorptive. Process I is represented by \square , with \diamond and Δ representing process II and III, respectively. The equations for the best fit lines along with the associated R^2 values for Processes I-III are given as follows: $y=4.30x-0.101$, $R^2=0.996$; $y=3.00x+0.751$, $R^2=0.992$; $y=3.01x-0.454$, $R^2=0.993$.

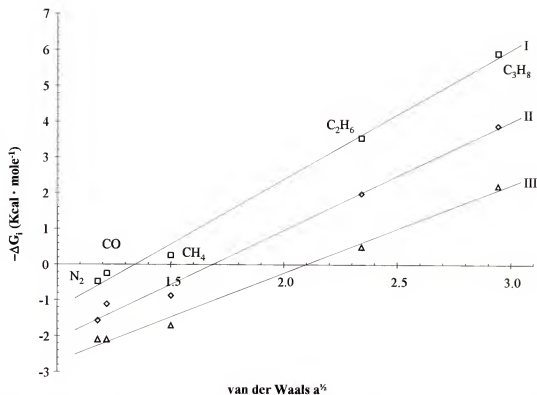


Figure 2.18: The free energies of adsorption on A572 at 25°C versus the square root of the van der Waals a constant for each adsorptive. Process I is represented by \square , with \diamond and Δ representing Process II and II, respectively. The equations for the best fit lines along with the associated R^2 values for Process I-III are given as follows: $y=3.63x-4.87$, $R^2=0.995$; $y=3.04x+5.13$, $R^2=0.991$; $y=2.47x-5.18$, $R^2=0.992$.

Concluding Remarks

The utility of the multiple equilibrium analysis (MEA) has been shown for the thermodynamic and physical characterization of porous carbonaceous materials. The thermodynamic characterization reveals differences in materials that are not readily apparent when traditional physical characterization techniques are used, for example, BET. The physical quantities that result from the n_i 's (surface area and pore volume) have been shown to be more realistic estimates than provided by other methods. Specifically, these values represent "usable" space within these materials.

The $-\Delta H_i$ values determined using the MEA make it possible to predict adsorption equilibrium constants based on a physical characteristic of an adsorptive molecule, the van der Waals α constant. The ability to predict an entire adsorption isotherm will result when the n_i values can be predicted in a reliable fashion from a MEA derived pore size distribution (MEA-PSD).

CHAPTER 3

THE MEA PORE SIZE DISTRIBUTION (MEA-PSD)

The pore size distribution (PSD) for a porous material is an essential piece of information for selecting a material for a specific application. With crystalline materials such as zeolites, the width of the distribution is narrow and the average pore size(s) can be determined from crystallography [1,31]. The determination of pore sizes is a little more difficult for amorphous materials, for example, carbons, silicas, and aluminas, which usually have a wide distribution of pore sizes [1]. Different methodologies have been developed to determine PSDs and each has advantages and potential shortcomings. The focus of this chapter will be to examine a few of the current methods for determining PSDs and to introduce a method that takes advantage of the information provided by the MEA.

Heterogeneity and PSDs

Activated carbons, in general, contain a distribution of pore sizes. As was mentioned in Chapter 2, the driving force for adsorption in these pores is the addition of potential fields that exists between the opposite walls of slit-shaped pores, which are dominate in activated carbon materials. Everett and Powl have shown that the maximum enhancement from the addition of potential fields, versus adsorption on a single graphitic plane, occurs in slit-

shaped pores roughly 1 molecular diameter in width [10]. At widths greater than ~ 2 molecular diameters, the enhancement is negligible and adsorption approaches that on a single graphitic surface, refer to Figure 2.2.

Others have proposed potential functions for adsorption in slit-shaped pores with Everett and Powl's 10-4 potential as the basis of many of them [34,99]. Closely resembling Everett and Powl's 10-4 potential is that used by Horvath and Kawazoe [61] and later, Mariwala and Foley [64]. Steele's 10-4-3 potential is a better approximation of the potential function and has been used in recent work using Monte Carlo simulation to determine PSDs [100-102]. Some of the elegance of these models comes with a price, however. Specifically, a potential function must be chosen that may or may not justly describe the interactions encountered [103-106].

Determining PSDs

Jaroniec, et.al., have examined the structural heterogeneity of micropores and the surface heterogeneity of mesopores using a Γ distribution function [56,62,80,107,108]. Their PSDs are based on the relationship between micropore dimension (χ) and the characteristic energy of adsorption (ε_0). The characteristic energy ε_0 comes from the fit of experimental adsorption data to the Dubinin-Radushkevich (D-R) equation [70,72,76]. The PSD is determined by choosing an isotherm equation to approximate the adsorption occurring in the solid being studied (the local isotherm) and using it with the adsorption integral equation, Equation 3.1 [7,109]. In Equation 3.1, $F(\varepsilon)$ is the local

$$\mathcal{G}_t(P) = \int_{\Delta} \mathcal{G}(P, \varepsilon) F(\varepsilon) d\varepsilon \quad (3.1)$$

isotherm function, ε is the adsorption energy, P is the pressure, θ is the coverage, and Δ is the integration range covering all possible adsorption energies. Comparison of the calculated adsorption to the experimental isotherm allows determination of the PSD.

Gubbins, et. al., have used Density Functional Theory (DFT) to determine PSDs [63,110,111]. Their DFT method simulates adsorption in slit-like pores as a function of pressure and pore width. The simulated adsorption isotherms are combined using linear combinations to best fit the experimental isotherms giving a composite simulated isotherm. The PSD is extracted from the composite, as the widths of the pores used to simulate the adsorption are known.

The Horvath - Kawazoe Model

The use of the Horvath-Kawazoe model has become a standard method for determining PSDs of microporous materials, because it only requires the use of a single N_2 isotherm collected at 77K [61]. Since the H-K model is used as the basis for the MEA-PSD, a brief summary of its derivation follows. A complete derivation may be found in the original Horvath and Kawazoe paper or in a later paper by Mariwala and Foley [64]. Baksh and Yang have also applied the principles of the H-K model to microporous pillared clays [112].

Derivation

As mentioned in Chapter 1, the free energy change upon adsorption of an adsorptive gas by a porous solid can be expressed by Equation 3.2. The free

$$\Delta G_{\text{ads}} = \Delta H_{\text{ads}} - T\Delta S_{\text{ads}} \quad (3.2)$$

energy change can also be calculated from the equilibrium relative pressure of the gas over the solid using Equation 3.3, where R is the gas constant, T is

$$\Delta G_{\text{ads}} = RT\ln(P/P_0) \quad (3.3)$$

the experimental temperature, P is the equilibrium pressure of the adsorptive over the solid, and P_0 is the saturation pressure of the adsorptive at the experimental temperature. Combining Equations 3.2 and 3.3 results in an equation that relates the equilibrium relative pressure to the molar enthalpy and the molar entropy of adsorption, Equation 3.4.

$$RT\ln(P/P_0) = \Delta H_{\text{ads}} - T\Delta S_{\text{ads}} \quad (3.4)$$

At the molecular level the adsorption can be expressed as the contribution from the adsorbate–adsorbent interaction, U_0 , and the adsorbate–adsorbate interaction, P_a . The result is Equation 3.5. A potential function that takes

$$RT\ln(P/P_0) = U_0 + P_a \quad (3.5)$$

into account the adsorbate–adsorbent and adsorbate–adsorbate–adsorbent interactions is expressed by Equation 3.6. Equation 3.6 is derived by

$$\varphi(z) = N_{AV} \frac{N_s A_s + N_a A_a}{2\sigma^4} \left[-\left(\frac{\sigma}{z}\right)^4 + \left(\frac{\sigma}{z}\right)^{10} - \left(\frac{\sigma}{1-z}\right)^4 + \left(\frac{\sigma}{1-z}\right)^{10} \right] \quad (3.6)$$

summing the overlapping potentials from two parallel planes of carbon atoms separated by a distance z . This function assumes the pores are slit-shaped and extend to infinity in the x and y directions. In this way, the potential varies significantly only along the z -axis, the pore width. N_s and N_A are the densities per unit area of the solid atoms and the adsorbate molecules, respectively. The latter is usually determined from the liquid density of the adsorptive as it is assumed that the liquid and adsorbed states are similar. A_s and A_A are the Kirkwood-Muller dispersion constants given by Equations 3.7 and 3.8, where m_e is the mass of an electron, c is the speed of light, α and

$$A_s = \frac{6m_e c^2 \alpha_s \alpha_A}{\alpha_s + \alpha_A} \frac{\chi_s}{\chi_A} \quad (3.7)$$

$$A_A = \frac{3m_e c^2 \alpha_A \chi_A}{2} \quad (3.8)$$

χ are the polarizabilities and diamagnetic susceptibilities of the solid and adsorptive atoms, respectively. A_s corresponds to the adsorbate-adsorbent interaction while A_A refers to adsorbate-adsorbate interactions. σ is the collisional diameter or the diameter at zero interaction, recall the Lennard-Jones function in Figure 1.3. The collisional diameter is estimated in this case by Equation 3.9, where $d_0 = (d_s + d_A) / 2$ is the arithmetic mean of

$$\sigma = (2/5)^{1/6} d_0 \quad (3.9)$$

the solid and adsorptive diameters. The average potential is calculated by integrating 3.6 over the pore widths leading to Equation 3.10, which is the Horvath-Kawazoe equation.

$$RT \ln(P/P_0) = N_{AV} \frac{N_s A_s + N_A A_A}{\sigma^4 (l-d)} \left[- \left(\frac{\sigma^4}{3 \cdot \left(l - \frac{d}{2} \right)^3} \right) + \left(\frac{\sigma^{10}}{9 \cdot \left(l - \frac{d}{2} \right)^9} \right) - \left(\frac{\sigma^4}{\left(\frac{d}{2} \right)^3} \right) + \left(\frac{\sigma^{10}}{\left(\frac{d}{2} \right)^9} \right) \right] \quad (3.10)$$

In the Horvath-Kawazoe equation, l is the distance between the centers of two model graphitic planes, and d is the distance of the molecule from the surface of the planes. With each parameter on the right side of Equation 3.10 fixed, l is varied to obtain corresponding values of P/P_0 . Given the relationship between l and P/P_0 and the experimental volume adsorbed at each relative pressure, an integral pore size distribution can be obtained. The integral pore size distribution is then differentiated to obtain the more familiar pore size distribution. The final PSD is dependent on both the temperature of the adsorption experiment and the size of the adsorptive relative to the size of the pore.

Mariwala and Foley

Mariwala and Foley have adapted the Horvath-Kawazoe model to calculate PSDs from the methyl chloride adsorption isotherm collected at or near ambient temperature rather than from the nitrogen isotherm collected at 77K [64]. The advantages of CH_3Cl are that more is taken up by the solid

in the adsorption experiment, ultrahigh vacuum is not necessary, experiments can be run at ambient temperature, and ambient temperature allows shorter equilibrium times as a result of higher molecular diffusivities. Their results confirmed those of Horvath and Kawazoe and showed that molecules other than N_2 can be used to effectively characterize porous solids.

The MEA-PSD

Again, one purpose for determining a PSD is for comparing different porous solids for use in a particular application. Another reason for determining a PSD for a material is for the prediction of adsorption isotherms for an adsorptive that has not necessarily been studied on the solid of interest. The MEA is potentially useful for each of the above applications. First, MEA-PSDs are based on more than one adsorptive molecule allowing a more precise estimation of the true PSD than a single molecule allows. Second, the n_i 's determined from MEA give an indication of the number densities for adsorption in the different pore size regimes (Processes), which could lead to accurate estimations of new n_i 's based on adsorptive size. Finally, the free energies of adsorption determined from MEA are a better prediction of the sum of observed adsorbate-adsorbent and adsorbate-adsorbate interactions than the estimation methods used in other models.

MEA Extension of the Horvath – Kawazoe Model

The MEA allows the resolution of different pore size regimes based on differences in the average free energies of adsorption, $\ln K$'s, in each regime. In microporous activated carbon materials, the free energy of adsorption is proportional to the width of the pore used for adsorption. Thus, the determination of the distribution of free energies can be correlated to the distribution of pore sizes used for adsorption. The major assumptions associated with the MEA-PSD are:

1. The error in ΔG_{ads} determined from MEA directly reflects the width of the distribution of ΔG_{ads} values for the pores in each size regime.
2. The n_i 's corresponding to each ΔG_{ads} is a measure of the density of pores and thus, is the area under the curve in the distribution.

Modification of 3.10 begins with the substitution of 3.11 for 3.3 resulting in an equation relating the equilibrium constant for adsorption to pore width, Equation 3.12. The term $N_S A_S + N_A A_A$ is the estimated interaction potential

$$\Delta G_{\text{ads}} = RT \ln K_{\text{eq}} \quad (3.11)$$

$$-RT \ln K_{\text{eq}} = N_{A'} \frac{N_S A_S + N_A A_A}{\sigma^4 (l-d)} \left[- \left(\frac{\sigma^4}{3 \cdot \left(l - \frac{d}{2} \right)^3} \right) + \left(\frac{\sigma^{10}}{9 \cdot \left(l - \frac{d}{2} \right)^9} \right) - \left(\frac{\sigma^4}{\left(\frac{d}{2} \right)^3} \right) + \left(\frac{\sigma^{10}}{\left(\frac{d}{2} \right)^9} \right) \right] \quad (3.12)$$

(IP) determined from the solid and liquid adsorptive densities and the Kirkwood–Muller constants calculated from 3.7 and 3.8. The units of this

term are $\text{cal}\cdot\text{nm}^4\cdot\text{molecule}^{-1}$. The IP includes contributions from both the adsorbate–adsorbent (N_sA_s) and the adsorbate–adsorbate ($N_A A_A$) interactions. Dividing the IP by σ^4 converts the units to $\text{cal}\cdot\text{molecule}^{-1}$. This is then converted to a molar quantity by multiplying by Avogadro's number, N_{AV} , giving the units of $\text{cal}\cdot\text{mole}^{-1}$. When the IP is calculated in this way for nitrogen, methane, and sulfur hexafluoride, the resulting values are similar to the MEA ΔG_{ads} values calculated at the critical temperatures of the adsorptives. This suggests that ΔG_{ads} can be substituted into 3.12 as an appropriate approximation of the IP in the given pore size regime (Process),

$$\Delta G_{\text{ads}} = N_{AV} \frac{N_s A_s + N_A A_A}{\sigma^4} \quad (3.13)$$

$$\ln K_{eq} = \frac{-\Delta G_{\text{ads}}}{RT(l-d)} \left[- \left(\frac{\sigma^4}{3 \cdot \left(l - \frac{d}{2}\right)^3} \right) + \left(\frac{\sigma^{10}}{9 \cdot \left(l - \frac{d}{2}\right)^9} \right) - \left(\frac{\sigma^4}{\left(\frac{d}{2}\right)^3} \right) + \left(\frac{\sigma^{10}}{\left(\frac{d}{2}\right)^9} \right) \right] \quad (3.14)$$

Equation 3.13. Equation 3.14 connects the MEA equilibrium constant and pore width allowing the calculation of effective pore sizes and then the PSD.

To determine the PSD with respect to the adsorptive gas and MEA Process, assumption 1 above is used. The distribution of $\ln K$ is determined using a Monte Carlo simulation program and the MEA derived ΔH_i 's, ΔS_i 's, and their associated errors. The Monte Carlo simulation program used was Crystal Ball® (Decisioneering, Denver, CO), which is a plug-in application for use with the Microsoft Excel spreadsheet program. A spreadsheet model was constructed allowing the calculation of $\ln K_i$ from $-\Delta H_i$, $-\Delta S_i$, and

temperature. The temperature used in was the critical temperature of the associated adsorptive gas. Crystal Ball allows the choice of distribution function for the variable parameters ($-\Delta H_i$ and $-\Delta S_i$ in this case). It was assumed that the errors in $-\Delta H_i$ and $-\Delta S_i$ were normally distributed. Like most Monte Carlo simulation programs, Crystal Ball computes a value for $\ln K_i$ using randomly generated $-\Delta H_i$ and $-\Delta S_i$ values chosen from the distribution assigned for each of these variables. This is repeated for a specified number of trials, 100,000 was used in each simulation here, with each result appearing in a probability histogram to give a picture of the overall distribution in $\ln K_i$. In each case, it was found that the resulting histogram was best fit by a normal distribution function. The mean value for $\ln K_i$ and its standard distribution were taken from the fitted distribution function.

The pore width is calculated from Equation 3.14 using the $\ln K_i$ determined from the Monte Carlo simulation to get the corresponding value of l , which is found by varying l until the value of $\ln K_i$ calculated is the same as the value determined from the simulation. The PSD is calculated from the normal (Gaussian) distribution function using the associated n_i as the normalization constant. Alternatively, n_i can be converted to the accessible volume as described in Chapter 2 resulting in a pore volume distribution. The distributions from each Process/adsorptive are then overlayed to get the resulting distribution for the solid.

MEA – PSD of Selected Carbons

The MEA $\ln K_i$ distributions for A563, A600, A572, F300, and BPL are shown in Figures 3.1-3.5, respectively. Each figure shows the accessible pore volume versus $\ln K$. Nitrogen is represented by the solid line, methane by the long-dashed line, and sulfur hexafluoride is represented by the dotted line. Each process is represented going from right to left for each of the three adsorptives used.

An examination of the $\ln K$ distribution for A563, Figure 3.1, reveals a few of the features of the MEA-PSD. First is the overlap of the different $\ln K$ distributions for the adsorptives used. The Process II pores for nitrogen, the second peak from the right, overlap the Process I pores for methane. Additionally, the Process III pores for methane fall between the process II and Process II pores used by SF_6 . The successive overlap of the different Process designations for the adsorptives used shows the micropore mapping that is possible using the MEA and multiple adsorptives.

It was mentioned in Chapter 2 that A563 and A600 are very similar when compared using conventional characterization methods. This is partially confirmed by the MEA-PSDs of the two materials. Figures 3.1 and 3.2 show the features of the MEA-PSD for A563 and A600, respectively. The major difference between the two PSDs is that the widths of the peaks in the A600 distribution are greater. Additionally, it appears that the distribution of A563 increases and then levels out while that for A600 shows a maximum in

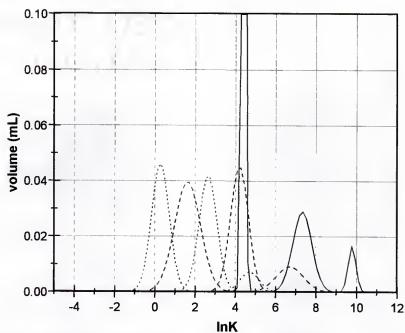


Figure 3.1: The MEA-PSD of A563, volume versus $\ln K$. Peak assignment is described in the text.

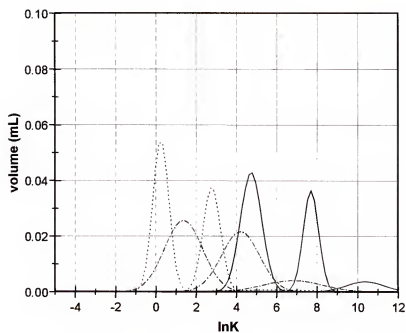


Figure 3.2: The MEA-PSD of A600, volume versus $\ln K$. Peak assignment is described in the text.

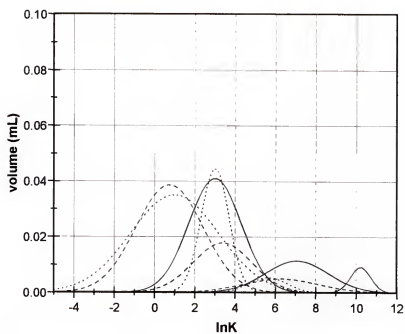


Figure 3.3: The MEA-PSD of A572, volume versus $\ln K$. Peak assignment is described in the text.

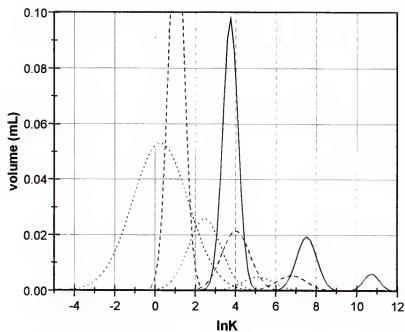


Figure 3.4: The MEA-PSD of F300, volume versus $\ln K$. Peak assignment is described in the text.

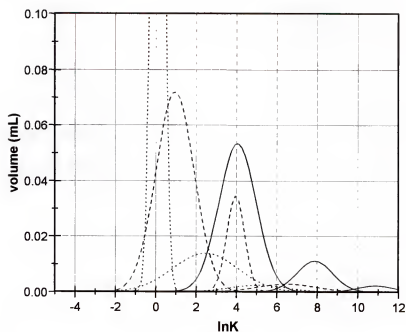


Figure 3.5: The MEA-PSD of BPL, volume versus $\ln K$. Peak assignment is described in the text.

the area of a $\ln K$ value of five. This could be confirmed by using a larger molecule that would use the same range of pores.

A563, A600, and A572 are all prepared via the controlled pyrolysis of a synthetic resin. The final pore structure depends on the starting material and the treatment the material receives during synthesis. It is clear from a comparison of Figures 3.1-3.3 (A563, A600, and A572, respectively) that A572 is probably derived from a different starting material or it received a much different synthesis treatment than the other two. Not only does A572 show a greater volume of pores, the pores are wider on average. The PSD of A572 shows that the average pore size is centered around a $\ln K$ of ~ 1.5 while the average pore size is not easily discerned from the A563 or A600 plots. The MEA-PSD of A572 shows the process overlap much better than either A563 or A600.

F300 and BPL are both coal derived carbons that show some similarity in their MEA-PSDs. While the PSD of F300 suggests a maximum at a $\ln K$ value of 2, the BPL distribution shows a steady increase in pore size through the peak for the Process III adsorption of SF_6 . Again, the use of a larger adsorptive would help to fill in the gaps in each distribution.

A comparison of A572 to BPL based on the properties presented in Table 2.2 suggest that they are similar materials, although one is synthetically derived while the other is coal derived. A comparison of Figures 3.3 and 3.5, A572 and BPL, respectively, shows that A572 has a broad distribution of

pores that go through a maximum at a $\ln K$ value of 1.5, while BPL has a broad distribution of pores that gradually increase in size. The MEA of a wide variety of different carbons may reveal that those derived from coals have a broad distribution of pores while those derived from synthetic materials have distributions that may contain a maximum volume at a particular pore size.

Predicting n_i 's from the MEA-PSD

From the MEA-PSD for a particular solid, it should be possible to predict the n_i 's for an adsorptive not previously studied on the solid. To determine the new n_i 's, it will be necessary to have the MEA-PSD in a pore volume versus pore width format and that the dimensions of the adsorptive molecule be known. The n_i 's for Processes I-III are determined by determining the available volume in the pore size regimes associated with each Process and calculating the number of moles of adsorptive that corresponds to the determined volume. The prediction of n_i 's has not been accomplished to date, but it will continue to be actively pursued.

Concluding Remarks

The goal of the Multiple Equilibrium Analysis derived Pore Size Distribution was to obtain a method for predicting n_i values for a new adsorptive on a MEA characterized solid. Although this goal has not been reached, progress has been made in its attainment. The $-\Delta H_i$'s and $-\Delta S_i$'s from the MEA have been used to find $\ln K$ distributions associated with N_2 ,

CH₄, and SF₆ adsorption on the solids studied. The use of several spherically symmetric adsorptive molecules allows the effective mapping of the micropore region, < 10 Å in width. The lnK distributions correlate to pore width and will permit the determination of a pore volume / pore width distribution. It is hoped that volume / width distribution will allow the direct calculation of n_i values for use in isotherm prediction.

CHAPTER 4

A MEA DESCRIPTION OF MULTILAYER FORMATION

With the introduction of the multiple equilibrium analysis it is possible to examine adsorption data collected at temperatures below the critical temperature (T_C) of the adsorptive rather than above it (Chapters 2 and 3). The transition from the filling of the smaller micropores to filling the larger (> 2 molecular dimensions) micropores where multiple layers of condensed adsorptive are probable is of particular interest. The purpose of the study of adsorption below T_C is not to necessarily gather information about the larger pores using the MEA, although that may be a result, but rather to gain insight into the adsorption processes that occur in the liquid phase. The adsorption of ethane and sulfur hexafluoride at temperatures below their respective critical temperatures is examined using MEA.

Multilayer Formation on a Homogeneous Surface

Figure 4.1 shows a simple representation of multiple layers of adsorptive condensed on a homogeneous surface. The first layer is characterized by a strong interaction with the surface and provides a new adsorption surface for the second layer. The layers continue to form until one layer cannot be

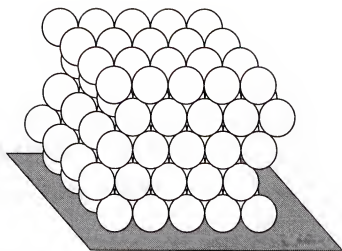


Figure 4.1: Representation of multiple adsorbed layers on a homogeneous surface.

differentiated from the previous layer and the sum of the layers resembles the bulk liquid.

Brunauer, Emmett, and Teller used the above view to derive the BET equation, described in Chapter 1 [59]. The BET equation is an adaptation of Langmuir's model that attempts to extrapolate from the last adsorbed layer, through the bulk of the fluid, to the surface layer, and extract surface area information regarding the solid. It is also possible to gain information concerning the interaction between the surface and the first adsorbed layer from the BET C constant [1,59]. However, lateral interactions between adsorbed molecules are neglected in the BET treatment, limiting the values that are obtained [1].

Other treatments of multilayer formation on homogeneous surfaces exist [111,113], but the BET is by far the most encountered model and is valid for many cases of multiple layer formation on homogeneous surfaces. Many attempts have been made to modify the BET to include lateral interactions between adsorbed molecules, but their relevance to the following discussion is limited [73,74,114].

Pore Filling and Cooperative Adsorption

Since most, if not all, of the activity of carbonaceous adsorbents is found within the microporosity of these materials, it is important that the mechanism of pore filling be understood. The volume filling micropore theory (VFMT) proposes a progressive filling of the micropore volume with the

smallest pores filling first [14]. VFMT is consistent with the definition of MEA described in Chapter 2. There are other proposed mechanisms but two in particular are significant enough to warrant further discussion, specifically, these are primary and cooperative micropore filling.

Primary micropore filling occurs in the smallest micropores with widths of ~ 1 -2 molecular diameters. The driving force for adsorption in these pores is the potential field overlap that exists between the opposite walls of the pores. Everett and Powl have shown that the maximum enhancement from this effect occurs in slit-shaped pores roughly 1 molecular diameter in width [10]. At widths greater than ~ 2 molecular diameters, the enhancement is negligible and adsorption approaches that on a single graphitic surface. The micropores associated with this mechanism range from 3 to 7\AA in width. The pores associated with primary micropore filling are associated with Processes I-III in the MEA of adsorption above T_C .

In cooperative micropore filling, Figure 4.2, a surface site adjacent to an adsorbate molecule attracts another adsorptive molecule [115,116]. The combination of the attractive potential of the surface and adsorbate effectively increases the overall potential "seen" by the adsorptive. This interaction not only involves adsorbent/adsorbate interactions but also adsorbate/adsorbate interactions and an entropic contribution. The monolayer-induced micropore filling model (MIMF) has recently been applied

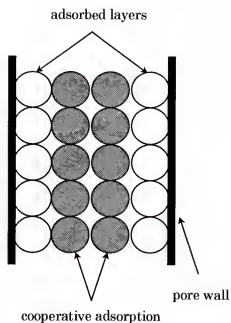


Figure 4.2: Representation of cooperative adsorption in a large micropore (~ 4 molecular diameters in width).

to cooperative micropore filling [115,116]. It postulates that a distinct monolayer forms on each of the opposite walls in slit-shaped pores that are 3-4 molecular diameters in width. Completion of these layers is described as a phase transition to a disordered solid state. The result is a pore with a width of ~ 1.2 molecular diameters. As in the primary micropore filling mechanism, the potential overlap of the walls of the pore that is now effectively 2 molecular diameters in width may enhance additional adsorption, filling the pore. In either case, adsorption of this type is restricted to larger micropores with widths between 7 and 18\AA [115,116]. It is adsorption in this size regime and the smaller mesopores that will be most important to the MEA of adsorption below T_C .

MEA Multilayers

To examine the effects of multilayer formation in microporous carbons, adsorption isotherms were collected at temperatures below the T_C of the adsorptive used. The experimental details have been outlined in Chapter 2. Isotherms were collected for ethane adsorption by A572 at 100, 70, 55, 40, 25, -16, -43, -62, and -84°C . Isotherms for sulfur hexafluoride adsorption were collected at 95, 80, 65, 50, 30, 0, and -16°C . Details of the MEA fits of the experimental data will be presented where appropriate.

Figure 4.3 shows the experimental (solid triangles) and MEA calculated adsorption isotherms for ethane adsorption by A572. At temperatures above T_C , 32.3°C for ethane, the adsorption is dominated by surface/adsorptive

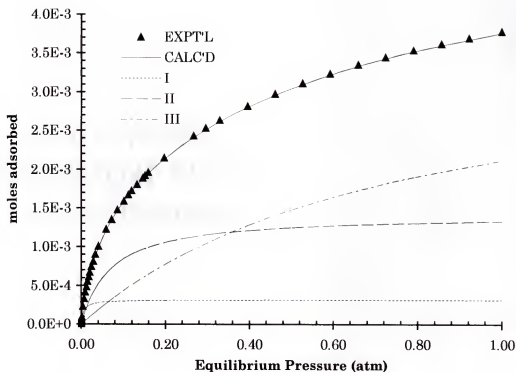


Figure 4.3: Experimental and calculated adsorption isotherms for ethane adsorption by A572 at 40°C. The Process resolved isotherms are included to show the progression to saturation. At 1 atm, Process I is >99% complete, II is 94% complete, and III is 57% complete.

interactions in the smaller micropores ($\leq \sim 2$ molecular diameters). As the temperature decreases, the adsorptive/adsorptive interactions increase, thus increasing the total adsorption more than is predicted by the MEA. The increasing adsorptive/adsorptive interaction is shown in Figure 4.4 in the form of van der Waals isotherms calculated at the experimental temperatures. The increasing minimum is a consequence of the increasing adsorptive/adsorptive interaction with decreasing temperature. The negative pressure at -84°C shows the limitations of the model.

At 7°C below the critical temperature of ethane, Figure 4.5, the adsorption predicted from the MEA of the adsorption data collected above T_C is close to that experimentally obtained. However, when the 25°C data is included in the MEA fit with the four temperature sets collected above T_C , an unacceptable fit results. Since the 25°C data does not work in the overall fit, normally data collected below the critical temperature of the adsorptive are not included in MEAs, it could be concluded that another interaction is occurring that is not present above T_C .

The "new" interaction is more visible in the lower temperature adsorption data. Figure 4.6 shows the deviation of the experimental data from the MEA calculated isotherm at -16°C . The calculated isotherms are based on the n_i 's and K_i 's obtained from the MEA of the data collected at temperatures above T_C . The K_i 's are calculated from the weighted least-squares regression of the $\ln K_i$ versus T^{-1} data.

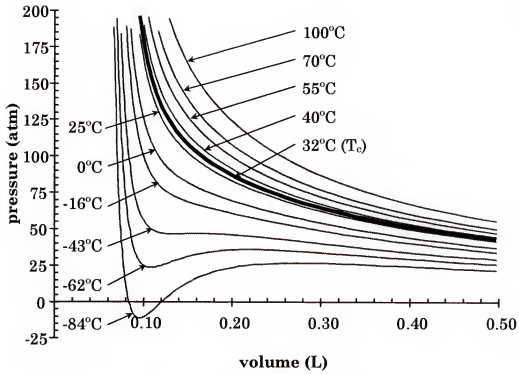


Figure 4.4: Ethane van der Waals isotherms.

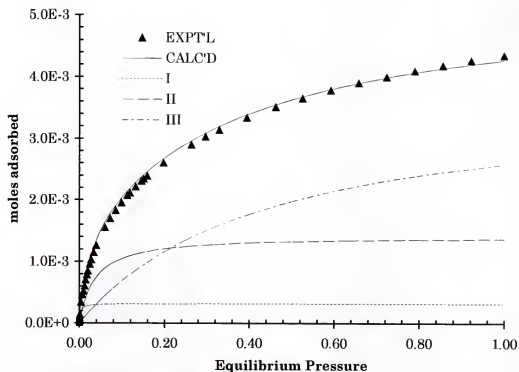


Figure 4.5: Experimental and calculated adsorption isotherms for ethane adsorption by A572 at 25°C. At 1 atm, Process I is >99% complete, II is 97% complete, and III is 70% complete.

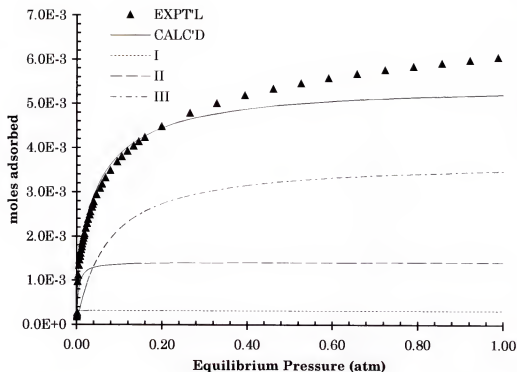


Figure 4.6: Experimental and calculated adsorption isotherms for ethane adsorption by A572 at -16°C. At 1 atm, Process I is 100% complete, II is >99% complete, and III is 93% complete.

The deviation of the calculated isotherm from the experimental isotherm has two reasonable explanations. First, the MEA value for n_3 for ethane was underestimated because of a small number of points available to adequately define Process III. If this were the case, it would have been apparent in the MEA fit of the adsorption data collected above T_C . Additionally, if the MEA fit of the data were acceptable, the error in n_3 is 0.3 mmoles while difference between the calculated and the experimental isotherms is ~ 1 mole at 1 atm. The second possibility, as mentioned above, is that another Process is occurring below T_C . The physical significance of this new Process is not yet known, but it will be designated Process IV for now.

Examination of the ethane adsorption at -84°C shows the potential magnitude of Process IV, Figure 4.7. The difference between the experimental and calculated adsorption at 1 atm is ~ 4 mmoles. This is approximately twice the amount adsorbed at 40°C . Again, the question arises "What is the physical reality of Process IV?" It is possible that Process IV is associated with cooperative pore filling in the larger micropores ($< 3\text{-}4$ molecular diameters) or capillary condensation in the mesopores. Capillary condensation would likely have an equilibrium constant consistent with the enthalpy and entropy of vaporization (condensation) and would be considered as the last Process to occur as one approaches the normal boiling point of the adsorptive. At -84°C , the experimental adsorption was collected only 5°C from the normal boiling point of ethane.

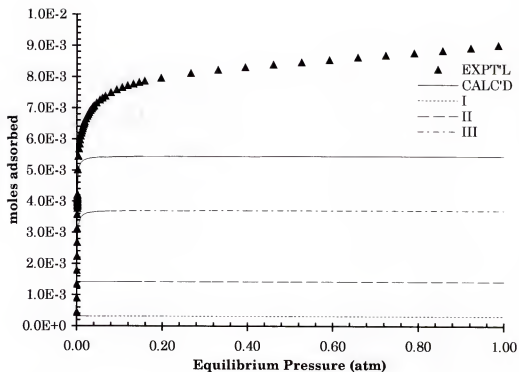


Figure 4.7: Experimental and calculated adsorption isotherms for ethane adsorption by A572 at -84°C . At 1 atm, Process I is 100% complete, II is 100% complete, and III is >99% complete.

It is probable that Process IV is associated with cooperative pore filling in pores a few molecular diameters in width, Figure 4.2. The K associated with this type of adsorption will be similar to that found for Process III in adsorption above T_C . As was mentioned before, the pore restriction that occurs as a monolayer is adsorbed on opposite walls creates a new effective "pore" that is ~ 2 molecular diameters wide (using the example in Figure 4.2), which leads to the enhanced adsorption introduced by Everett and Powl. Seemingly, many possible "effective pore sizes" are possible in the micropore region ($< 20 \text{ \AA}$). It is also more than likely that the Processes that define the "effective pore sizes" overlap with the Processes defining the adsorption above T_C . The overlapping Processes make resolution much more difficult and attempts to do so have not been successful to date.

Concluding Remarks

The purpose of studying adsorption data collected below the critical temperature of the adsorptive using the MEA was to attempt to explain multilayer formation in qualitative as well as quantitative terms. The information gained would be particularly useful in studying liquid-solid adsorption processes where several competing equilibria are occurring simultaneously. However, it seems that the MEA may not be well suited for studying adsorption below T_C . The adsorption processes occurring below T_C are so quantitatively similar to those that occur above T_C that they may preclude resolution, although their physical interpretation is different from

the above T_C case. An area to be explored in the near future is the possible separation of adsorptive/adsorptive from solid/adsorptive interactions at temperatures below T_C . If this can be achieved, resolution of these "subcritical" Processes may be possible.

CHAPTER 5

SUMMARY AND CONCLUDING REMARKS

The research presented in this dissertation focused on the theoretical description of micropore filling using a new adsorption model and on the evaluation of the model parameters used to quantify specific properties of the gas / solid adsorption system. In Chapter 2, the basis of the model, the Multiple Equilibrium Analysis (MEA), was described and MEA derived quantities were used to compare and contrast five activated carbon materials. In Chapter 3, MEA derived quantities were used to introduce pore size distributions (PSDs) for the solids studied and suggested the use of MEA-PSDs in the prediction of adsorption isotherms. In chapter 4, multilayer formation was addressed in a manner consistent with the MEA.

The ultimate goal of developing the MEA was to gain a fundamental understanding of adsorptive-adsorbent interactions and apply the information obtained to the rational design of new adsorbents tailored to specific adsorptives of interest. The utility of the MEA to interpret adsorption isotherms was examined and the parameters obtained were shown to be meaningful within the context of the model. Adsorptives were selected that vary in size and polarizability to permit adsorbent characterization in terms of these physical properties. The equilibrium

constants (K_i 's), capacities (n_i 's), and enthalpies ($-\Delta H_i$'s) obtained from the analysis of the varied adsorptives were then used to directly compare five activated carbon adsorbents.

The utility of the multiple equilibrium analysis (MEA) has been shown for the thermodynamic and physical characterization of porous carbonaceous materials. The thermodynamic characterization reveals differences in materials that are not readily apparent when traditional physical characterization techniques are used, for example, BET. The physical quantities that result from the n_i 's, surface area and pore volume, have been shown to be more realistic estimates than other methods provide. Specifically, these values represent "usable" space within these materials.

The $-\Delta H_i$ values determined in the MEA make it possible to predict adsorption equilibrium constants based on a physical characteristic of an adsorptive molecule, the van der Waals α constant. The ability to predict an entire adsorption isotherm will result when the n_i values can be predicted in a reliable fashion from a MEA pore size distribution (MEA-PSD).

The pore size distribution (PSD) for a porous material is an essential piece of information for selecting a material for a specific application. With crystalline materials such as zeolites, the width of the distribution is narrow and an idea of the average pore size(s) can be determined from crystallography. The determination of pore sizes is a little more difficult for amorphous materials, for example, carbons, silicas, and aluminas, which

usually have a wide distribution of pore sizes and may actually possess more than one average pore size.

The goal of pursuing a Multiple Equilibrium Analysis derived Pore Size Distribution (MEA-PSD) was to obtain a method for predicting n_i values for a new adsorptive on a MEA characterized solid. Although this goal has not been reached, progress has been made in its attainment. The $-\Delta H_i$'s and $-\Delta S_i$'s from the MEA have been used to find $\ln K$ distributions associated with N_2 , CH_4 , and SF_6 adsorption on the solids studied. The use of several spherically symmetric adsorptive molecules allowed the effective mapping of the micropore region $< 10 \text{ \AA}$ in width. The $\ln K$ distributions correlate to pore width and permit the determination of a pore volume / pore width distribution. It is hoped that volume / width distribution will allow the direct calculation of n_i values for use in isotherm prediction.

The purpose of studying adsorption data collected below the critical temperature of the adsorptive using the MEA was to attempt to explain multilayer formation in qualitative as well as quantitative terms. The information gained would be particularly useful in studying liquid-solid adsorption processes where several competing equilibria occur simultaneously. However, it seems that the MEA is not well suited for studying adsorption below T_C . The adsorption processes occurring below T_C are so quantitatively similar to those that occur above T_C that they preclude resolution, although the physical interpretation of the below T_C adsorption

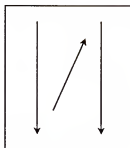
Processes is different from the above T_C case. An area to be explored in the near future is the possible separation of adsorptive/adsorptive from solid/adsorptive interactions at temperatures below T_C . If this can be achieved, resolution of the Processes associated with adsorption below T_C may be possible.

APPENDIX A ADSORPTION DATA

The following is a typical pressure table used in the adsorption experiments described in the text (pressure in torr).

1.0	11.0	28.0	100.0	500.0
2.0	12.0	30.0	110.0	550.0
3.0	13.0	35.0	120.0	600.0
4.0	14.0	40.0	150.0	650.0
5.0	16.0	45.0	200.0	700.0
6.0	18.0	50.0	250.0	750.0
7.0	20.0	60.0	300.0	
8.0	22.0	70.0	350.0	
9.0	24.0	80.0	400.0	
10.0	26.0	90.0	450.0	

The following data was collected as described in the text and should be read as shown in the graphic below.



PRESSURE (torr)	VOL ADS (cc/g STP)	PRESSURE (torr)	VOL ADS (cc/g STP)	PRESSURE (torr)	VOL ADS (cc/g STP)
N₂ / A563 / -93°C				N₂ / A563 / -43°C	
1.0452	1.1372	1.0064	0.1797	0.3894	0.0261
3.0429	3.2003	1.9884	0.3734	0.5709	0.0402
5.0370	4.8902	3.0419	0.5745	0.7111	0.0509
7.1056	6.4120	3.9924	0.7523	0.8285	0.0597
9.2260	7.7882	4.9967	0.9375	0.8926	0.0645
11.0877	8.8601	6.2896	1.1779	0.9769	0.0711
13.1563	9.9789	7.2204	1.3233	1.0571	0.0772
15.2766	11.0276	8.4616	1.5388	2.0071	0.1569
18.1209	12.4522	9.6511	1.7493	3.0274	0.2419
21.1721	13.8380	10.1165	1.8195	4.0002	0.3223
25.1025	15.3787	10.9439	1.9698	5.0008	0.4045
35.6006	18.8884	12.0299	2.1354	5.9834	0.4856
45.6333	21.6600	13.2194	2.3508	7.1212	0.5827
55.3557	23.9455	14.2537	2.5063	8.8278	0.7183
65.3367	25.9878	16.5809	2.8725	9.3966	0.7618
75.4212	27.8522	18.2875	3.1383	10.4309	0.8383
85.4022	29.4766	19.9423	3.3941	10.9481	0.8815
90.4702	30.2640	22.4764	3.7655	12.3444	0.9852
100.3478	31.6727	24.0795	4.0013	12.9650	1.0340
110.1736	32.9537	26.0447	4.2674	14.2578	1.1321
115.1383	33.5477	27.8030	4.5085	15.8610	1.2620
120.8786	34.2223	30.3371	4.8547	17.8779	1.4096
150.4079	37.3666	35.1983	5.4827	19.8430	1.5620
201.7609	41.7944	40.2663	6.1208	22.0668	1.7308
225.8601	43.5244	45.3861	6.7391	24.0320	1.8681
250.7350	45.1095	49.7302	7.2321	25.9971	2.0104
301.1054	47.9800	60.1766	8.3794	27.9623	2.1578
350.7518	50.3885	70.3645	9.4074	29.9792	2.2954
400.5016	52.4763	80.0352	10.3404	35.4093	2.6694
451.0789	54.3437	89.2922	11.1726	39.7016	2.9612
500.4667	55.9924	100.3074	12.1312	44.7180	3.2880
550.1649	57.4791	109.2541	12.8485	49.5275	3.6030
601.2076	58.8818	120.0626	13.6925	60.3359	4.2812
650.1816	60.1110	150.0573	15.8283	69.4377	4.8333
701.1209	61.3052	200.8931	18.9394	79.2636	5.4051
760.2829	62.5673	249.9707	21.5109	90.2272	6.0198
N₂ / A563 / -62°C		299.8756	23.7947	99.3807	6.5224
0.2943	0.0441	349.9358	25.8325	109.3100	7.0500
0.4691	0.0788	400.0476	27.6681	119.2910	7.5479
0.5787	0.0992	450.0043	29.3343	150.1648	9.0082
0.6775	0.1174	500.0644	30.8663	200.5870	11.1599
0.7649	0.1337	550.2280	32.2840	250.1299	13.0500
0.8435	0.1487	600.2363	33.5969	300.0349	14.7706
0.8838	0.1566	650.1414	34.8251	350.0950	16.3505
0.9474	0.1687	700.1497	35.9788	400.4137	17.8074
		750.2098	37.0629		

PRESSURE (torr)	VOL ADS (cc/g STP)	PRESSURE (torr)	VOL ADS (cc/g STP)	PRESSURE (torr)	VOL ADS (cc/g STP)
450.1636	19.1493	399.4937	55.9897	349.7801	35.7324
500.1720	20.4198	450.0710	57.7867	399.8919	37.7837
550.2838	21.5908	499.9243	59.3651	449.7969	39.6316
600.0853	22.6902	550.0361	60.7832	500.1156	41.3110
650.2489	23.7418	599.9410	62.0732	549.9171	42.8381
700.3090	24.7335	650.0529	63.2574	600.1841	44.2508
750.1623	25.6776	700.1647	64.3271	649.9340	45.5626
CO / A563 / -93°C		749.9146	65.3073	700.2526	46.7778
1.1615	3.3829	CO / A563 / -62°C		749.9507	47.9085
2.0076	5.3238	1.0224	0.4233	CO / A563 / -43°C	
3.0739	7.3229	1.9833	0.8114	1.3275	0.2013
3.9722	8.6912	3.0114	1.2101	1.9962	0.3094
4.9600	9.9207	3.9976	1.5779	3.0155	0.4728
5.9426	10.3283	4.9962	1.9380	4.0038	0.6291
6.9769	11.3867	6.1856	2.3365	5.0019	0.7845
8.2180	12.5630	7.2199	2.6793	5.9845	0.9477
8.9938	13.2099	8.2542	3.0072	7.3808	1.1547
9.9246	13.9454	9.2885	3.3250	8.1048	1.2609
11.0624	14.7495	9.9091	3.5317	9.0356	1.3989
11.9415	15.2865	11.3054	3.9453	10.2768	1.5746
12.8724	15.8629	11.9260	4.1318	11.4145	1.7395
13.9067	16.4982	13.3740	4.5354	12.5523	1.8993
16.1304	17.7236	13.9429	4.7169	12.9143	1.9524
17.8887	18.6484	16.1666	5.3070	13.8969	2.0860
20.0091	19.6557	18.2869	5.8770	16.1206	2.3854
22.0777	20.5440	19.8384	6.2654	18.6546	2.7275
24.2497	21.3673	22.3207	6.8606	20.1027	2.9251
26.3183	22.0967	23.8722	7.2339	21.9127	3.1562
27.8180	22.5808	26.5096	7.8294	24.6536	3.4955
30.2486	23.3333	27.9576	8.1526	25.9982	3.6774
34.7995	24.7305	29.8711	8.5616	27.9633	3.9150
40.3330	26.2862	34.8357	9.5910	29.7216	4.1308
45.1425	27.4589	40.2658	10.6257	34.9449	4.7427
50.1589	28.5406	45.0236	11.4838	40.2198	5.3306
59.8813	30.5181	50.0917	12.3471	45.3396	5.8921
70.4312	32.4014	59.7107	13.8826	49.7354	6.3574
79.9985	33.8679	70.2605	15.3929	60.4404	7.4116
89.8243	35.2131	79.8795	16.6767	70.0593	8.3066
100.1673	36.4729	90.1708	17.9399	79.2129	9.1186
110.0449	37.5463	99.9966	19.0727	90.2799	10.0387
120.0259	38.5388	110.1845	20.1654	99.1749	10.7438
150.6929	41.5423	120.0621	21.1621	110.1902	11.5798
199.5635	45.6621	149.3327	23.8127	119.2403	12.2323
250.9165	49.0769	201.0477	27.7163	150.1659	14.2940
300.2526	51.7294	249.6599	30.7449	200.9500	17.2331
350.4162	54.0127	299.2545	33.3898	249.9758	19.6693

PRESSURE (torr)	VOL ADS (cc/g STP)	PRESSURE (torr)	VOL ADS (cc/g STP)	PRESSURE (torr)	VOL ADS (cc/g STP)
299.5705	21.8485	151.5591	50.6487	100.0959	30.1308
349.9409	23.8119	201.4123	54.9734	109.7149	31.4010
399.7942	25.5804	250.2830	58.3100	120.3165	32.6839
450.1129	27.2028	299.1537	61.0136	149.1217	35.7507
499.9661	28.6874	349.2138	63.3695	201.4056	40.2034
550.0262	30.0750	399.8428	65.4128	249.1386	43.4351
600.1898	31.3554	449.7478	67.1859	299.6124	46.2816
649.8879	32.5523	499.9113	68.7778	349.4657	48.6792
700.1549	33.6817	550.0749	70.1894	399.6292	50.7864
749.9564	34.7479	599.8247	71.4779	449.8445	52.6511
CH ₄ / A563 / -62°C		650.1434	72.6643	499.9563	54.3125
0.7038	1.9257	699.8932	73.7229	549.9647	55.8050
0.8771	2.4060	749.8499	74.7256	599.9214	57.1683
1.0684	2.8889	CH ₄ / A563 / -43°C		650.0333	58.4285
1.9874	5.0646	0.9764	1.0235	700.0416	59.5895
3.0227	6.9860	0.9929	1.0399	750.0500	60.6617
3.9691	8.5416	1.0090	1.0564	CH ₄ / A563 / -16°C	
4.9988	10.0169	1.9869	1.9972	0.6407	0.1530
6.0331	11.2708	3.0248	2.8991	1.1367	0.2817
7.0157	12.4043	3.9681	3.6618	2.0314	0.5152
7.9465	13.3925	4.9920	4.4349	3.0165	0.7663
8.9808	14.4301	6.0263	5.1499	3.9991	1.0113
9.9117	15.3127	7.0606	5.8154	5.0003	1.2554
10.9460	16.2098	8.0432	6.4508	6.2932	1.5586
12.0320	17.1417	8.9741	7.0114	7.0689	1.7347
12.9112	17.8742	10.0084	7.5875	8.1032	1.9743
13.8938	18.5961	10.9910	8.1385	9.1375	2.1992
15.9106	20.0248	12.0770	8.6998	9.9650	2.3761
18.0310	21.4183	13.0079	9.1959	10.9475	2.5952
20.0996	22.6515	14.0939	9.7423	12.3439	2.8855
21.9613	23.6803	16.1108	10.6858	13.1196	3.0320
23.9265	24.7089	18.0759	11.5495	13.9987	3.2246
26.0985	25.7364	20.1445	12.4041	16.0156	3.6143
28.0637	26.6499	22.2131	13.2288	18.3428	4.0589
30.1840	27.5775	24.3852	14.0145	19.9977	4.3635
35.2520	29.5649	26.2986	14.7147	21.8077	4.6954
39.9581	31.2527	27.8501	15.2391	23.8246	5.0605
45.1296	32.9084	30.1773	16.0061	26.4103	5.5094
49.9391	34.3101	34.7799	17.4014	28.1686	5.7961
60.1787	36.9606	40.0031	18.8798	29.9787	6.0888
70.1597	39.1711	45.1746	20.2042	35.2536	6.9243
79.7787	41.0468	49.9324	21.3576	40.4768	7.7046
89.9148	42.8154	60.2237	23.5502	44.6140	8.2989
99.9475	44.4040	69.8427	25.4017	50.1992	9.0658
110.1354	45.8416	80.1339	27.1579	60.3871	10.3854
120.0646	47.1259	89.9081	28.6836	70.2647	11.5518

PRESSURE (torr)	VOL ADS (cc/g STP)	PRESSURE (torr)	VOL ADS (cc/g STP)	PRESSURE (torr)	VOL ADS (cc/g STP)
80.0388	12.6374	50.1149	18.4261	34.8409	10.7561
90.1749	13.6900	60.8199	20.0797	40.9950	11.8792
99.0699	14.5642	70.0769	21.4047	45.0805	12.4880
110.1886	15.5855	79.4891	22.5489	50.3554	13.3374
119.1870	16.3770	90.1423	23.8124	60.6984	14.7829
150.4229	18.8535	99.8648	24.7703	70.0588	15.9876
201.0002	22.2383	109.3286	25.6763	79.5227	17.0057
249.9743	24.9947	120.2922	26.6705	90.2794	18.1423
299.4655	27.4007	151.2178	28.8993	99.0709	19.0608
349.7842	29.5553	199.7782	31.6077	109.7242	19.8927
399.9995	31.4664	250.3554	33.8962	120.4292	20.8491
449.9562	33.1844	299.7433	35.6910	151.3548	22.9362
500.2232	34.7711	349.4413	37.1946	199.7083	25.5873
550.3867	36.2084	399.8118	38.5010	249.5099	27.8451
599.8780	37.5257	449.3547	39.6632	299.5700	29.8029
650.1967	38.7582	499.5183	40.6882	349.7336	31.2684
699.9982	39.9081	549.7336	41.5714	400.7762	32.6345
750.1617	40.9948	599.5351	42.4030	450.2675	33.8548
C₂H₆ / A563 / 40°C		649.4918	43.2334	499.3450	34.9030
0.4587	0.4969	700.1725	43.8933	551.3186	35.9020
0.8724	0.9364	751.0601	44.5840	601.2236	36.7801
1.3079	1.3767	C₂H₆ / A563 / 55°C		649.1634	37.6139
1.9931	2.0424	0.3848	0.2098	699.9475	38.2832
3.0108	2.8970	0.7126	0.4025	751.3522	39.0217
3.9903	3.6721	1.0033	0.5679	C₂H₆ / A563 / 70°C	
5.0712	4.4101	1.9972	1.1174	0.3837	0.0276
6.1055	5.1024	3.0393	1.6490	0.2281	0.0544
7.1398	5.6973	4.0120	2.1146	0.4137	0.1042
8.1224	6.2602	5.0014	2.5521	0.5389	0.1412
9.3118	6.9206	6.1391	3.0303	0.6376	0.1703
10.1910	7.3630	7.1734	3.4365	0.7142	0.1933
11.2253	7.8454	8.4145	3.9021	0.7778	0.2109
11.8976	8.1442	9.1903	4.1881	0.8285	0.2245
12.9836	8.5920	10.2763	4.5855	0.8445	0.2279
14.2247	9.1206	11.0520	4.8118	0.8662	0.2319
16.2933	9.9315	12.2932	5.2227	0.8869	0.2354
18.3619	10.6760	13.0172	5.4577	0.9019	0.2385
19.8099	11.1841	13.8963	5.7559	0.9169	0.2405
22.3957	12.0034	15.9132	6.3135	0.9371	0.2449
23.9471	12.4836	18.1887	6.9314	0.9748	0.2545
25.8606	13.0448	20.4124	7.5631	1.0110	0.2644
28.3946	13.7705	22.2225	7.9568	2.0024	0.5726
30.0495	14.2124	24.2393	8.4447	3.0915	0.9037
35.1176	15.3973	25.7908	8.8275	4.0069	1.1717
39.9788	16.4650	28.3248	9.4363	5.0076	1.4502
45.3054	17.4932	30.2383	9.7876	5.9901	1.6372

PRESSURE (torr)	VOL ADS (cc/g STP)	PRESSURE (torr)	VOL ADS (cc/g STP)	PRESSURE (torr)	VOL ADS (cc/g STP)
6.9727	1.8952	5.0065	0.6825	3.9831	1.7303
8.0070	2.1548	6.0408	0.8295	5.2398	2.1286
9.3516	2.4947	7.7474	1.0377	6.1701	2.3734
10.1273	2.6854	8.2646	1.1038	7.0493	2.6019
11.0582	2.8962	9.2989	1.2310	8.2904	2.9300
11.9374	3.0951	10.9020	1.4210	9.0662	3.1256
13.1268	3.3643	11.3675	1.4854	10.0487	3.3417
14.0060	3.5634	12.2983	1.5995	11.0830	3.5992
16.1263	4.0279	13.7981	1.7813	12.0139	3.7937
17.9363	4.3866	14.3669	1.8342	12.8931	3.9919
20.4703	4.8737	16.4355	2.0739	13.9274	4.2142
22.0735	5.1806	18.0904	2.2460	16.2028	4.6192
23.9870	5.5222	19.8487	2.4609	18.5817	5.0466
25.8487	5.8724	21.9173	2.6711	20.0815	5.3060
27.9173	6.1882	23.9342	2.8748	21.8915	5.6134
29.7790	6.4925	25.7960	3.0930	24.4772	6.0363
35.2091	7.3450	28.1231	3.2920	26.1838	6.2708
39.6566	8.0008	30.4503	3.5252	27.9938	6.5229
44.6213	8.6619	35.4667	4.0089	29.8039	6.7603
50.3099	9.3699	39.9659	4.3821	34.9754	7.3500
60.1875	10.5170	45.6028	4.8910	40.4054	7.9768
70.3236	11.5912	50.1020	5.2346	44.8012	8.4359
79.6840	12.4641	60.3416	6.0363	49.8176	8.8811
90.5442	13.4628	70.5811	6.8035	59.7986	9.7055
99.6460	14.2019	79.7347	7.4171	69.3658	10.3942
109.5236	14.9581	89.5088	8.0713	79.4503	11.0556
120.3320	15.7329	99.7484	8.6364	89.4313	11.6494
150.3267	17.6370	109.2640	9.2223	99.5674	12.1929
201.1626	20.2303	119.6070	9.7957	109.7035	12.6598
250.4470	22.3230	150.2740	11.3122	119.6328	13.1180
299.8348	24.0394	200.6961	13.4034	150.5067	14.2492
351.2912	25.6427	251.1182	15.1941	199.7394	15.6748
399.4896	26.9734	299.5235	16.7366	249.2823	16.8071
450.3771	28.0852	350.3076	18.0610	299.9113	17.7232
501.1613	29.1733	401.4020	19.3118	349.5577	18.5167
549.6699	30.2096	449.5487	20.4666	400.2901	19.1900
600.6609	31.0150	501.1085	21.3867	449.7814	19.7898
649.3765	31.8844	549.6689	22.3626	500.5138	20.2918
701.0397	32.5425	601.2288	23.1505	550.8325	20.7683
750.3242	33.2561	650.4614	24.0251	600.1686	21.2248
C₂H₆ / A563 / 100°C		701.4007	24.6648	650.6425	21.6058
0.5839	0.0772	750.9954	25.4380	701.4266	21.9643
1.1165	0.1496	SF₆ / A563 / 50°C		751.2281	22.3523
1.9915	0.2746	1.2406	0.5759	SF₆ / A563 / 65°C	
3.0491	0.4183	2.0133	0.9698	1.1036	0.3111
4.0255	0.5509	3.2115	1.4133	2.0179	0.5763

PRESSURE (torr)	VOL ADS (cc/g STP)	PRESSURE (torr)	VOL ADS (cc/g STP)	PRESSURE (torr)	VOL ADS (cc/g STP)
3.0843	0.8503	2.0205	0.3383	1.0529	0.1016
3.9738	1.1006	3.0553	0.5046	2.0091	0.2014
5.2165	1.3802	4.0146	0.6571	3.0372	0.3046
6.3025	1.5942	5.0262	0.8087	3.9898	0.4000
7.3368	1.8018	6.4737	1.0160	5.0039	0.5010
8.5263	2.0138	7.7666	1.1777	6.1417	0.6106
9.1985	2.1813	8.2320	1.2429	7.6931	0.7528
10.1294	2.3316	9.2146	1.3798	8.2620	0.8000
11.5774	2.5906	10.6626	1.5614	9.1411	0.8918
11.9912	2.6815	11.1280	1.6317	10.7443	1.0102
13.0772	2.8511	12.1623	1.7651	11.2615	1.0609
13.9563	3.0047	13.6104	1.9365	12.2958	1.1523
16.2835	3.3187	14.0758	2.0068	14.1575	1.2934
18.3521	3.6253	16.6098	2.2721	14.1575	1.2934
20.0587	3.8277	18.2647	2.4549	16.3812	1.4706
21.8170	4.0611	20.1264	2.6234	18.2430	1.6067
24.5062	4.4202	21.8848	2.7939	20.2082	1.7762
26.2128	4.6029	23.8499	2.9963	22.0699	1.9174
27.8677	4.7988	25.8151	3.1935	24.1385	2.0445
29.7294	5.0254	28.1423	3.3760	26.0002	2.1657
35.3146	5.5720	29.8489	3.5348	27.9137	2.3084
39.8655	5.9853	35.4858	3.9857	29.9306	2.4592
44.6750	6.4057	39.8816	4.3021	35.7744	2.7996
50.5705	6.9119	44.7428	4.6786	39.7564	3.0542
60.7584	7.6513	49.7591	5.0290	45.0314	3.3220
69.4465	8.2333	60.0504	5.6865	49.8926	3.5723
79.6861	8.8158	69.9280	6.1885	60.3390	4.0996
89.3051	9.3508	79.4436	6.7057	69.8546	4.5285
99.6998	9.8538	89.6831	7.1988	79.6287	4.9904
109.6291	10.3187	99.8710	7.6231	90.0751	5.3812
119.9721	10.7315	109.5934	8.0589	99.8493	5.7319
149.8116	11.7983	119.9364	8.4367	109.8302	6.1240
200.7509	13.3066	150.6034	9.4673	120.1215	6.4647
250.3973	14.3582	200.7152	10.8988	149.7542	7.3741
300.7160	15.3007	250.6719	11.8861	199.3489	8.5171
350.2590	16.1023	299.1806	12.8168	251.0122	9.5951
400.1122	16.8042	350.6887	13.5795	300.3483	10.4650
450.5344	17.3597	400.4386	14.3098	350.0464	11.2068
501.1116	17.9444	450.9124	14.8778	400.0031	11.8600
551.1201	18.3694	501.3862	15.4855	451.1493	12.4676
601.8525	18.8349	551.0844	15.9226	501.4680	13.0053
652.2746	19.2176	601.8168	16.4061	551.7866	13.4873
702.3347	19.5901	652.3423	16.7965	601.8467	13.9516
752.2914	19.9780	702.5576	17.1418	651.6483	14.4436
SF ₆ / A563 / 80°C		751.9971	17.5809	703.3116	14.6927
1.1026	0.1770	SF ₆ / A563 / 95°C		752.2857	15.0641

PRESSURE (torr)	VOL ADS (cc/g STP)	PRESSURE (torr)	VOL ADS (cc/g STP)	PRESSURE (torr)	VOL ADS (cc/g STP)
N₂ / A572 / -93°C					
4.8162	6.3654	29.7713	4.0630	16.0668	1.1736
24.1057	19.0389	34.8911	4.6317	18.1871	1.3102
47.8428	28.3492	40.5280	5.2448	19.9454	1.4371
96.5580	40.9078	44.7686	5.6815	21.9106	1.5767
146.8244	50.0079	49.6816	6.1633	23.9792	1.7075
199.4164	57.4874	59.4040	7.0858	25.9961	1.8478
298.1404	68.3134	70.3158	8.0470	28.3233	2.0019
397.2824	76.7411	80.0900	8.8846	30.0816	2.1189
496.6296	83.6401	89.2435	9.6215	35.5117	2.4666
598.1428	89.6134	100.1037	10.4554	39.8040	2.7301
698.9340	94.7597	109.2055	11.1271	44.8204	3.0325
753.1296	97.2431	119.0831	11.8384	49.7850	3.3242
		149.3881	13.8654	60.0763	3.9169
N₂ / A572 / -62°C		199.3965	16.8450	69.3333	4.4366
0.3108	0.0441	250.0772	19.5481	79.3143	4.9599
0.5006	0.0757	300.1373	21.9493	89.1401	5.4762
0.6361	0.0991	349.8354	24.1567	99.3280	5.9826
0.7349	0.1162	400.3093	26.2245	109.2572	6.4748
0.7840	0.1243	450.4728	28.1501	119.3934	6.9443
0.8316	0.1320	500.1192	29.9546	150.0604	8.3327
0.8714	0.1389	550.2311	31.6813	200.1722	10.3847
0.9076	0.1448	600.2912	33.3260	250.0772	12.2524
0.9391	0.1502	650.2996	34.8745	300.1890	13.9904
0.9666	0.1549	700.1011	36.3553	350.1457	15.6154
0.9919	0.1593	750.3164	37.7994	400.2058	17.1352
1.0162	0.1636	N₂ / A572 / -43°C		450.1108	18.5719
2.0014	0.3389	0.4334	0.0232	500.0675	19.9490
3.0321	0.5135	0.6563	0.0378	550.3345	21.2626
3.9877	0.6714	0.7535	0.0434	600.1877	22.5211
5.0003	0.8346	0.8367	0.0486	650.2996	23.7322
6.0341	0.9576	0.9066	0.0530	700.1528	24.8947
7.2753	1.1476	0.9640	0.0567	750.3164	26.0096
8.6199	1.3484	1.0136	0.0601	CO / A572 / -93°C	
9.2922	1.4488	2.0262	0.1421	0.1339	0.4882
10.2230	1.5761	3.0553	0.2232	0.2498	0.9799
11.5159	1.7613	3.9950	0.2967	0.3584	1.4730
11.9813	1.8301	4.9998	0.3747	0.4691	1.9658
13.0673	1.9736	6.0858	0.4331	0.5927	2.4538
14.4119	2.1642	7.6890	0.5532	0.7225	2.9475
15.8600	2.3607	8.2579	0.6055	0.8502	3.4368
18.3423	2.6851	9.3439	0.6841	0.9919	3.9283
20.2040	2.9145	10.1713	0.7394	1.1320	4.4150
21.9623	3.1432	11.1539	0.8168	2.0174	7.1018
23.8241	3.3776	11.9296	0.8716	2.9777	9.3552
25.8927	3.6135	13.1708	0.9672	3.9686	11.3754
27.7544	3.8275	14.8774	1.0784	4.9745	13.1372

PRESSURE (torr)	VOL ADS (cc/g STP)	PRESSURE (torr)	VOL ADS (cc/g STP)	PRESSURE (torr)	VOL ADS (cc/g STP)
5.9571	14.5796	0.5223	0.3050	449.9065	57.0155
6.9396	15.9937	0.5927	0.3561	499.9149	59.7657
7.9739	17.3366	0.6645	0.4069	550.0268	62.3050
9.0082	18.6278	0.7349	0.4580	599.8801	64.6886
9.9908	19.7882	0.8150	0.5116	650.2504	66.9226
11.0251	20.8963	0.8874	0.5623	699.9485	69.0016
11.9043	21.8279	0.9635	0.6119	750.1121	70.9930
13.0420	22.8877	1.0271	0.6533	CO / A572 / -43°C	
13.9729	23.7391	1.9864	1.2599	0.2596	0.0476
15.8863	25.4315	3.0465	1.8742	0.4323	0.0904
18.0066	27.1120	3.9784	2.3881	0.5616	0.1236
19.9201	28.5560	5.0029	2.9224	0.6470	0.1455
22.0921	30.0629	5.9850	3.4013	0.7235	0.1652
23.9539	31.3346	7.1744	3.9647	0.7907	0.1829
25.7639	32.4755	8.0536	4.3685	0.8512	0.1991
27.7291	33.6427	9.0879	4.8052	0.8833	0.2094
29.7460	34.8093	10.0705	5.2137	0.9376	0.2236
34.8140	37.4584	11.0530	5.6645	0.9836	0.2351
39.9338	39.9102	12.1908	6.1247	1.0234	0.2457
44.8467	42.0644	13.1734	6.4911	2.0040	0.5080
49.8114	44.0682	14.1559	6.8854	3.0295	0.7704
60.1027	47.8515	16.1211	7.6131	3.9877	1.0094
70.1871	51.1120	18.1897	8.3503	4.9998	1.2558
79.7544	53.9195	20.2583	9.0595	6.3444	1.5219
90.0456	56.6488	22.3786	9.7262	7.2236	1.7290
99.8715	59.0697	23.7749	10.1910	8.0510	1.9143
110.1628	61.3736	26.2573	10.9425	9.2404	2.1784
119.8852	63.4077	27.8604	11.4169	10.0162	2.3470
150.7073	69.1787	30.1359	12.0886	10.9987	2.5398
201.4915	76.9508	34.7902	13.3572	12.2399	2.8045
250.0518	83.0093	39.9617	14.6914	13.0156	2.9734
299.9568	88.2513	45.0815	15.9412	13.9982	3.1608
349.1895	92.7355	50.0979	17.0872	15.9117	3.5507
399.6116	96.7785	60.0789	19.1975	18.2906	4.0261
449.6718	100.3592	70.0599	21.1572	19.9454	4.3335
499.8870	103.5878	80.1443	22.9714	21.8072	4.6755
549.8954	106.4954	89.8667	24.6267	24.2378	5.1200
599.8004	109.1566	99.9511	26.2259	25.8927	5.4168
650.0157	111.6083	110.0356	27.7397	27.8578	5.7494
699.8689	113.8675	120.1200	29.1560	30.2884	6.1621
750.1359	115.9615	150.3733	33.0326	34.8394	6.9149
CO / A572 / -62°C		201.2608	38.5843	40.1660	7.7521
0.1469	0.0645	249.6143	43.0705	45.1824	8.5165
0.2539	0.1229	299.1573	47.1043	50.2504	9.2658
0.3258	0.1695	349.6829	50.7494	59.8694	10.5892
0.4530	0.2537	399.5878	54.0114	70.1090	11.8995

PRESSURE (torr)	VOL ADS (cc/g STP)	PRESSURE (torr)	VOL ADS (cc/g STP)	PRESSURE (torr)	VOL ADS (cc/g STP)
79.9866	13.1105	44.9889	41.5400	198.1553	48.4162
90.2261	14.2783	50.1087	43.7604	223.5474	51.3422
100.1554	15.3741	59.6760	47.5477	249.1980	54.0953
110.2915	16.4148	70.1741	51.2606	298.4307	58.9103
119.0831	17.2895	79.7931	54.3696	350.4043	63.3988
149.4398	20.1188	90.0844	57.3887	399.5335	67.2096
199.3448	24.1936	99.8586	60.0600	449.7488	70.7759
249.9220	27.7871	109.7878	62.5636	500.0675	74.0458
299.5685	30.9284	119.9757	64.9720	549.9725	77.0222
349.7837	33.8036	150.9530	71.4564	599.8774	79.7910
399.8955	36.4292	201.5820	80.1389	649.9893	82.3912
449.9040	38.8500	249.9355	87.0131	700.1011	84.8204
499.9641	41.1119	299.1165	92.8809	759.8320	87.5868
550.1276	43.2118	350.0557	98.2282	CH₄ / A572 / 0°C	
599.9809	45.1705	400.0641	102.7783	0.9779	0.1737
650.0410	47.0267	449.2968	106.8118	2.9395	0.5385
700.1011	48.7772	499.9775	110.5437	5.0520	0.9165
750.0578	50.4367	549.9859	113.8764	7.4309	1.0890
CH₄ / A572 / -62°C		599.8392	116.9239	9.1375	1.3575
0.2943	0.9824	649.9510	119.7623	10.7407	1.6357
0.5678	1.9648	700.1146	122.3818	12.7059	1.9279
0.8678	2.9434	749.8644	124.8066	15.2916	2.3739
1.0948	3.6028	CH₄ / A572 / -43°C		17.6705	2.7665
1.9884	6.2129	0.9753	1.2263	20.5665	3.1825
3.1008	8.5362	2.9405	3.1511	25.2209	3.8553
3.9665	10.2432	4.8964	4.6822	34.8399	5.1892
5.0650	12.0505	7.3270	5.3418	43.7349	6.3177
5.9958	13.4135	9.0336	6.4616	53.3538	7.5225
6.9784	14.7818	11.4125	8.0258	63.4383	8.6881
8.0644	16.1706	12.7053	8.7850	73.5227	9.7927
8.9436	17.2481	14.5671	9.7729	83.6588	10.8373
9.9779	18.4074	17.6700	11.2504	89.9681	11.4774
10.9088	19.4187	20.9280	12.7119	99.0182	12.3585
11.9431	20.4406	24.9618	14.4781	108.5855	13.2690
12.8739	21.4010	35.7702	18.4526	114.9464	13.8246
14.0117	22.4488	44.5101	21.2886	119.9111	14.3019
15.9768	24.1663	53.7671	23.8951	150.0092	16.8427
18.0971	25.9042	64.7306	26.6749	199.7073	20.5882
19.8555	27.2592	73.4705	28.6943	224.1168	22.2756
21.8723	28.7014	83.1929	30.7767	249.9743	23.9652
23.9409	30.1286	89.6055	32.0459	299.4655	26.9526
26.0613	31.4949	98.4488	33.7124	350.1462	29.7522
27.8713	32.6619	107.8609	35.3616	399.8444	32.3213
30.0433	33.9469	114.4805	36.4746	447.2153	34.5875
35.0597	36.7127	120.0657	37.3633	499.9646	36.9559
39.9209	39.1567	147.5781	41.6238	547.3355	38.9597

PRESSURE (torr)	VOL ADS (cc/g STP)	PRESSURE (torr)	VOL ADS (cc/g STP)	PRESSURE (torr)	VOL ADS (cc/g STP)
597.2405	40.9499	30.0950	158.4096	2.9741	83.9575
649.8864	42.9798	34.9562	160.5533	3.9650	90.7098
697.5676	44.7092	40.3863	162.6154	4.9558	95.9758
759.8842	46.8746	44.9889	164.0870	6.0419	100.4122
C₂H₆ / A572 / -84°C					
0.1169	10.0028	50.1087	165.4827	6.9727	103.6259
0.1882	20.0130	60.0897	167.8901	7.9553	106.4789
0.1862	30.0881	70.3293	169.9431	8.9379	109.0181
0.2327	40.1243	79.8966	171.5321	9.9205	111.3007
0.2906	50.1421	89.8776	172.9394	10.9031	113.4740
0.3884	60.1560	99.9620	174.1844	11.9891	115.4914
0.5621	70.1600	110.1498	175.2687	13.0234	117.4226
0.7623	80.1607	119.9757	176.1888	13.9543	118.7972
0.8833	84.7160	149.2981	178.6362	15.9711	121.7428
0.9060	86.2293	202.2025	181.9708	18.0397	124.1845
0.9040	86.9922	250.7112	184.3536	19.9015	126.4063
0.9045	87.7548	299.6336	186.4257	21.8149	128.1533
0.9081	88.5167	349.6420	188.3450	23.7801	129.9147
0.9143	89.2774	400.0124	190.1413	25.7970	131.5482
0.9221	90.0371	449.8140	191.8645	27.8139	133.0344
0.9309	90.7947	500.1327	193.5506	29.8825	134.4684
0.9428	91.5508	549.9342	195.2128	35.3126	137.8160
0.9557	92.3067	599.9943	196.9091	40.0703	140.2990
0.9759	93.0665	650.1061	198.6545	44.8798	142.4829
0.9965	93.8234	700.0629	200.4526	49.8445	144.5347
1.0059	94.5736	749.8644	202.3591	59.6703	147.9865
C₂H₆ / A572 / -62°C					
1.9978	112.4188	0.2281	10.0190	70.0133	151.0092
2.9757	122.1549	0.2201	20.0390	79.6323	153.4284
3.9660	127.3554	0.4758	30.0498	89.8719	155.6710
4.9615	131.0248	0.7075	40.0536	99.9563	157.6322
5.9441	133.9879	0.8481	45.2674	109.9373	159.3844
7.0301	136.6327	0.8611	46.5690	120.1769	160.9758
8.0644	138.8344	0.8533	47.2269	150.5336	164.9448
8.9436	140.4394	0.8817	48.5245	201.9383	169.8904
10.0296	142.1295	0.8817	49.1792	249.4127	173.3136
10.9605	143.5226	0.8848	49.8333	299.7314	176.1800
11.9431	144.8038	0.8905	50.4868	349.1709	178.4656
12.9256	145.9906	0.8947	51.1400	399.2310	180.4478
13.9082	147.0997	0.9024	51.7925	449.8083	182.1748
15.9251	149.1614	0.9123	52.4439	499.6615	183.6991
18.0971	151.0651	0.9257	53.0936	549.9802	185.0882
19.9589	152.5191	0.9391	53.7422	600.0403	186.3513
21.9758	153.9205	0.9578	54.3884	649.9453	187.5278
23.8892	155.1462	0.9826	55.0402	700.0054	188.6429
26.0095	156.3793	1.0084	55.6890	750.0139	189.7056
C₂H₆ / A572 / -43°C					
28.0781	157.4689	1.9905	72.5269	0.2229	10.0067

PRESSURE (torr)	VOL ADS (cc/g STP)	PRESSURE (torr)	VOL ADS (cc/g STP)	PRESSURE (torr)	VOL ADS (cc/g STP)
0.5228	20.0039	399.6442	154.4658	201.6678	107.3497
0.8564	27.5820	449.7043	156.4096	249.2973	112.2253
0.9117	29.0639	499.9713	158.1117	299.1506	116.2873
0.9195	29.8102	549.9280	159.6304	350.0381	119.7502
0.9340	30.5546	600.2467	161.0005	399.7363	122.5692
0.9547	31.2958	649.9448	162.2328	449.2792	125.0473
0.9676	32.0365	700.0049	163.3820	500.0117	127.2839
0.9971	32.7728	750.0651	164.4439	549.9166	129.2441
1.0286	33.5050	C₂H₆ / A572 / -16°C		599.9767	131.0216
1.9853	45.7134	0.7354	3.9315	650.1403	132.6279
2.9746	54.9979	0.8548	4.6887	699.8901	134.1046
4.0069	60.4079	0.9671	5.4346	750.1054	135.4777
4.9553	65.0695	1.0721	6.1699	C₂H₆ / A572 / 25°C	
6.0413	69.0223	1.9848	21.8827	0.0740	0.0772
6.9722	72.0958	2.9762	25.1710	0.1081	0.1575
7.9548	74.8756	3.9655	30.2209	0.2063	0.6169
8.9374	77.3011	5.0474	32.9124	0.3067	0.9517
9.9200	79.6070	6.0817	34.7481	0.4122	1.4059
10.9543	81.7717	6.9608	36.3724	0.5001	1.6776
11.9369	83.7722	7.9951	38.1914	0.6030	2.0239
13.0229	85.6924	8.9260	39.5497	0.8181	2.6406
13.9020	87.2124	9.9086	41.0080	0.9965	3.1569
15.8672	90.1021	10.9429	42.5664	3.1391	7.5656
17.9358	93.0420	11.9772	43.9364	4.9672	10.4386
20.1078	95.6124	12.9598	45.2895	7.1915	11.7017
21.8661	97.6387	13.8906	46.2819	9.0015	13.5355
23.7796	99.5192	15.8558	49.0990	11.1218	15.7972
26.0033	101.5776	18.3899	51.2486	13.1387	17.5908
27.9168	103.1471	19.8379	53.5142	14.8970	19.0718
29.7785	104.5742	22.5788	55.7481	18.3102	21.5165
35.2603	108.2946	23.7682	57.4133	20.8442	23.1887
40.0181	111.0585	26.7677	59.6096	25.0332	25.7207
44.9827	113.5727	27.7503	61.1238	29.9978	28.2948
49.9474	115.8040	29.7672	62.3442	45.2537	34.7950
60.1870	119.6437	34.9387	66.0337	54.6141	38.0758
69.7542	122.6588	40.9376	69.2286	64.4400	41.0507
79.7869	125.3514	44.7128	71.4128	74.5761	43.8535
89.9231	127.7012	51.1255	74.3885	85.1777	46.4667
99.8524	129.7496	59.4516	78.1567	89.5735	47.4558
110.0919	131.6052	71.3460	82.5829	99.7096	49.6543
119.8661	133.2212	79.5687	85.1854	110.4663	51.7775
149.7056	137.3064	89.5497	88.0477	114.5001	52.5906
200.9552	142.6141	100.5133	90.6613	120.4473	53.6791
250.2913	146.5045	109.7185	92.7879	149.7697	58.4495
300.0928	149.6379	120.4235	95.0507	199.6747	65.0064
349.8944	152.2480	151.1423	100.5335	225.0668	67.9145

PRESSURE (torr)	VOL ADS (cc/g STP)	PRESSURE (torr)	VOL ADS (cc/g STP)	PRESSURE (torr)	VOL ADS (cc/g STP)
249.9417	70.3847	249.7555	59.1006	299.6982	49.7412
299.3812	74.7661	300.0742	63.1898	350.0169	53.0908
350.7859	78.6114	350.0826	66.7363	400.4391	55.9872
399.0878	81.7964	399.8842	69.8315	449.2063	58.5827
449.7685	84.7674	449.4789	72.6603	500.4042	61.0156
499.9837	87.3677	500.5215	75.1965	549.5334	63.2198
549.7853	89.6812	549.5991	77.3881	600.3176	65.3078
599.6902	91.8232	599.9178	79.4286	650.2742	67.1274
649.9055	93.8427	650.0814	81.2637	699.6620	68.8362
700.4828	95.6571	699.9346	82.9277	760.1686	70.7890
759.5930	97.6207	759.5103	84.8600	C₂H₆ / A572 / 70°C	
C₂H₆ / A572 / 40°C		C₂H₆ / A572 / 55°C		0.3206	0.1896
0.0440	0.1051	0.0796	0.1002	0.6035	0.3755
0.0884	0.2119	0.1593	0.1950	0.8290	0.5228
0.1298	0.3141	0.2462	0.2787	1.0374	0.6532
0.2032	0.4900	0.3139	0.3558	2.0055	1.2582
0.3232	0.7380	0.4220	0.4772	3.0114	1.8179
0.4117	0.9480	0.5099	0.5734	4.0141	2.3581
0.5228	1.1947	0.6195	0.6932	5.0127	2.8603
0.6071	1.3677	0.8135	0.8937	6.0988	3.3646
0.7980	1.7469	0.9997	1.0830	7.1331	3.8367
0.9950	2.1113	3.0926	2.9001	8.1674	4.2932
3.1236	5.2261	4.9750	4.2720	9.3568	4.7904
4.9884	7.4652	7.1982	5.6671	10.0291	5.0209
7.1087	9.3871	8.9565	6.6594	11.1668	5.4805
8.9705	10.8685	11.0768	7.7562	12.0460	5.7685
11.0391	12.4873	13.1972	8.7966	13.2871	6.2622
13.1077	13.8043	15.3175	9.7428	14.1146	6.5127
15.1763	15.1086	18.2135	10.9374	16.0797	7.2331
18.1240	16.7505	20.9544	12.0394	17.9415	7.7763
21.1752	18.2814	25.2985	13.5768	20.1652	8.5199
25.1056	20.2939	29.9528	15.0535	22.2338	9.0438
30.7942	22.5789	45.1053	19.3120	23.9404	9.6283
44.8090	27.5355	54.9312	21.6213	25.9573	10.1046
54.5831	30.3652	64.6019	23.6500	27.8708	10.6849
64.7193	33.1603	74.7380	25.6794	29.9911	11.1590
76.1483	35.6628	85.5464	27.5702	34.7489	12.4403
84.6295	37.5601	89.5285	28.2304	41.0581	13.9333
90.4733	38.7355	100.0784	29.9084	45.1436	14.6979
99.8337	40.5236	110.2145	31.4230	49.8496	15.7374
110.2802	42.3459	115.0757	32.0821	60.5546	17.7172
114.6242	43.1231	119.8852	32.7472	69.8633	19.3477
120.5197	44.0472	150.2419	36.5433	80.5166	21.0499
149.3250	48.2431	201.4397	41.8512	89.8771	22.4668
202.6949	54.5361	224.8666	44.0161	100.1683	23.9223
224.5703	56.7852	250.1036	46.0798	110.2528	25.2290

PRESSURE (torr)	VOL ADS (cc/g STP)	PRESSURE (torr)	VOL ADS (cc/g STP)	PRESSURE (torr)	VOL ADS (cc/g STP)
120.6992	26.5201	352.0829	29.0342	90.0575	74.3208
150.1250	29.7772	400.1779	31.2671	99.6765	75.9410
200.9091	34.5557	451.9446	33.2419	109.0887	77.2685
250.8658	38.5969	500.3499	35.1484	119.5351	78.6389
300.0468	41.9463	551.6511	36.8558	149.4781	81.8222
350.4689	45.0286	600.6769	38.4850	200.7276	85.8357
400.8911	47.8909	650.2199	40.1131	249.3914	88.6965
450.5375	50.4168	699.8663	41.4120	300.1239	91.0850
501.8387	52.7629	760.1143	43.1476	349.3565	92.9920
551.2783	54.7861	SF₆ / A572 / -16°C		399.5718	94.6532
601.1832	56.7668	0.3548	4.0225	449.8905	96.0951
650.4160	58.5995	0.6035	6.7664	499.9506	97.3488
701.9241	60.4346	0.6718	7.4494	549.9073	98.4804
750.6913	61.9661	0.7318	8.1477	600.3295	99.4824
C₂H₆ / A572 / 100°C		0.8047	8.8428	649.7690	100.4066
0.2663	0.0632	0.8719	9.5267	700.2946	101.2643
0.4644	0.1111	0.9495	10.2042	750.0961	102.0480
0.6051	0.1452	1.0322	10.8637	SF₆ / A572 / 0°C	
0.7980	0.1926	1.9843	19.2088	0.1189	1.0340
1.0643	0.2575	3.0383	23.0191	0.2637	2.0684
3.0310	0.7188	3.9660	26.5125	0.4054	3.1001
5.0236	1.1579	5.0381	29.1928	0.5678	4.1291
7.5576	1.6597	5.9689	31.0305	0.6899	4.7955
9.5745	2.0556	7.0032	32.9544	0.8233	5.4779
11.0225	2.3503	7.9341	34.6469	0.9603	6.1328
13.7634	2.8465	8.9684	36.3105	1.1026	6.7737
15.0563	3.0792	10.0027	37.8591	1.9869	11.1618
18.4695	3.6989	10.9853	39.1820	3.0439	13.9817
21.1070	4.0909	11.9162	40.4440	3.9753	16.1176
25.6579	4.8122	13.0022	41.6881	4.9667	17.8535
30.5191	5.5318	14.0365	42.9414	5.9493	19.3417
44.8959	7.4637	16.1568	45.0490	6.9836	20.6921
54.5666	8.7057	18.0185	46.9572	7.9662	21.9227
65.1164	9.8520	20.2940	48.9065	9.0005	23.0256
75.4077	10.9706	21.8455	50.1714	9.9313	24.1709
85.2336	12.0049	24.1726	51.8861	11.1725	25.3813
90.1465	12.5004	25.7758	52.9968	11.9482	26.1179
99.5586	13.3238	27.7927	54.3075	13.1377	27.0749
110.3671	14.3341	29.9130	55.5592	13.8617	27.6671
115.5903	14.7827	35.0328	58.3188	16.1889	29.4317
120.1929	15.1359	40.0491	60.6621	18.0506	30.7076
150.7565	17.5248	44.8586	62.6731	20.1192	32.4525
202.1095	21.0296	50.0301	64.6034	22.1878	33.7026
225.3812	22.5368	60.0628	67.7096	23.8427	34.6680
250.7733	23.9281	69.8370	70.2079	26.0147	35.8457
299.4888	26.6187	79.7145	72.3865	28.0833	36.8679

PRESSURE (torr)	VOL ADS (cc/g STP)	PRESSURE (torr)	VOL ADS (cc/g STP)	PRESSURE (torr)	VOL ADS (cc/g STP)
30.1002	37.8249	24.1431	19.4105	18.2673	10.6856
35.2717	40.0760	26.0566	20.2501	19.8187	11.2432
40.1846	41.9758	28.3321	21.1627	22.3011	12.0814
44.8907	43.6590	29.7801	21.7302	23.8008	12.6121
50.1139	45.3712	34.7447	23.4422	26.2314	13.4287
60.0949	48.1881	39.8645	25.0686	28.0931	13.9187
69.9725	50.5821	44.9843	26.6067	30.1617	14.5976
79.9535	52.7255	50.1558	28.0413	35.1781	15.8625
89.9345	54.6559	60.2402	30.5063	39.7290	17.0840
100.1223	56.3918	69.9626	32.6334	46.0900	18.4980
109.7930	57.9147	79.9436	34.6083	49.9686	19.3900
119.9809	59.4267	89.9763	36.4282	60.9839	21.3970
149.9239	62.9987	100.0091	38.1182	69.6720	22.9365
200.2426	67.5117	110.1969	39.6857	80.5839	24.6495
250.5095	70.8748	120.0745	41.0668	89.7891	26.0301
299.7939	73.4926	149.0866	44.5979	99.2530	27.2650
350.2678	75.7106	201.2153	49.6853	109.5443	28.5788
399.9142	77.5177	249.2585	53.3706	120.3010	29.8749
450.3880	79.1216	299.8358	56.5462	150.3474	32.9670
499.9310	80.5209	349.3271	59.1571	200.6144	37.1495
550.3014	81.7470	399.6458	61.4294	249.2782	40.4337
600.1547	82.8496	449.8093	63.4069	299.8555	43.3835
650.1113	83.8600	499.9729	65.1594	350.5362	45.8296
700.1198	84.7871	550.0330	66.7138	400.6997	47.9659
750.1282	85.6499	600.0414	68.1012	449.9324	49.8524
SF ₆ / A572 / 30°C		649.9464	69.3780	500.3545	51.5374
0.4189	0.9962	700.2651	70.5464	549.3803	52.9596
0.7473	1.7002	750.1700	71.5943	600.5782	54.4368
1.0907	2.3665	SF ₆ / A572 / 50°C		649.4489	55.6561
1.9895	3.9484	0.3879	0.4985	700.0778	56.7050
2.9907	5.3400	0.8135	0.9959	751.2757	57.7747
3.9727	6.6474	1.2427	1.4425	SF ₆ / A572 / 65°C	
5.0603	7.7621	2.0014	2.2097	0.5911	0.4792
6.0429	8.7020	3.0517	3.0769	1.1470	0.8925
6.9738	9.5164	3.9727	3.7963	1.9993	1.4875
8.0081	10.3324	5.0800	4.5399	3.0558	2.1312
9.0941	11.1854	6.0625	5.1585	3.9862	2.6678
9.9215	11.7955	7.0451	5.6853	4.9946	3.1896
11.0075	12.4979	7.9760	6.2158	6.1324	3.7244
12.0418	13.1944	9.0620	6.7863	7.2184	4.2060
13.0761	13.8284	10.0963	7.2789	8.2010	4.6384
14.0587	14.4097	11.0789	7.7444	9.2870	5.0858
16.0756	15.5211	12.1649	8.2587	10.0627	5.3857
17.9891	16.5218	12.9406	8.5758	11.3039	5.9011
20.0059	17.5448	14.1301	9.1235	12.0796	6.1611
22.1780	18.5390	16.0435	9.8952	12.9587	6.4531

PRESSURE (torr)	VOL ADS (cc/g STP)	PRESSURE (torr)	VOL ADS (cc/g STP)	PRESSURE (torr)	VOL ADS (cc/g STP)
14.1999	6.8999	11.4352	4.1459	9.0279	2.2303
16.1651	7.5822	12.0041	4.2727	10.1139	2.4310
18.4923	8.3053	13.2452	4.6035	11.7688	2.7835
19.9920	8.7094	14.1244	4.8237	12.2859	2.8696
22.3709	9.4055	16.1413	5.3295	13.3202	3.0846
24.0775	9.8565	18.3650	5.8886	14.5097	3.3207
25.7841	10.3248	20.1233	6.2330	15.9060	3.5579
28.2664	10.9559	22.1919	6.7452	18.4400	4.0081
29.9213	11.3766	24.1054	7.0988	20.0949	4.2698
35.1962	12.5521	26.1740	7.5842	22.0084	4.5504
40.0574	13.6226	28.1392	7.9178	23.9218	4.8473
45.1772	14.6960	30.1560	8.3755	26.6110	5.2546
50.1935	15.6689	35.0690	9.2600	28.0073	5.4918
60.4331	17.4622	40.0853	10.0831	29.9207	5.8259
70.0521	18.9888	45.2051	10.9143	35.2991	6.5225
79.4642	20.2517	50.3249	11.7668	40.4189	7.1681
90.2210	21.7203	60.5645	13.2104	45.3835	7.8781
99.4262	22.8164	70.0800	14.4547	50.2447	8.3711
110.1312	24.2263	80.1645	15.6652	59.9154	9.4889
120.2157	25.1807	89.9903	16.7836	71.2927	10.6201
150.3655	28.1604	100.1264	17.8674	79.5671	11.3885
204.2525	32.3646	109.3317	18.7406	90.6342	12.4344
250.0720	35.4193	120.6056	19.7900	99.8911	13.1542
300.9079	38.3231	150.7037	22.2821	110.8547	14.0785
349.8820	40.7113	200.7638	25.7556	119.9048	14.7445
400.8213	42.9395	251.0825	28.7722	149.5893	16.7676
450.4677	44.8393	300.2118	31.2357	201.1491	19.7670
500.9932	46.6431	350.7373	33.4740	250.8472	22.2440
549.7087	48.1235	400.9009	35.4524	301.2177	24.4251
601.2686	49.6310	451.0644	37.2267	351.2778	26.3667
649.5187	50.9133	501.1245	38.8251	401.4930	28.0993
700.0959	52.0799	551.0812	40.3236	451.8117	29.6590
751.0869	53.3060	600.4174	41.6669	501.6650	31.0980
SF ₆ / A572 / 80°C		651.2532	42.9378	551.7251	32.4417
0.4872	0.2337	701.4684	44.1066	601.6818	33.6797
0.9603	0.4632	751.1149	45.2451	651.8970	34.8404
1.3751	0.6547	SF ₆ / A572 / 95°C		701.8020	35.9381
2.0081	0.9439	0.7085	0.2056	749.3281	37.0279
3.0522	1.3835	1.2903	0.3703		
4.0058	1.7452	2.0102	0.5705		
4.9708	2.1058	3.0031	0.8366		
6.2120	2.5274	4.0110	1.0904		
6.9360	2.7702	4.9941	1.3309		
8.3840	3.2345	6.3387	1.6308		
9.3666	3.5001	7.3213	1.8708		
10.5044	3.8604	8.2522	2.0504		

PRESSURE (torr)	VOL ADS (cc/g STP)	PRESSURE (torr)	VOL ADS (cc/g STP)	PRESSURE (torr)	VOL ADS (cc/g STP)
N₂ / A600 / -93°C		120.1588	35.3117	35.0990	5.6879
0.0786	0.0984	149.1709	38.3895	40.3222	6.3491
0.1396	0.2005	200.9893	42.7996	45.3903	6.9798
0.2575	0.3566	249.2911	46.0892	49.7860	7.5001
0.3243	0.4576	299.4547	48.9254	60.3359	8.6597
0.3925	0.5582	349.7216	51.3409	70.1100	9.6738
0.4608	0.6588	399.7818	53.4452	80.2979	10.6575
0.5306	0.7590	450.0488	55.3079	89.9686	11.5299
0.6009	0.8592	499.9537	56.9656	99.0187	12.3231
0.6718	0.9593	550.1690	58.4609	110.3960	13.2489
0.7447	1.0589	600.0223	59.8228	119.3427	13.9362
0.8192	1.1583	650.1341	61.0840	150.2166	16.1364
0.8947	1.2573	700.2459	62.2273	201.1558	19.2333
0.9697	1.3566	749.9957	63.2935	249.9231	21.7550
1.0452	1.4558	N₂ / A600 / -62°C		299.9315	24.0200
2.0252	2.6393	0.2808	0.0472	350.0433	26.0195
3.0269	3.7068	0.4535	0.0837	399.8449	27.8119
3.9696	4.6234	0.5668	0.1065	450.1118	29.4557
4.9895	5.5313	0.6630	0.1258	500.0685	30.9546
5.9720	6.3315	0.7483	0.1435	550.1804	32.3363
7.0063	7.1362	0.8249	0.1590	600.3439	33.6174
8.0924	7.9247	0.8678	0.1678	650.0937	34.8030
8.9715	8.5114	0.9066	0.1760	700.4642	35.9319
9.9024	9.1231	0.9640	0.1876	750.2140	36.9699
10.9884	9.7788	1.0203	0.1991	N₂ / A600 / -43°C	
12.0744	10.4243	1.9967	0.4038	0.3837	0.0276
13.0570	11.0047	3.0310	0.6133	0.5606	0.0428
14.0913	11.5689	3.9919	0.8044	0.7199	0.0558
16.1082	12.5858	5.0008	1.0011	0.8342	0.0653
18.0216	13.4763	6.3454	1.2473	0.8947	0.0703
20.0385	14.4013	7.0177	1.3781	0.9774	0.0770
22.2106	15.3038	7.9486	1.5540	1.0529	0.0835
24.2792	16.1259	9.4483	1.8102	2.0086	0.1690
26.3478	16.9276	10.2241	1.9508	3.0134	0.2582
27.7958	17.4612	11.1032	2.1117	4.0012	0.3449
30.1230	18.2544	12.4995	2.3376	4.9993	0.4320
34.6739	19.7246	12.9650	2.4180	6.4473	0.5635
40.4660	21.3890	14.0510	2.5937	7.4299	0.6513
45.0169	22.6191	16.1713	2.9604	7.9470	0.6954
50.1884	23.8974	18.1364	3.2613	9.0331	0.7941
60.0659	26.0453	19.8430	3.5323	10.5845	0.9263
69.9435	27.9841	22.3771	3.9134	11.1017	0.9703
80.2348	29.7641	24.0320	4.1642	12.0842	1.0530
89.9055	31.2965	25.8937	4.4301	13.5840	1.1744
100.1968	32.7697	28.5312	4.7959	14.1011	1.2185
110.0226	34.0708	30.1860	5.0216	16.5834	1.4125

PRESSURE (torr)	VOL ADS (cc/g STP)	PRESSURE (torr)	VOL ADS (cc/g STP)	PRESSURE (torr)	VOL ADS (cc/g STP)
18.1349	1.5344	9.0491	14.8096	0.7447	0.3088
20.1001	1.6843	9.9800	15.6554	0.7824	0.3268
21.9101	1.8282	11.0143	16.4720	0.8161	0.3418
23.9270	1.9887	11.8934	17.1275	0.8440	0.3546
26.1507	2.1607	12.9277	17.8654	0.8704	0.3665
28.1159	2.2952	13.9620	18.5744	0.8967	0.3783
29.9259	2.4289	16.0306	19.8642	0.9236	0.3900
35.2008	2.8085	17.9441	20.9764	0.9490	0.4020
41.0446	3.2171	20.0127	22.0965	0.9759	0.4137
45.0267	3.5020	21.8744	22.9936	1.0028	0.4254
49.7845	3.8222	23.8396	23.8987	2.0050	0.8563
60.1792	4.4934	26.0116	24.8116	3.0279	1.2715
70.3671	5.1328	28.0285	25.6049	3.9960	1.6496
79.4172	5.6629	30.1488	26.3852	4.9993	2.0271
90.1739	6.2903	34.8549	28.0320	6.1887	2.4333
99.4826	6.8015	40.2850	29.7593	7.1713	2.7775
109.3084	7.3210	45.0427	31.1074	8.2573	3.1427
119.1860	7.8305	50.0074	32.3682	8.9296	3.3638
150.2667	9.3268	59.8849	34.6776	10.2742	3.7910
200.7923	11.5127	70.4348	36.7991	10.9982	4.0227
250.2318	13.4106	79.7952	38.4427	11.9291	4.3012
300.1368	15.1270	89.8796	40.0265	13.1703	4.6471
350.0935	16.7056	100.0158	41.4566	13.8943	4.8735
400.2570	18.1555	110.1002	42.7204	15.9629	5.4366
450.0586	19.4819	119.9260	43.8489	18.1866	6.0409
500.1704	20.7282	149.9725	47.0166	20.4621	6.6053
550.1271	21.8969	199.8257	51.2446	21.9101	6.9679
600.2906	22.9901	249.6273	54.5718	24.4441	7.5794
650.0922	24.0247	300.1011	57.3021	25.9956	7.9476
700.3592	25.0105	350.5232	59.5889	27.8573	8.3581
750.1090	25.9370	399.4973	61.5052	30.1845	8.8573
CO / A600 / -93°C		449.7126	63.2546	34.6837	9.7892
0.1614	0.4860	500.1347	64.7929	40.1655	10.8482
0.3175	0.9728	549.8328	66.1468	44.9750	11.7321
0.4644	1.4611	600.0481	67.3702	50.0948	12.6131
0.6175	1.9483	649.9531	68.4703	59.9723	14.1758
0.7773	2.4346	700.0132	69.4791	70.1085	15.6339
0.9448	2.9194	750.0733	70.3962	79.9860	16.9399
1.1196	3.4034	CO / A600 / -62°C		90.0187	18.1715
2.0009	5.5958	0.1665	0.0610	100.0515	19.3216
3.0010	7.5741	0.3077	0.1160	110.1359	20.3874
3.9717	9.2421	0.4023	0.1568	119.9617	21.3750
5.0153	10.7399	0.4897	0.1945	149.5427	24.0223
6.0496	11.7304	0.5699	0.2303	200.9474	27.8324
7.0322	12.8659	0.6454	0.2634	249.6112	30.8160
8.0148	13.8357	0.6997	0.2879	299.3611	33.4171

PRESSURE (torr)	VOL ADS (cc/g STP)	PRESSURE (torr)	VOL ADS (cc/g STP)	PRESSURE (torr)	VOL ADS (cc/g STP)
349.6798	35.7053	80.0036	9.1674	30.0299	27.6836
399.8433	37.7198	90.1398	10.0184	35.1497	29.7100
449.8517	39.5255	100.2242	10.8063	40.0626	31.4332
500.0153	41.1573	109.0675	11.4786	44.9755	32.9997
549.9720	42.6499	120.2896	12.2771	50.1470	34.4662
600.0838	44.0287	150.1292	14.2394	60.0246	36.9463
650.0922	45.2910	199.3101	17.0468	70.1607	39.1311
699.9454	46.4662	250.0943	19.5194	79.8314	40.9670
750.1090	47.5694	299.5855	21.6417	89.9676	42.6886
CO / A600 / -43°C					
0.2917	0.0340	349.9042	23.5686	100.0520	44.2198
0.4872	0.0647	399.9643	25.2990	110.0330	45.5944
0.5994	0.0816	449.9727	26.8881	120.0140	46.8617
0.6976	0.0967	500.1363	28.3436	150.2155	50.1295
0.7824	0.1099	549.9896	29.6756	200.4308	54.3336
0.8450	0.1193	600.0497	30.9200	249.9738	57.5827
0.9138	0.1305	650.1098	32.0908	300.4993	60.2788
0.9712	0.1396	700.0665	33.1973	349.3183	62.4502
1.0224	0.1477	750.1783	34.2250	399.4818	64.3830
CH4 / A600 / -62°C					
1.9941	0.3125	0.1629	0.4846	449.8005	66.0913
3.0455	0.4855	0.3274	0.9691	499.9641	67.6046
3.9924	0.6391	0.4820	1.4553	549.9725	68.9610
5.0169	0.8027	0.6428	1.9404	600.0326	70.1906
6.0512	0.9323	0.8119	2.4243	649.9893	71.3172
7.2923	1.1164	0.9888	2.9062	699.9977	72.3662
8.0681	1.2308	1.1734	3.3871	750.1095	73.3380
CH4 / A600 / -43°C					
8.9472	1.3700	2.0236	5.3754	0.1034	0.1172
9.9815	1.5143	3.0667	7.3595	0.1996	0.2328
11.3261	1.6987	3.9712	8.8715	0.3558	0.4005
12.0501	1.8179	4.9998	10.3609	0.4737	0.5380
13.0327	1.9475	6.1375	11.5831	0.5802	0.6615
14.1704	2.1068	7.0167	12.6279	0.6847	0.7801
16.1356	2.3806	8.1027	13.8057	0.7912	0.8974
18.5145	2.6943	8.9301	14.6648	0.8693	0.9827
19.9625	2.8933	9.9127	15.5932	0.9588	1.0806
21.8242	3.1373	10.9470	16.5415	1.0508	1.1784
24.4100	3.4761	12.0330	17.4074	1.9983	2.1170
26.0649	3.6755	12.9639	18.1502	3.0305	3.0314
27.9266	3.9048	13.9982	18.9621	3.9665	3.7884
29.7884	4.1340	16.2220	20.5189	4.9889	4.5470
35.0633	4.7617	18.0837	21.6781	6.0750	5.2457
40.2348	5.3404	20.1006	22.8775	7.0058	5.8510
45.3029	5.8939	21.9623	23.8756	8.0918	6.5599
49.5435	6.3381	23.8758	24.8695	9.0744	7.0947
59.4211	7.3167	26.0995	25.9388	9.9536	7.5979
70.1778	8.3069	28.1164	26.8410	11.0913	8.2009

PRESSURE (torr)	VOL ADS (cc/g STP)	PRESSURE (torr)	VOL ADS (cc/g STP)	PRESSURE (torr)	VOL ADS (cc/g STP)
12.0739	8.7053	10.0684	2.5053	6.9438	6.1999
13.2116	9.2523	10.9993	2.7039	7.9781	6.8379
14.1942	9.6854	12.4990	3.0306	9.0124	7.3964
15.9525	10.4426	13.5333	3.2408	10.0984	7.9611
18.0728	11.3157	14.0504	3.3632	11.0810	8.4685
20.1932	12.1379	16.0673	3.7678	12.1670	8.9786
22.3135	12.9045	18.3428	4.2111	13.1496	9.4364
23.8132	13.4145	19.8942	4.5188	13.8736	9.7434
26.2955	14.2410	22.4800	5.0019	16.2525	10.6943
27.9504	14.7632	24.0314	5.2898	18.3728	11.5092
29.8121	15.3132	25.9966	5.6188	19.8725	11.9950
34.9319	16.7702	28.3238	6.0283	22.2514	12.7917
40.2586	18.1434	30.0304	6.3186	24.0097	13.3141
44.9129	19.2752	35.0467	7.1334	26.4403	14.0425
50.2396	20.4355	40.1665	7.9054	28.0952	14.4777
59.6517	22.3233	45.2346	8.6564	29.8535	14.9453
70.2533	24.2200	49.7855	9.2850	35.2836	16.2876
80.1826	25.8049	60.2837	10.6487	40.1965	17.3635
90.0084	27.2320	70.1095	11.8380	44.6440	18.2432
100.2480	28.6060	80.2974	12.9642	50.0224	19.2569
110.2290	29.7962	89.9681	13.9821	60.4688	20.8726
119.0722	30.7895	100.3111	14.9958	69.9326	22.2290
149.1187	33.8602	109.1026	15.8111	79.3965	23.3674
202.3334	38.1647	120.2213	16.7925	90.0498	24.5910
249.5492	41.2147	150.4229	19.1701	99.3585	25.5109
300.0747	43.9341	200.7933	22.5144	109.2878	26.4169
349.6177	46.1985	249.8708	25.2476	119.8376	27.3935
399.7296	48.1854	299.4655	27.6217	151.0735	29.5475
449.8414	49.9471	349.6808	29.7355	199.2719	32.2544
500.0566	51.5197	399.9995	31.6195	250.2111	34.4568
550.0651	52.9209	449.9045	33.3084	300.5298	36.3054
600.0217	54.1894	500.0680	34.8624	350.1245	37.7229
650.0302	55.3623	550.1281	36.2659	399.0986	38.9388
700.3488	56.4162	600.0848	37.5528	450.7102	40.2189
750.7192	57.4171	649.9381	38.7748	500.3049	41.1247
CH ₄ / A600 / -16°C		700.3085	39.9153	550.7787	42.0722
0.6170	0.1545	750.0066	40.9657	599.8563	42.8550
1.0938	0.2853	C ₂ H ₆ / A600 / 40°C		649.5544	43.6193
2.0040	0.5370	0.3884	0.5098	699.8730	44.2949
3.0233	0.8111	0.7716	0.9991	749.7263	44.9287
3.9981	1.0665	1.1584	1.4494	C ₂ H ₆ / A600 / 55°C	
5.0003	1.3223	1.9910	2.3652	0.3987	0.2655
6.2932	1.6309	3.0046	3.2993	0.7333	0.5054
7.0172	1.8063	3.9898	4.1512	1.0436	0.7190
7.9481	2.0247	5.0303	4.9279	1.9972	1.3505
9.2410	2.3233	6.1163	5.6617	3.0470	1.9810

PRESSURE (torr)	VOL ADS (cc/g STP)	PRESSURE (torr)	VOL ADS (cc/g STP)	PRESSURE (torr)	VOL ADS (cc/g STP)
4.0074	2.5265	1.0421	0.4013	C₂H₆ / A600 / 100°C	
4.9812	3.0268	1.9998	0.7876	0.5735	0.0806
6.0672	3.5295	3.0600	1.1807	1.0596	0.1506
7.1015	3.9953	3.9971	1.5247	2.0340	0.2989
8.1875	4.4727	5.0448	1.8822	3.0362	0.4488
8.9632	4.7639	6.2342	2.2673	4.0193	0.5874
10.1527	5.2494	7.3203	2.5858	5.0350	0.7327
11.0318	5.5487	7.9926	2.7852	6.3278	0.9284
12.2730	6.0055	9.3371	3.1544	7.2070	1.0412
13.1004	6.2525	9.9577	3.3526	8.4999	1.2218
14.2382	6.6453	10.9920	3.6351	8.9653	1.2815
16.2033	7.2397	11.9746	3.8670	10.1030	1.4225
18.2719	7.8679	13.2675	4.2054	11.4993	1.5865
19.9268	8.3066	14.1466	4.4002	12.8957	1.7556
22.3057	8.9539	16.0084	4.8714	13.3611	1.8104
24.0123	9.3587	17.9218	5.2501	14.2920	1.9098
25.7706	9.8055	20.1456	5.7599	16.2571	2.1817
28.3564	10.3831	22.1107	6.1349	18.1706	2.3773
29.9595	10.7545	24.0242	6.4790	20.4460	2.6690
34.9759	11.7837	26.2997	6.9607	22.2044	2.8498
40.0440	12.7335	28.1097	7.2676	24.0661	3.0188
45.1637	13.6747	29.8163	7.5818	26.3933	3.3072
49.7147	14.3764	35.2981	8.5187	28.2550	3.4912
60.0059	15.9360	40.4179	9.3186	30.1167	3.6403
69.5215	17.0683	44.7619	9.9358	35.0814	4.1672
80.1231	18.3238	50.2437	10.6901	39.9426	4.5914
89.4318	19.2729	60.5350	11.9790	44.9590	4.9758
99.2059	20.2206	70.0506	13.0910	50.4407	5.5242
110.2729	21.2270	79.6695	13.9893	60.9389	6.3674
119.7368	21.9378	90.4263	15.0148	69.7822	6.9444
149.6798	24.0102	99.5281	15.7858	80.7974	7.7146
202.2222	26.8748	109.1471	16.5995	89.9510	8.2710
250.3689	29.0323	119.4384	17.3115	99.3631	8.8854
300.5324	30.7336	149.7434	19.2806	109.1890	9.5428
350.7477	32.2567	202.1307	22.0275	120.3594	10.0344
399.7735	33.5278	250.7428	24.0661	150.7161	11.5437
449.7819	34.6829	300.4926	25.9312	203.1034	13.7414
499.8420	35.7131	350.1907	27.2772	251.4052	15.4425
549.9539	36.6381	400.9231	28.6374	299.9139	16.9043
599.8588	37.4972	450.9832	29.8097	351.5255	18.3261
650.1776	38.2575	499.4402	30.8382	400.1893	19.4579
699.7722	38.9552	551.4138	31.8218	451.6974	20.5916
749.7289	39.6683	599.5604	32.6498	500.0510	21.5609
C₂H₆ / A600 / 70°C		649.1034	33.5379	549.1285	22.6330
0.4153	0.1469	700.5081	34.1864	601.9812	23.3088
0.7530	0.2845	750.8268	34.9753	650.3865	24.1158

PRESSURE (torr)	VOL ADS (cc/g STP)	PRESSURE (torr)	VOL ADS (cc/g STP)	PRESSURE (torr)	VOL ADS (cc/g STP)
700.7569	24.8121	651.9938	19.9615	550.3221	17.1529
751.3859	25.4662	702.2607	20.3266	599.8134	17.5899
SF ₆ / A600 / 50°C		752.3726	20.6830	650.2872	18.0165
1.3606	0.5291	SF ₆ / A600 / 65°C		700.4507	18.3766
1.9962	0.8423	0.8083	0.1566	751.0280	18.7671
3.3801	1.2859	1.3399	0.2834	SF ₆ / A600 / 80°C	
3.9784	1.5334	2.0453	0.4633	0.5358	0.0766
5.3494	1.9240	3.0269	0.6970	0.9552	0.1433
5.9700	2.0428	3.9831	0.9154	1.3053	0.2013
7.2629	2.3022	4.9874	1.1405	1.9983	0.3215
8.1420	2.4738	6.0217	1.2836	3.0248	0.4820
9.0729	2.6672	7.3663	1.4980	4.0012	0.6473
10.5209	2.9411	8.5040	1.6878	5.1275	0.8092
10.9346	3.0589	9.5900	1.8812	6.0067	0.9130
12.1758	3.2763	9.9520	1.9539	6.9376	1.0285
13.0549	3.4681	11.0380	2.1031	7.9202	1.1407
14.2961	3.6705	12.4861	2.3201	9.3165	1.3318
16.3130	3.9958	13.7272	2.5076	10.2990	1.4490
18.0196	4.2368	14.0375	2.5839	11.7988	1.6181
20.3985	4.6333	16.3647	2.8862	12.2125	1.6868
22.2085	4.8723	18.3299	3.1353	13.1951	1.7840
24.1737	5.1408	20.0365	3.3291	14.5397	1.9330
25.8285	5.3752	21.8982	3.5364	16.0911	2.0836
27.9489	5.6383	24.3805	3.8622	18.3149	2.3263
29.8623	5.8752	26.2423	4.0450	20.0215	2.4919
35.3958	6.4235	27.8454	4.2116	22.0383	2.6677
40.8776	6.9908	29.8106	4.4168	23.9001	2.8385
45.1182	7.3708	35.2407	4.8926	25.8653	3.0275
49.9794	7.7689	39.6364	5.2696	27.9856	3.2013
60.2190	8.5094	45.4285	5.7983	29.8990	3.3685
69.5277	9.1317	50.1863	6.1256	35.5877	3.7778
79.6121	9.7323	59.9087	6.7942	39.6732	4.1004
89.4897	10.2860	69.6829	7.3560	44.9998	4.4376
99.6258	10.8213	79.2501	7.9225	49.6024	4.7616
109.7103	11.3003	89.5414	8.4526	60.4109	5.3755
119.8464	11.7305	99.5224	8.9416	69.5644	5.8759
150.7720	12.7829	109.7620	9.3624	79.7006	6.3832
199.8495	14.1147	119.5878	9.7732	89.6816	6.8495
249.8062	15.1710	150.2548	10.7705	99.9729	7.2654
299.5560	16.0581	199.2289	12.0938	109.5918	7.6799
349.8230	16.8565	249.5476	13.1475	120.0383	8.0504
400.5554	17.5125	299.2458	14.0514	150.4984	9.0178
450.9258	18.1176	349.9265	14.8493	199.2657	10.2402
501.2963	18.6522	400.2451	15.5324	249.5326	11.2891
551.6149	19.1449	449.9950	16.1330	299.9547	12.1768
602.0888	19.5514	500.0551	16.6872	349.9632	12.9381

PRESSURE (torr)	VOL ADS (cc/g STP)	PRESSURE (torr)	VOL ADS (cc/g STP)
401.4713	13.6255	300.4124	10.2498
451.9969	14.2294	350.1623	10.9937
502.2121	14.7676	401.3601	11.6691
552.6860	15.2335	451.6788	12.2923
602.5909	15.7064	502.4112	12.7848
653.2717	16.0631	552.0059	13.3308
702.9697	16.4794	603.1003	13.7059
753.5988	16.7787	652.3330	14.1911
SF ₆ / A600 / 95°C		703.5309	14.4850
0.7142	0.0630	752.8152	14.8924
1.1920	0.1098		
1.9900	0.1941		
3.0238	0.3018		
3.9965	0.4032		
5.0169	0.5059		
6.3092	0.6355		
7.2918	0.7257		
8.7915	0.8519		
9.2053	0.9044		
10.3947	0.9912		
11.8427	1.1306		
12.3082	1.1749		
13.3942	1.2534		
14.8422	1.3780		
16.0834	1.4663		
18.4105	1.6629		
20.1171	1.7857		
22.1857	1.9098		
23.8923	2.0325		
25.9092	2.1848		
27.9261	2.3271		
30.0464	2.4479		
35.6316	2.7911		
40.1308	3.0309		
44.7335	3.3086		
49.9050	3.5794		
60.3514	4.1341		
70.2290	4.5223		
79.4342	4.9044		
89.6221	5.3271		
99.9134	5.6936		
109.7392	6.0654		
120.0822	6.3841		
150.4906	7.3253		
200.1888	8.3947		
249.4732	9.3719		

PRESSURE (torr)	VOL ADS (cc/g STP)	PRESSURE (torr)	VOL ADS (cc/g STP)	PRESSURE (torr)	VOL ADS (cc/g STP)
N₂ / BPL / -93°C		650.1625	73.4739	109.2055	11.1271
0.4194	0.4802	699.9641	75.6185	119.0831	11.8384
0.8305	0.9501	750.3862	77.6225	149.3881	13.8654
1.2500	1.3790	N₂ / BPL / -62°C		199.3965	16.8450
1.9879	2.0859	0.3108	0.0441	250.0772	19.5481
3.0419	2.9609	0.5006	0.0757	300.1373	21.9493
3.9722	3.6762	0.6361	0.0991	349.8354	24.1567
5.0184	4.4001	0.7349	0.1162	400.3093	26.2245
5.9488	4.9857	0.7840	0.1243	450.4728	28.1501
7.0348	5.6578	0.8316	0.1320	500.1192	29.9546
8.1208	6.2680	0.8714	0.1389	550.2311	31.6813
9.1551	6.8476	0.9076	0.1448	600.2912	33.3260
10.1377	7.3554	0.9391	0.1502	650.2996	34.8745
11.1203	7.8529	0.9666	0.1549	700.1011	36.3553
11.8960	8.2489	0.9919	0.1593	750.3164	37.7994
13.1372	8.8166	1.0162	0.1636	N₂ / BPL / -43°C	
13.8612	9.1460	2.0014	0.3389	0.4334	0.0232
15.9298	10.0269	3.0321	0.5135	0.6563	0.0378
18.1535	10.9374	3.9877	0.6714	0.7535	0.0434
20.1704	11.7053	5.0003	0.8346	0.8367	0.0486
22.2390	12.4881	6.0341	0.9576	0.9066	0.0530
23.8422	13.0479	7.2753	1.1476	0.9640	0.0567
26.1176	13.8084	8.6199	1.3484	1.0136	0.0601
27.7208	14.3425	9.2922	1.4488	2.0262	0.1421
30.1514	15.1227	10.2230	1.5761	3.0553	0.2232
34.9609	16.5338	11.5159	1.7613	3.9950	0.2967
40.0290	17.9477	11.9813	1.8301	4.9998	0.3747
45.3039	19.3034	13.0673	1.9736	6.0858	0.4331
49.9582	20.4633	14.4119	2.1642	7.6890	0.5532
60.1978	22.7651	15.8600	2.3607	8.2579	0.6055
69.9202	24.7875	18.3423	2.6851	9.3439	0.6841
80.2115	26.7540	20.2040	2.9145	10.1713	0.7394
90.0374	28.4922	21.9623	3.1432	11.1539	0.8168
100.1218	30.1563	23.8241	3.3776	11.9296	0.8716
109.9476	31.6876	25.8927	3.6135	13.1708	0.9672
120.1872	33.2000	27.7544	3.8275	14.8774	1.0784
150.8542	37.3320	29.7713	4.0630	16.0668	1.1736
201.1729	43.1719	34.8911	4.6317	18.1871	1.3102
249.8367	48.0052	40.5280	5.2448	19.9454	1.4371
299.3797	52.3353	44.7686	5.6815	21.9106	1.5767
349.8018	56.2905	49.6816	6.1633	23.9792	1.7075
400.2239	59.8493	59.4040	7.0858	25.9961	1.8478
449.9738	63.0530	70.3158	8.0470	28.3233	2.0019
500.2408	65.9908	80.0900	8.8846	30.0816	2.1189
549.8354	68.6824	89.2435	9.6215	35.5117	2.4666
600.3093	71.1969	100.1037	10.4554	39.8040	2.7301

PRESSURE (torr)	VOL ADS (cc/g STP)	PRESSURE (torr)	VOL ADS (cc/g STP)	PRESSURE (torr)	VOL ADS (cc/g STP)
44.8204	3.0325	26.1605	19.0652	6.2342	1.9536
49.7850	3.3242	28.2809	19.8598	7.1651	2.2161
60.0763	3.9169	30.2460	20.5987	7.9408	2.4383
69.3333	4.4366	35.3141	22.3394	8.9234	2.6908
79.3143	4.9599	39.9167	23.8235	10.2163	3.0036
89.1401	5.4762	45.1400	25.3649	11.0437	3.1904
99.3280	5.9826	49.8977	26.6990	12.0263	3.4276
109.2572	6.4748	59.8270	29.2312	13.2158	3.7306
119.3934	6.9443	70.0149	31.6058	14.1984	3.9324
150.0604	8.3327	80.0476	33.7293	16.0601	4.3361
200.1722	10.3847	89.9251	35.6677	18.1804	4.8057
250.0772	12.2524	100.0096	37.5244	19.8353	5.1336
300.1890	13.9904	110.0940	39.2575	22.3693	5.6128
350.1457	15.6154	120.0233	40.8659	23.9208	5.9055
400.2058	17.1352	150.5868	45.3376	26.4548	6.3899
450.1108	18.5719	201.2158	51.5713	28.0580	6.6723
500.0675	19.9490	249.2074	56.5969	29.8680	6.9950
550.3345	21.2626	299.2675	61.1668	34.8844	7.8376
600.1877	22.5211	349.5862	65.2364	40.1593	8.6498
650.2996	23.7322	399.8531	68.8790	45.1239	9.3915
700.1528	24.8947	449.7581	72.1718	49.5714	10.0271
750.3164	26.0096	499.9734	75.2043	59.4490	11.3588
CO / BPL / -93°C					
0.1960	0.5219	549.9301	77.9734	70.2574	12.6791
0.4173	1.0316	599.9385	80.5344	79.8764	13.7926
0.6532	1.5385	649.8951	82.9348	90.2194	14.8963
0.8952	2.0027	700.0587	85.1939	99.8901	15.8983
1.1553	2.4621	750.0154	87.3098	110.2331	16.9108
CO / BPL / -62°C					
2.0453	3.8166	0.1976	0.0523	149.8468	20.3676
3.0041	5.0356	0.3584	0.1035	200.5275	24.1605
3.9727	6.1170	0.4639	0.1457	249.9670	27.3850
4.9574	7.0913	0.5518	0.1811	299.6134	30.2880
6.1468	8.1489	0.6113	0.2041	349.8287	32.9597
7.0777	8.9169	0.6666	0.2257	399.9922	35.3986
8.0086	9.6407	0.7183	0.2456	449.8972	37.6531
8.9912	10.3587	0.7643	0.2643	500.1642	39.7464
10.0255	11.0511	0.8099	0.2812	549.8623	41.7030
11.0598	11.7092	0.8523	0.2970	600.1293	43.5776
11.8872	12.2337	0.8916	0.3113	650.1377	45.3308
12.9732	12.8466	0.9272	0.3246	700.1461	46.9669
13.9041	13.3986	0.9712	0.3407	749.8959	48.5286
16.2830	14.6406	1.0002	0.3512	CO / BPL / -43°C	
17.8344	15.4363	1.9931	0.7009	0.3201	0.0296
20.1099	16.4785	3.0295	1.0416	0.5280	0.0566
21.9199	17.3184	3.9857	1.3398	0.6439	0.0725
24.2988	18.3000	4.9931	1.6406	0.7406	0.0865

PRESSURE (torr)	VOL ADS (cc/g STP)	PRESSURE (torr)	VOL ADS (cc/g STP)	PRESSURE (torr)	VOL ADS (cc/g STP)
0.8233	0.0992	650.0415	31.2172	449.7529	79.2538
0.8942	0.1100	700.2568	32.5429	500.0199	82.7144
0.9557	0.1196	750.0583	33.8071	549.8215	85.8746
1.0090	0.1277	CH ₄ / BPL / -62°C		600.0367	88.8091
2.0107	0.2810	0.2601	0.5310	649.9417	91.5170
3.0227	0.4290	0.5042	1.0416	699.8984	94.0689
4.0152	0.5708	0.7638	1.5366	750.1136	96.4709
5.0003	0.7085	1.0353	1.9986	CH ₄ / BPL / -43°C	
5.9829	0.8091	1.9967	3.4430	0.5746	0.4587
7.3275	1.0025	2.9907	4.6969	1.1041	0.8729
8.2584	1.1181	3.9707	5.8092	2.0474	1.5502
9.5512	1.2960	5.0039	6.8465	3.0015	2.1733
10.0167	1.3589	5.9865	7.7382	3.9815	2.7637
10.9993	1.4849	7.0208	8.5894	4.9848	3.3293
12.4990	1.6638	7.9517	9.3450	6.0708	3.8899
13.3782	1.7640	9.0377	10.1458	7.1051	4.4140
14.5676	1.9010	10.0720	10.8911	8.1394	4.8968
15.9122	2.0642	10.9512	11.4903	9.2254	5.4005
18.2911	2.3384	11.9855	12.1447	9.9494	5.7054
19.9460	2.5282	12.9681	12.7638	11.2423	6.2418
21.8077	2.7443	14.0541	13.3932	11.9146	6.5360
24.4969	3.0299	16.0192	14.5258	12.8972	6.9151
25.9966	3.1990	17.9844	15.5727	14.1384	7.4099
28.0135	3.3956	19.9496	16.5743	16.3104	8.1956
29.7718	3.5756	22.0182	17.5760	18.3273	8.9181
34.7365	4.0798	24.0868	18.5122	19.8270	9.4200
40.2700	4.6069	26.2071	19.4180	22.2576	10.2077
44.6140	5.0069	28.0171	20.2030	23.8608	10.7000
49.5269	5.4450	30.2926	21.1336	26.4465	11.4838
60.1802	6.3564	34.7401	22.7834	28.0497	11.9400
70.2129	7.1435	39.9633	24.6249	29.8597	12.4598
80.1939	7.8942	45.0831	26.3157	35.3415	13.9010
90.0715	8.6097	50.0994	27.8403	39.8924	15.0512
99.0699	9.2357	59.8218	30.5816	45.2708	16.3218
110.1886	9.9722	70.1648	33.2423	49.9769	17.3906
119.2388	10.5469	79.9907	35.5616	60.3199	19.5361
150.0609	12.3955	89.9717	37.7551	69.9906	21.3875
200.4830	15.0947	100.0561	39.8128	80.0750	23.1803
250.0260	17.4550	109.9854	41.7287	90.0560	24.8477
299.7758	19.6185	120.0698	43.5740	100.1404	26.4291
349.9911	21.6244	150.7885	48.6386	110.0697	27.9009
399.9995	23.4742	201.0555	55.6946	120.1541	29.3181
450.0079	25.1999	249.5125	61.4697	149.0628	33.0621
499.9646	26.8392	300.2449	66.7969	201.1915	38.9219
550.2316	28.3844	349.8913	71.3629	249.6485	43.6494
600.0331	29.8256	399.4342	75.4566	299.6052	47.9786

PRESSURE (torr)	VOL ADS (cc/g STP)	PRESSURE (torr)	VOL ADS (cc/g STP)	PRESSURE (torr)	VOL ADS (cc/g STP)
349.6136	51.9212	120.1686	14.4980	100.5438	22.5335
399.8806	55.5569	150.2667	16.8989	109.4388	23.5145
449.4752	58.8621	200.8440	20.4877	120.0403	24.7811
499.9491	61.9992	250.0250	23.6035	151.6899	27.9387
550.1126	64.9021	299.9817	26.4706	200.1469	32.2300
599.9659	67.6274	349.9384	29.1264	250.1553	36.0145
650.1812	70.1954	400.1536	31.5903	299.6982	39.2803
699.8793	72.6254	449.9034	33.8924	349.3446	42.2582
750.1462	74.9562	500.2221	36.0887	400.1805	45.0011
CH₄ / BPL / -16°C		550.1788	38.1521	449.6200	47.4759
0.2679	0.0509	600.0321	40.1099	499.8870	49.8625
0.4551	0.0899	650.0405	41.9928	550.9814	51.9966
0.7173	0.1458	700.2557	43.7858	599.2833	53.9088
0.9241	0.1889	749.9022	45.4915	650.4294	55.7682
1.0896	0.2239	C₂H₆ / BPL / 40°C		699.7137	57.5039
2.0071	0.4287	0.5446	0.4239	750.4979	59.1616
3.0538	0.6524	1.0819	0.8496	C₂H₆ / BPL / 55°C	
3.9908	0.8468	2.0076	1.5292	1.0953	0.5077
4.9993	1.0503	3.0543	2.1911	1.9853	0.9177
6.4473	1.3260	3.9841	2.7424	3.0801	1.3662
7.6368	1.5615	5.0779	3.2919	3.9862	1.7199
8.1022	1.6410	6.2156	3.7424	5.0081	2.0950
9.0848	1.8217	7.2499	4.1857	6.3010	2.5157
10.3776	2.0485	8.1808	4.6026	7.2835	2.8507
11.6188	2.2589	9.2151	5.0314	8.2144	3.1076
12.0842	2.3386	9.9391	5.2843	9.4556	3.4755
13.1185	2.5251	11.2320	5.8108	10.1279	3.6635
14.5666	2.7493	12.0077	6.0938	11.0070	3.9085
16.4800	3.0579	12.9903	6.4154	11.8862	4.1484
17.9798	3.2931	14.1797	6.8285	13.4376	4.5507
20.6172	3.7008	16.0932	7.4365	14.4202	4.8089
22.2204	3.9375	18.3169	8.0951	16.0234	5.1615
24.1338	4.2204	19.8684	8.5356	18.0920	5.6551
26.0990	4.5143	22.3507	9.2291	19.8503	6.0478
27.9090	4.7646	23.9539	9.6659	22.3843	6.5852
29.8742	5.0328	25.8673	10.1438	23.9358	6.9309
34.9423	5.7263	28.2979	10.7393	26.0044	7.3168
39.7001	6.3269	29.9528	11.1193	28.3315	7.7563
44.5613	6.9393	35.0209	12.2569	29.9864	8.0588
49.5776	7.5344	40.3475	13.3478	35.0545	8.9440
60.0758	8.7463	45.1570	14.2918	40.0191	9.7952
70.4705	9.8638	50.1734	15.2113	45.2941	10.6300
79.3137	10.7616	59.7924	16.8569	49.6381	11.2696
90.1739	11.8302	70.3422	18.4656	60.1880	12.7034
99.2757	12.6744	79.9612	19.8070	69.9621	13.9816
109.1016	13.5507	89.7354	21.1615	80.3051	15.2413

PRESSURE (torr)	VOL ADS (cc/g STP)	PRESSURE (torr)	VOL ADS (cc/g STP)	PRESSURE (torr)	VOL ADS (cc/g STP)
89.2518	16.2257	59.5622	9.0046	45.9203	5.1218
99.2328	17.2692	69.6467	9.9382	49.7472	5.4977
109.8344	18.4119	80.0931	10.9807	60.6074	6.4151
119.4017	19.3219	89.8155	11.7461	69.5024	7.1191
149.6549	21.9549	100.7274	12.6825	79.6902	7.8442
201.0596	25.8158	109.7775	13.3809	90.8090	8.6411
249.5683	28.9973	120.8962	14.2595	99.2385	9.3301
299.7319	31.9169	150.9944	16.3630	110.1504	9.9598
350.1540	34.5963	200.0202	19.3989	120.3899	10.6152
400.1624	37.0060	249.9769	22.1486	151.3672	12.4374
449.9639	39.2155	300.6576	24.6705	200.7033	15.0360
500.0758	41.2750	350.2523	26.8933	249.9360	17.3886
550.1876	43.1814	400.8812	28.9978	299.9444	19.5704
599.8340	44.9725	451.0448	30.9544	349.5908	21.6425
650.0493	46.7231	501.1049	32.7947	401.3058	23.4722
700.4714	48.3626	550.1824	34.4754	451.4694	25.1865
749.9109	49.8962	601.3803	36.1051	501.0641	26.8448
C₂H₆ / BPL / 70°C		651.1301	37.6607	550.7621	28.3467
0.4344	0.1122	701.3971	39.1409	601.4429	29.8441
0.7690	0.2055	751.2504	40.5512	650.3135	31.2267
1.0090	0.2712	C₂H₆ / BPL / 100°C		701.0460	32.6279
2.0179	0.5445	0.6113	0.0744	750.8992	33.8462
3.0331	0.8021	1.0922	0.1436	SF₆ / BPL / 50°C	
3.9810	1.0336	1.9936	0.2874	0.7928	0.6195
5.0029	1.2724	3.0864	0.4499	1.6089	1.1560
6.3475	1.5516	3.9857	0.5922	1.9998	1.4002
7.0715	1.6952	5.1172	0.7433	3.0693	1.9811
7.9507	1.8874	6.3066	0.9261	3.9707	2.4454
9.3470	2.1434	7.1858	1.0268	4.9626	2.8987
10.0710	2.2819	8.4787	1.2077	6.1003	3.3721
11.2087	2.5209	10.0301	1.4022	7.2897	3.8421
12.6050	2.7619	10.0301	1.4022	8.2723	4.2255
13.0187	2.8326	11.3747	1.5745	8.9963	4.4637
14.1565	3.0270	12.7193	1.7415	10.2375	4.8968
16.2251	3.4053	13.2365	1.7892	11.1167	5.1965
18.2419	3.7128	14.2708	1.9308	11.9441	5.4660
20.5691	4.1179	16.4428	2.1708	12.8750	5.7525
22.3274	4.3540	18.5114	2.4180	14.1678	6.1390
24.2926	4.6997	20.1663	2.5952	16.0813	6.6989
26.1543	4.9633	21.8211	2.8136	18.3050	7.3098
28.0678	5.1987	24.0449	3.0296	19.8565	7.7267
30.3950	5.5593	26.4755	3.2987	22.4422	8.3754
35.4630	6.1630	28.2855	3.4501	24.0971	8.7471
40.3760	6.7723	30.4576	3.6696	26.4243	9.3366
45.3406	7.4230	35.4222	4.1646	28.2343	9.6977
49.8915	7.9041	39.9731	4.6055	30.2512	10.1886

PRESSURE (torr)	VOL ADS (cc/g STP)	PRESSURE (torr)	VOL ADS (cc/g STP)	PRESSURE (torr)	VOL ADS (cc/g STP)
34.9573	11.1305	30.0211	6.9762	25.9930	4.6137
39.9219	12.0832	34.9857	7.7096	27.8547	4.8908
45.1968	13.0247	40.0021	8.4401	29.9750	5.1243
50.2132	13.9073	44.8633	9.2038	34.8363	5.7455
60.3493	15.4782	49.7245	9.7904	40.6283	6.4247
70.0200	16.8513	60.0158	11.1323	44.8690	6.8672
80.1562	18.1597	71.1862	12.3835	50.2990	7.5105
90.0337	19.3278	79.6675	13.2321	60.9006	8.5897
99.8079	20.4549	90.4242	14.3423	69.4853	9.3399
109.9957	21.6402	99.4743	15.1677	80.3455	10.2874
119.4079	22.5477	110.5413	16.2070	89.1370	11.0613
149.9197	25.3931	119.6949	16.9509	99.4283	11.8466
202.4622	29.5589	150.1033	19.3954	110.6505	12.6889
249.4711	32.7226	203.2146	22.8942	119.4420	13.3159
299.3243	35.6667	249.8615	25.6232	150.1607	15.3389
349.9533	38.2861	299.9217	28.2356	200.7897	18.2486
399.2895	40.6782	349.8784	30.5939	249.9189	20.6964
451.2113	42.8124	400.0936	32.7246	299.6171	22.9157
499.5131	44.7943	451.7052	34.7407	350.6081	24.8433
549.2112	46.4434	500.2139	36.4698	400.5130	26.6381
599.4782	48.1928	551.1531	38.1331	450.1594	28.3330
649.3315	49.6118	601.1098	39.6835	500.1678	29.9520
700.0639	51.1055	651.0665	41.1825	551.1588	31.3310
751.2617	52.4537	700.7646	42.5114	600.6501	32.7197
SF ₆ / BPL / 65°C		751.3419	43.8063	650.6585	34.0797
1.0529	0.4394	SF ₆ / BPL / 80°C		701.2875	35.1974
2.0003	0.7878	0.6201	0.1617	750.0547	36.4241
2.9990	1.1304	1.1139	0.2929	SF ₆ / BPL / 95°C	
4.0022	1.4495	2.0257	0.5288	0.5430	0.0887
4.9910	1.7437	3.0124	0.7726	0.9826	0.1678
6.2322	2.0963	4.0472	0.9978	1.3260	0.2289
6.9562	2.3009	4.9967	1.2116	2.0210	0.3527
7.9388	2.5584	6.2379	1.4616	3.0176	0.5197
9.3868	2.9115	6.9619	1.6132	3.9924	0.6816
10.2659	3.1477	8.4099	1.8820	5.0293	0.8434
11.1451	3.3467	9.4442	2.0644	6.3734	1.0311
12.3345	3.5908	10.5819	2.2683	7.1491	1.1476
13.2137	3.8271	10.9956	2.3402	8.0800	1.2787
14.0929	3.9935	12.3919	2.5689	9.3728	1.4647
16.0580	4.4386	13.1677	2.7021	10.6657	1.6316
18.4886	4.9420	14.0468	2.8616	11.0794	1.6930
20.0918	5.2242	16.1671	3.1880	12.1654	1.8532
21.9535	5.5408	18.5460	3.5637	13.7169	2.0378
24.0738	5.9896	20.2009	3.7780	14.1823	2.1057
26.0907	6.3054	22.4247	4.1358	16.4061	2.3888
28.2628	6.6902	24.1830	4.3718	18.1127	2.5686

PRESSURE (torr)	VOL ADS (cc/g STP)	PRESSURE (torr)	VOL ADS (cc/g STP)	PRESSURE (torr)	VOL ADS (cc/g STP)
19.8710	2.7887	N₂ / F300 / -93°C		650.1522	65.1962
22.0430	3.0316	0.3775	0.4938	700.0054	66.8590
23.9565	3.2276	0.7385	0.9681	750.1173	68.4105
25.8182	3.4462	1.1145	1.4046	N₂ / F300 / -62°C	
27.8868	3.6616	1.9890	2.3305	0.4804	0.0916
30.1623	3.8739	3.0233	3.2563	0.8409	0.1633
35.4372	4.3940	3.9790	4.0366	1.1341	0.2206
39.6778	4.8184	5.0076	4.7886	2.0127	0.3999
44.6942	5.2726	6.3522	5.6490	3.0310	0.6042
49.6071	5.6849	7.0244	6.0924	4.0079	0.7937
60.0018	6.5363	8.0070	6.6896	4.9983	0.9803
70.2414	7.3731	9.0413	7.2603	6.4463	1.2408
79.7569	8.0178	10.0756	7.8205	7.2220	1.3896
89.1691	8.7075	11.1616	8.3699	8.2046	1.5546
99.4086	9.3750	12.0925	8.8370	9.5492	1.7782
109.4414	9.9778	13.2820	9.3907	10.0146	1.8580
119.1121	10.6273	13.9543	9.6775	11.0489	2.0233
150.5031	12.3946	16.1780	10.6556	12.1866	2.2097
199.2703	14.7940	18.2466	11.4836	13.2727	2.3752
250.2613	16.9317	20.2635	12.2391	14.7207	2.5940
301.0454	18.8575	22.3321	12.9680	15.9618	2.7756
351.0021	20.5926	23.9353	13.5235	18.3924	3.1385
401.1657	22.2163	26.3659	14.3226	20.0990	3.3790
451.3809	23.7029	27.9690	14.8151	22.0125	3.6462
501.5962	25.0782	29.7790	15.3739	23.7708	3.8921
551.5012	26.3752	35.5711	17.0054	26.4083	4.2504
599.2341	27.6139	39.6049	18.0620	28.1666	4.4650
650.5871	28.6770	45.1384	19.4242	30.1317	4.7063
701.2161	29.7996	50.1548	20.5664	34.9930	5.3173
749.8799	30.8053	59.9806	22.6338	40.5265	5.9670
		70.2719	24.5817	44.8705	6.4565
		80.0977	26.2628	49.6800	6.9681
		89.9753	27.8331	60.2299	8.0569
		100.2149	29.3531	70.3143	9.0248
		110.1959	30.7292	79.3644	9.8320
		120.3837	32.0365	90.0694	10.7595
		149.0856	35.4232	99.2230	11.4897
		201.1626	40.6156	110.0831	12.3324
		249.8264	44.7029	120.4261	13.0803
		299.3176	48.3034	150.1105	15.1179
		349.7915	51.5296	201.2050	18.2128
		399.9033	54.3939	250.1273	20.8052
		449.3428	56.9353	299.8772	23.1657
		499.9718	59.3165	350.0924	25.3135
		550.2388	61.4499	399.9974	27.2672
		599.9370	63.3957	450.0576	29.0803

PRESSURE (torr)	VOL ADS (cc/g STP)	PRESSURE (torr)	VOL ADS (cc/g STP)	PRESSURE (torr)	VOL ADS (cc/g STP)
500.2211	30.7633	0.4996	1.4655	750.5336	81.8304
550.3329	32.3302	1.0622	2.7517	CO / F300 / -62°C	
600.1862	33.7928	1.9859	4.5249	0.4722	0.1854
650.2463	35.1726	3.0502	6.0911	0.8786	0.3567
700.2030	36.4423	3.9681	7.2760	1.2391	0.5023
750.0045	37.6384	4.9590	8.3876	1.9921	0.7982
N ₂ / F300 / -43°C		6.0444	9.5042	3.0253	1.1788
0.3848	0.0322	7.0270	10.4452	3.9888	1.5148
0.6040	0.0529	8.0096	11.2683	4.9957	1.8488
1.0136	0.0919	8.9405	12.0037	6.2373	2.2209
3.0083	0.2820	9.9748	12.7918	7.2716	2.5301
5.0189	0.4685	11.0608	13.5399	7.9439	2.7395
7.6047	0.7146	11.8882	14.0948	9.2368	3.0964
9.2596	0.8494	12.9743	14.7890	9.9608	3.2906
11.0179	1.0013	13.9568	15.3863	11.4606	3.6744
12.9313	1.1708	16.2323	16.6753	12.2363	3.8949
14.9482	1.3361	17.9389	17.5686	13.1154	4.1106
18.6717	1.6258	19.9041	18.5617	13.8912	4.3156
21.0506	1.8051	21.9727	19.5734	16.1149	4.8474
25.7049	2.1627	24.1447	20.5296	18.3904	5.3643
29.7904	2.4667	25.9030	21.2845	19.9418	5.6869
45.0981	3.5416	28.2302	22.2090	22.4241	6.2045
55.0791	4.1827	30.2471	22.9950	24.0790	6.5377
64.9566	4.8066	34.8497	24.6238	25.7856	6.8918
74.3688	5.3668	39.9695	26.3005	28.2679	7.3583
84.2463	5.9264	45.0376	27.8451	29.8711	7.6604
90.1418	6.2520	50.1056	29.2522	34.8357	8.5367
99.3988	6.7509	59.9315	31.7559	40.0590	9.4196
109.1212	7.2642	70.1193	34.0979	45.1787	10.2197
115.1202	7.5735	80.1003	36.1724	50.1434	10.9671
120.3434	7.8280	90.0813	38.0700	60.1761	12.3649
150.0278	9.2562	100.0106	39.8110	70.0537	13.6389
201.2774	11.4637	110.0433	41.4476	80.1381	14.8371
224.4974	12.3993	120.0243	42.9717	90.0674	15.9522
250.1998	13.3810	150.5362	47.1638	100.1001	17.0111
300.3116	15.1853	201.2169	52.9814	110.1328	18.0228
350.4234	16.8349	249.4669	57.5810	120.1655	18.9739
400.0181	18.3503	300.1994	61.7599	149.6430	21.5404
450.0782	19.7996	349.7941	65.2768	200.9443	25.3917
500.5521	21.1693	399.2336	68.4390	249.6599	28.5603
550.0950	22.4472	450.1212	71.3405	299.6165	31.4327
600.2586	23.6827	499.8193	73.8783	349.9352	34.0347
650.2670	24.8577	550.1379	76.1427	399.8402	36.3950
700.2237	25.9785	602.8873	77.5225	450.1072	38.5753
760.3165	27.2760	650.0513	78.9559	499.8053	40.5982
CO / F300 / -93°C		701.0941	80.4844	550.1757	42.4986

PRESSURE (torr)	VOL ADS (cc/g STP)	PRESSURE (torr)	VOL ADS (cc/g STP)	PRESSURE (torr)	VOL ADS (cc/g STP)
599.9772	44.2699	349.7832	23.2867	120.0315	42.9681
650.0374	45.9502	400.0502	25.1682	150.9054	47.5231
700.0458	47.5386	449.9034	26.9199	201.3275	53.7231
750.0542	49.0435	500.1704	28.5639	249.2673	58.6810
CO / F300 / -43°C		549.9720	30.0984	299.2240	63.1384
0.2741	0.0418	600.0838	31.5501	349.5944	67.0663
0.4660	0.0745	650.0405	32.9220	399.8097	70.5577
0.7323	0.1199	699.9454	34.2389	449.9732	73.6985
0.9635	0.1583	750.1090	35.5030	499.9817	76.5405
1.1527	0.1901	CH4 / F300 / -62°C		549.9901	79.1429
2.0262	0.3435	0.2389	0.5423	600.1019	81.5318
3.0331	0.5161	0.4525	1.0705	650.0069	83.7333
4.0017	0.6778	0.6769	1.5733	700.1187	85.7915
4.9993	0.8407	0.9159	2.0641	750.0754	87.7077
6.2922	1.0472	1.1682	2.5290	CH4 / F300 / -43°C	
7.0679	1.1632	1.9931	3.8860	0.3175	0.2799
7.9988	1.3043	3.0036	5.2837	0.5983	0.5361
9.3433	1.5011	3.9696	6.4802	0.8709	0.7736
10.0674	1.6071	5.0174	7.6007	1.1300	0.9886
10.9982	1.7433	6.0000	8.5494	2.0107	1.6731
12.3428	1.9303	6.9826	9.4014	3.0321	2.3839
13.0668	2.0312	8.0169	10.2633	3.9660	2.9813
14.0494	2.1529	9.1546	11.1301	4.9879	3.5871
16.0663	2.4309	9.9303	11.7282	6.2291	4.2596
18.6520	2.7701	10.9646	12.4374	7.1082	4.7152
20.0484	2.9423	11.9989	13.1212	8.0908	5.2081
21.9101	3.1755	12.9815	13.7545	9.1768	5.7122
24.5476	3.5099	14.0675	14.3822	10.2111	6.1690
26.1507	3.6882	16.0327	15.5263	11.2454	6.6100
27.9090	3.9010	18.0496	16.5992	11.9177	6.8917
29.7191	4.1096	19.9630	17.5655	13.2106	7.4234
34.8906	4.6846	22.0833	18.5718	13.9863	7.7060
40.2689	5.2449	24.1002	19.4716	15.8998	8.4353
45.3887	5.7707	26.0137	20.3058	18.3304	9.2677
49.7845	6.2050	28.1340	21.1903	20.3990	9.9617
60.4378	7.1886	30.1509	21.9889	21.9504	10.4377
70.0568	8.0307	34.7018	23.6608	24.2776	11.1754
80.1412	8.8653	40.2870	25.5382	25.9842	11.6578
90.0705	9.6500	45.0448	27.0314	27.7425	12.1718
100.1032	10.4098	50.1646	28.5241	30.2765	12.8535
109.1016	11.0534	59.9387	31.0978	34.7758	14.0192
120.1686	11.8207	70.0231	33.5031	40.2575	15.3224
150.2150	13.7389	80.0559	35.6848	45.0153	16.4067
200.7923	16.5775	89.9851	37.6947	50.1868	17.4987
249.7664	19.0153	100.1213	39.5906	59.8058	19.3798
299.8782	21.2488	110.1023	41.3292	70.2005	21.2252

PRESSURE (torr)	VOL ADS (cc/g STP)	PRESSURE (torr)	VOL ADS (cc/g STP)	PRESSURE (torr)	VOL ADS (cc/g STP)
79.9747	22.8199	34.8906	5.9512	25.8715	12.2363
90.0591	24.3595	40.3723	6.6570	28.1986	12.8869
100.1435	25.7895	44.6130	7.1818	29.9569	13.3151
110.0728	27.1297	50.4051	7.8767	35.1802	14.6298
120.1572	28.4031	60.3343	8.9799	40.6102	15.8762
149.4279	31.7516	70.2636	10.0152	44.7474	16.7265
200.9878	36.7905	80.2446	11.0095	50.1258	17.8411
249.8067	40.8545	89.2430	11.8372	60.4171	19.6312
299.5048	44.4863	99.9997	12.7912	69.9844	21.2265
349.6684	47.7718	109.1533	13.5742	80.3791	22.8415
399.9354	50.7500	119.1343	14.3751	89.2223	24.0227
449.9438	53.4602	149.8530	16.6694	100.0308	25.4699
499.9522	55.9668	200.9474	20.0025	109.3912	26.5641
550.0640	58.2914	249.9215	22.8119	120.1996	27.8442
600.1758	60.4491	299.9817	25.3792	149.9875	30.8906
649.9774	62.4635	349.8349	27.7190	199.9959	35.2502
700.0375	64.3754	400.2053	29.8755	250.0043	38.9011
750.2010	66.1720	449.8517	31.8782	300.4264	42.2119
CH₄ / F300 / -16°C		500.2221	33.7626	350.7451	45.0084
0.2586	0.0531	550.0754	35.5137	399.2538	47.4435
0.4406	0.0943	600.1355	37.1734	450.4516	49.6777
0.5983	0.1304	650.0405	38.7473	499.9946	51.7770
0.7768	0.1708	700.1006	40.2447	550.7270	53.7269
0.9407	0.2077	750.0573	41.6726	600.2183	55.4076
1.0876	0.2408	C₂H₆ / F300 / 40°C		650.4852	57.0483
2.0076	0.4650	0.4153	0.5149	700.3385	58.5540
3.0781	0.7107	0.8409	0.9965	749.7780	59.9872
3.9800	0.9111	1.2882	1.4323	C₂H₆ / F300 / 55°C	
4.9993	1.1306	1.9952	2.0931	0.3879	0.2223
6.2922	1.4012	3.1117	2.9585	0.6847	0.4236
7.1713	1.5662	4.0064	3.5986	0.9722	0.6170
8.3090	1.7926	5.0303	4.2451	1.2494	0.7856
9.4468	2.0034	6.0646	4.8392	2.0003	1.2252
10.4811	2.2126	7.0989	5.3809	3.0227	1.7572
10.8948	2.2869	8.0815	5.9058	3.9805	2.2329
11.9291	2.4647	9.1675	6.4384	5.0732	2.7033
12.9117	2.6470	10.2535	6.8978	6.1075	3.1604
13.9460	2.8196	11.1844	7.2961	6.9867	3.4743
16.2214	3.1993	12.2187	7.7595	8.1761	3.9462
17.9280	3.4815	13.0461	8.0560	9.0553	4.2241
20.0484	3.8168	13.8736	8.3838	10.2447	4.6449
22.7892	4.2402	15.9422	9.1329	11.0205	4.8940
24.3924	4.4897	18.3728	9.9481	11.9513	5.1684
26.1507	4.7463	19.9242	10.4393	13.1408	5.5532
27.8056	4.9804	22.3548	11.2389	14.0717	5.8173
29.7708	5.2509	24.0614	11.7285	16.0368	6.3691

PRESSURE (torr)	VOL ADS (cc/g STP)	PRESSURE (torr)	VOL ADS (cc/g STP)	PRESSURE (torr)	VOL ADS (cc/g STP)
18.3640	7.0036	13.2540	3.7931	11.0825	1.6628
20.0189	7.4024	13.9263	3.9769	12.0651	1.7767
22.3461	8.0011	16.0984	4.3898	13.6166	1.9709
24.1044	8.3773	18.0635	4.8370	14.1337	2.0287
25.9144	8.7601	19.9770	5.1844	16.4092	2.3130
28.0864	9.2771	22.3042	5.6404	18.1675	2.5082
30.0516	9.6441	23.9590	5.9619	19.8224	2.7368
35.2748	10.7147	25.9759	6.2873	22.0978	2.9740
39.7223	11.4898	28.2514	6.7174	23.9596	3.1515
45.2041	12.4757	30.1648	6.9910	26.5970	3.4521
49.7033	13.1754	34.9743	7.7889	28.2519	3.6078
59.8394	14.8143	41.0767	8.6879	29.7516	3.8109
71.2167	16.3420	45.0070	9.1985	35.3886	4.3396
79.5428	17.3418	49.8165	9.7756	40.5601	4.7968
90.2478	18.6595	60.0044	11.1533	46.0936	5.3327
99.5565	19.6427	69.8302	12.1446	50.2825	5.6392
110.4684	20.8281	80.0698	13.2493	60.3669	6.4618
119.3117	21.6887	90.9300	14.2860	70.9168	7.2981
149.7718	24.4126	99.5147	15.0506	79.7083	7.9184
201.2800	28.3418	110.8920	16.0606	90.7236	8.7645
249.6852	31.5070	119.7869	16.7731	100.6012	9.3345
301.0382	34.5088	149.6265	19.0430	111.3062	10.0291
350.3743	36.9932	201.8069	22.4185	119.9426	10.5505
400.5896	39.3397	250.5742	25.1369	150.2993	12.2108
450.3394	41.4360	300.7894	27.6350	200.3594	14.6370
500.9684	43.4149	350.9013	29.8674	250.9884	16.8142
550.0977	45.1949	401.0648	31.9174	301.3071	18.7311
600.1060	46.8933	451.1249	33.7894	351.1086	20.4907
650.2696	48.4475	501.2885	35.5548	401.4791	22.1007
700.8986	49.9643	551.2969	37.1643	451.4875	23.5862
750.0795	51.3768	601.3570	38.6675	500.9787	25.0333
C₂H₆ / F300 / 70°C		651.4689	40.0934	550.9871	26.3080
0.3879	0.1527	701.6324	41.4170	601.9781	27.5497
0.7323	0.2917	751.6408	42.6828	651.7280	28.7272
1.0281	0.4074	C₂H₆ / F300 / 100°C		701.4778	29.8420
2.0345	0.7703	0.5492	0.0889	751.8482	30.9192
3.0238	1.1134	1.0090	0.1623	SF₆ / F300 / 50°C	
4.0286	1.4340	2.0153	0.3317	0.6056	0.4760
5.0314	1.7445	3.0403	0.4996	1.2117	0.8876
6.2725	2.1098	4.0162	0.6499	1.9993	1.3677
6.9965	2.3049	5.0319	0.8075	3.0315	1.9211
7.9791	2.5555	6.3765	1.0058	3.9903	2.3668
9.1686	2.8900	7.4108	1.1578	4.9972	2.8008
10.2029	3.1222	8.9105	1.3660	6.1867	3.2845
11.0303	3.3002	9.3759	1.4326	6.9624	3.5703
12.2715	3.5867	10.4619	1.6019	8.3587	4.0546

PRESSURE (torr)	VOL ADS (cc/g STP)	PRESSURE (torr)	VOL ADS (cc/g STP)	PRESSURE (torr)	VOL ADS (cc/g STP)
9.0310	4.2805	6.2870	2.1654	4.0012	0.9972
10.1687	4.6282	6.9593	2.3543	5.0169	1.2240
11.0996	4.9390	8.3556	2.7288	6.3097	1.4954
12.0305	5.2188	9.2347	2.9239	7.1372	1.6538
12.9613	5.4675	10.3208	3.1849	8.2749	1.8710
14.3059	5.8829	11.1482	3.3586	9.2058	2.0423
16.3745	6.4277	12.0274	3.5488	10.1884	2.2252
18.1845	6.8460	13.3202	3.8159	11.6364	2.4613
20.3566	7.3834	14.1477	4.0194	12.1535	2.5361
22.0115	7.7508	16.3197	4.4221	12.9810	2.6647
23.9249	8.1358	18.3366	4.8004	14.3773	2.8894
26.3038	8.6838	19.9398	5.0917	16.4459	3.2182
28.1138	9.0245	22.3704	5.5417	18.0491	3.4340
29.8204	9.3677	24.0770	5.8212	20.5831	3.7914
34.9919	10.2477	25.9904	6.1068	22.2897	4.0201
39.9048	11.1310	28.4727	6.4988	23.8928	4.2658
45.5418	12.0503	30.0759	6.7456	25.9614	4.5051
49.9376	12.6609	35.2991	7.4730	28.4438	4.8213
59.4531	13.9740	40.4189	8.1523	30.0986	5.0187
70.7787	15.3235	44.7112	8.6878	35.1667	5.5992
80.3460	16.4680	50.2965	9.3661	40.4934	6.2270
89.7581	17.4060	60.4843	10.4798	44.9926	6.6668
100.4114	18.5246	70.1550	11.4489	49.6469	7.1504
109.7718	19.3379	80.0843	12.4413	60.8174	8.1818
119.5459	20.2084	89.8067	13.2282	70.3846	9.0571
150.5750	22.6256	99.1671	14.0141	79.9519	9.7691
200.5833	25.9391	110.6479	14.9378	90.7086	10.6350
249.9712	28.6809	119.9566	15.5485	100.0690	11.2467
300.6002	31.0992	149.8478	17.5197	109.2743	11.9225
350.7120	33.1903	202.6488	20.4522	119.6173	12.5520
399.2207	34.9696	250.6921	22.7285	150.1809	14.3190
450.2117	36.7722	300.8556	24.8500	201.3270	16.8937
501.3061	38.2724	349.1574	26.6103	249.7323	19.0358
549.2976	39.5774	401.1310	28.3216	300.2578	21.0209
601.0643	40.9371	451.0360	29.8422	349.5939	22.8865
649.6247	42.0462	499.4930	31.1804	400.0677	24.3568
699.1677	43.1930	549.6048	32.4292	450.3864	25.8936
750.0035	44.1545	599.4581	33.6054	501.6360	27.2491
SF ₆ / F300 / 65°C		649.6216	34.7018	551.2307	28.5067
0.5316	0.2281	699.2680	35.7972	599.3774	29.6624
0.9738	0.4213	750.3624	36.7128	650.1615	30.6717
1.4491	0.6093	SF ₆ / F300 / 80°C		700.6353	31.8454
2.0071	0.8334	0.5828	0.1415	750.6954	32.7439
3.0895	1.2240	1.0436	0.2695	SF ₆ / F300 / 95°C	
4.0027	1.5088	2.1151	0.5506	0.5285	0.0941
4.9941	1.8088	2.9964	0.7671	0.9697	0.1712

PRESSURE (torr)	VOL ADS (cc/g STP)	PRESSURE (torr)	VOL ADS (cc/g STP)
1.3125	0.2308	40.9816	4.7118
1.9900	0.3488	45.2739	5.0343
3.0264	0.5182	49.6180	5.3978
3.9971	0.6754	60.4781	6.2064
5.0396	0.8304	70.7177	6.9409
6.3842	1.0192	79.8195	7.5177
7.2117	1.1479	89.1799	8.1713
8.5562	1.3120	99.8849	8.7376
8.9700	1.3738	109.3488	9.2860
10.0043	1.5235	119.1746	9.8955
11.4006	1.6941	150.8242	11.4628
12.7452	1.8582	199.7983	13.5939
13.2106	1.9167	250.5824	15.4152
14.2449	2.0172	301.1597	17.0918
16.2618	2.2658	351.0130	18.6381
18.0201	2.4524	401.1248	20.1050
20.5541	2.7511	449.9955	21.3061
22.2607	2.9113	501.7105	22.4160
23.8639	3.0881	551.6155	23.5007
25.8291	3.3055	601.6756	24.5359
28.1045	3.5027	649.4085	25.5546
29.8628	3.6742	700.8132	26.3792
35.3446	4.1806	749.2702	27.3602

APPENDIX B

FITTING ROUTINE AND INPUT FORMAT

The Fortran code for the MEA fitting program is followed by a typical data input file with a brief explanation of the parameters. The program reads an input file with experimental adsorption data, estimated parameter values, and fitting instructions. On termination the program outputs a file that includes the experimental and calculated data points with relative errors, the best fit parameters and associated errors, $\ln K_i$ versus T^{-1} regression results, and surface areas and pore volumes. A new input file with the best-fit parameters is output to allow another fit of the data to be run. The number of read-output cycles is controlled by the user.

The original program was written by Dr. N. Wong. Modifications to the original code were made by Ben Gordon, Edwin Webster, and myself for fitting the gas adsorption data. The fortran code as it appears here is the work of Edwin Webster.

The MEA Fitting Routine Fortran Code

```

c -----
c -- Title      : MEA Fitting Routine (Fortran Code)
c -- Description : This program implements NELDER and MEAD's
c --             Modified Simplex Method. It is set up
c --             to constrain the simplex to positive space
c --             by not allowing any of the parameters to
c --             become less than 0.
c -----
      implicit none

      integer MAXNTEMP,MAXNPOINT,MAXNSITE
      parameter (MAXNTEMP=5)
      parameter (MAXNSITE=5)
      parameter (MAXNPOINT=200)

      CHARACTER*60 INFILE, OUTFILE, NEWINFILE

      double precision B(MAXNTEMP,MAXNPOINT),H(MAXNTEMP,MAXNPOINT)
      double precision P(MAXNTEMP*2*MAXNSITE)
      double precision Dup(MAXNTEMP*2*MAXNSITE)
      double precision Ddown(MAXNTEMP*2*MAXNSITE)
      double precision DIF(MAXNTEMP,MAXNPOINT),HH(MAXNTEMP,MAXNPOINT)
      double precision SD(MAXNTEMP,MAXNSITE,2),br
      double precision avge(MAXNTEMP),ge(MAXNTEMP),ep,devn,b1,hcal
      double precision per,tot_sq, square(maxntemp)
      double precision CAL, n_tot, n_sd
      double precision temp(MAXNTEMP)
      double precision sx(MAXNTEMP),sx2(MAXNTEMP)
      double precision sxy(MAXNTEMP),sy(MAXNTEMP)
      double precision slope(MAXNTEMP),yinter(MAXNTEMP)
      double precision rbx(MAXNTEMP),rby(MAXNTEMP)
      double precision rt(MAXNTEMP),r(MAXNTEMP)
      double precision AREA, MVL
      double precision wgt(MAXNTEMP,MAXNSITE),t_wgt(MAXNSITE)
      double precision sd_y(MAXNTEMP),dy(MAXNTEMP,MAXNSITE),D
      double precision sd_m(MAXNTEMP),sd_b(MAXNTEMP)
      integer i,is,k,nt,n(MAXNTEMP),ne(MAXNTEMP),ns(MAXNTEMP),ip,KX
      integer total_ns,fixdn,i1,i2,UPORDWN
      integer total_np,maxns,tot_n
      integer count, m, calc_dim, weight

      WRITE (6,10)
10  FORMAT (5X,'Name of Data File? ')
      READ (5,'(A)') INFILE

      WRITE (6,20)
20  FORMAT (/5X,'Name of Output File? ')
      READ (5,'(A)') OUTFILE

      WRITE (6,30)
30  FORMAT (/5X,'Name of New Input File? ')
      READ (5,'(A)') newinfile

```

```

OPEN (8,FILE=INFILE,STATUS='OLD')

call getline(8)
READ (8,*) EP, KX, fixedn
  print *, 'Read in EP(convergence), KX(loops), Fixedn(0,1)'
  print *, EP, KX, FIXEDN
call getline(8)
READ (8,*) UPORDWN, count, calc_dim, weight
  print *, 'Read in Upordown(0,1,2,3,4,5,10,15) Count(External Loops)'
  print *, UPORDWN, COUNT
  print *, 'Read in Calc Dimensions?(0,1), Weighted Regression?(0,1)'
  print *, calc_dim, weight
IF (calc_dim.eq.1) then
  call getline(8)
  READ (8,*) AREA, MVL
  print *, 'Read in AREA/Molecule (A^2), Molar Vol (mL/mole)'
  print *, AREA, MVL
endif

call getline(8)
READ (8,*) nt
  print *, 'Read in NT(number of temperature sets)'
  print *, NT
if (nt.gt.MAXNTEMP) then
  print 100,nt,MAXNTEMP
  stop
100 format(5X,'Sorry. You asked for ',I3,
*      ' temperature sets. The maximum number is ',I3)
endif

ip = 1

maxns = 0

tot_n = 0

do 1000 k=1,nt
  AVGE(k) = 0.00

  call getline(8)
  READ (8,*) NE(k),GE(k)
  print *, 'This is NE(k)[number of data points]',
*      'GE(k)[grams of solid]'
  print *, NE(k), GE(k)

  if (ne(k).gt.MAXNPOINT) then
    print 120,NE(k),MAXNPOINT
    stop
120 format(5X,'Sorry. You asked for ',I3,
*      ' data points. The maximum number is ',I3)
  endif

  N(k) = NE(k)
  tot_n = tot_n + n(k)

DO 150 l=1,N(k)

```



```

      call getline(8)
      READ (8,*) B(k,l),H(k,l)
      print *, B(k,l),H(k,l)
150 CONTINUE

      call getline(8)
      READ (8,*) ns(k), temp(k)
      print 160,ns(k),k,temp(k)
      if (ns(k).gt.MAXNSITE) then
        print 170,ns(k),MAXNSITE
        stop
160 format('Number of Sites [NS(k)]:',l2,5X,'Temp',l2,',',F7.2)
170 format(5X,'Sorry. You asked for ',l3,
*         ' sites. The maximum number is ',l3)
      endif

      if (ns(k).gt.maxns) maxns = ns(k)

      do 180 i=1,2*ns(k)
        call getline(8)

      if (UPORDWN.LT.0) then
        UPORDWN=0
      endif
      if (UPORDWN.EQ.0) then
        READ (8,*) P(ip),ddown(ip),dup(ip)
        print *, P(ip), ddown(ip), dup(ip)
      endif
      if (UPORDWN.EQ.15) then
        READ (8,*) P(ip)
        ddown(ip)=1e-15*P(ip)
        dup(ip)=1e-15*P(ip)
        print *, P(ip), ddown(ip), dup(ip)
      endif
      if (UPORDWN.EQ.10) then
        READ (8,*) P(ip)
        ddown(ip)=1e-10*P(ip)
        dup(ip)=1e-10*P(ip)
        print *, P(ip), ddown(ip), dup(ip)
      endif
      if (UPORDWN.EQ.5) then
        READ (8,*) P(ip)
        ddown(ip)=1e-5*P(ip)
        dup(ip)=1e-5*P(ip)
        print *, P(ip), ddown(ip), dup(ip)
      endif
      if (UPORDWN.EQ.4) then
        READ (8,*) P(ip)
        ddown(ip)=1e-4*P(ip)
        dup(ip)=1e-4*P(ip)
        print *, P(ip), ddown(ip), dup(ip)
      endif
      if (UPORDWN.EQ.3) then
        READ (8,*) P(ip)
        ddown(ip)=1e-3*P(ip)
        dup(ip)=1e-3*P(ip)

```

```

        print *, P(ip), ddown(ip), dup(ip)
    endif
    if (UPORDWN.EQ.2) then
        READ (8,*) P(ip)
        ddown(ip)=.01*P(ip)
        dup(ip)=.01*P(ip)
        print *, P(ip), ddown(ip), dup(ip)
    endif
    if (UPORDWN.EQ.1) then
        READ (8,*) P(ip)
        ddown(ip)=.1*P(ip)
        dup(ip)=.1*P(ip)
        print *, P(ip), ddown(ip), dup(ip)
    endif
    ip = ip + 1
180  continue

    DO 190 l=1,N(k)
        AVGE(k) = AVGE(k) + H(k,l) / NE(k)
190  CONTINUE

    IF (AVGE(k).EQ.0) AVGE(k) = 1.00

    DO 200 l=1,N(k)
        HH(k,l) = H(k,l) / GE(k)
200  CONTINUE

    DO 210 l=1,MAXNSITE
        SD(k,l,1)=0.0
        SD(k,l,2)=0.0
210  CONTINUE

1000 continue

    CLOSE(8)

    total_np = ip - 1
    total_ns = total_np / 2

    if (fixedn.ne.0) then
        do 500 i = 2*maxns + 1, total_np-1,2
            ddown(i) = 0.0
            dup(i) = 0.0
500  continue
        endif

        do 5000 m = 0, count-1
            do 1020 k=1,nt
                DO 1010 l=1,MAXNSITE
                    SD(k,l,1)=0.0
                    SD(k,l,2)=0.0
1010  CONTINUE
1020 continue

                tot_sq = 0.0

```

```

WRITE (6,1050)
1050 FORMAT (//5X,'WORKING')

CALL SIMPLEX(nt,EP,total_np,N,KX,P,Ddown,dup,HH,B,NS,fixedn,
*count,m,br)
WRITE (6,1060)
1060 FORMAT (/5X,'Fitting Routine Completed')

OPEN (7,FILE=OUTFILE)
OPEN (10,FILE=newinfile)
OPEN (9,FILE='Best.BR')
print 1070, OUTFILE,NEWINFILE
write (7,1080) br
write (9,1090) count-m, br
write (10,1100)
1070 FORMAT (/,Writing  ',1A12,', '1A12', and Best.BR')
1080 FORMAT ('BR = ',e25.17)
1090 FORMAT ('The Best Residual for count',i3,' is',e25.17,'.')
1100 FORMAT ('#,'1X,'ep(convergence)',1X,'kx(loops)',1X,'Fixedn(0/1)')
  if (UPORDWN.GT.2) then
    UPORDWN = 5
    write (10,1110) EP, KX, fixedn
    write (10,1120)
    write (10,1130) UPORDWN, count, calc_dim, weight
  if (calc_dim.eq.1) then
    write (10,1140)
    write (10,1150) AREA, MVL
  endif
else
  write (10,1110) EP, KX, fixedn
  write (10,1120)
  write (10,1130) UPORDWN, count, calc_dim, weight
  if (calc_dim.eq.1) then
    write (10,1140)
    write (10,1150) AREA, MVL
  endif
endif
1110 FORMAT (E16.4,3X,I10,3X,I1)
1120 FORMAT ('#,'1X,'Upordown(0,1,2,3,4,5,10,15)',1X,
*'Count(ext_loops) Calc_Dim(0,1) Weight(0,1)')
1130 FORMAT (I2,3X,I2,3X,I2,3X,I2)
1140 FORMAT ('#,'1X, AREA(A^2), MVL(mL/mole)')
1150 FORMAT (F7.3,3X,F7.3)

write (7,1160) count-m
write (10,1170)
write (10,1180) nt
1160 format(1X,'Count_is: ',I2)
1170 format ('#_number_of_temperature_sets')
1180 format (I3)

ip = 1

do 2010 k=1,nt
  DEVN=0.00

```

```

square(k) = 0.0
DO 1190 l=1,N(k)
  DIF(k,l) = H(k,l) - Ge(k) * CAL(k,l,ip,P,B,NS,fixedn)
  square(k) = square(k) + dif(k,l)**2
1190 CONTINUE

DO 2000 l=1,N(k)
  DEVN=DIF(k,l)**2

DO 2000 IS=0,NS(k)-1
  if (fixedn.eq.0) then
    L1 = ip + 2*is
  else
    L1 = 2*is + 1
  endif

  L2 = ip + 2*is + 1
  B1 = P(L2)*B(k,l)

  if (fixedn.eq.0) then
    SD(k,is+1,1)=SD(k,is+1,1)+(((1.0+B1)/B1)**2)*DEVN
  else
    SD(1,is+1,1)=SD(1,is+1,1)+(((1.0+B1)/B1)**2)*DEVN
  endif

  SD(k,is+1,2)=SD(k,is+1,2)+(dif(k,l)/(B(k,l)*
* (P(L1)-dif(k,l))))**2
2000 CONTINUE

ip = ip + 2*ns(k)

2010 continue

ip = 1
do 2030 k=1,nt

DO 2020 IS=0,NS(k)-1

  if (fixedn.eq.0) then
    L1 = ip + 2*is
  else
    L1 = 2*is + 1
  endif

  L2 = ip + 2*is + 1

  if (fixedn.eq.0) then
    SD(k,is+1,1) = SQRT(SD(k,is+1,1)/N(k))
    IF ((ddown(l1).eq.0.0).and.(dup(l1).eq.0.0)) then
      SD(k,is+1,1)=-1.00
    endif
  endif

  SD(k,is+1,2) = SQRT(SD(k,is+1,2)/N(k))
  IF ((ddown(l2).eq.0.0).and.(dup(l2).eq.0.0)) then

```

```

      SD(k,is+1,2)=-1.00
    endif

2020 CONTINUE

      ip = ip + 2*ns(k)

2030 continue

      if (fixedn.ne.0) then

DO 2040 IS=0,maxns-1
  L1 = 2*is + 1
  SD(1,is+1,1) = SQRT(SD(1,is+1,1)/tot_n)
  IF ((ddown(l1).eq.0.0).and.(dup(l1).eq.0.0)) then
    SD(1,is+1,1)=-1.00
  ENDIF
2040 CONTINUE

      endif

      ip = 1

      do 2260 k=1,nt
        write (10,2050)
        write (10,2060) ne(k), ge(k)
        write (7,2070) k, temp(k)
        write (10,2080) k, temp(k)
        IF (NE(k).GT.0) WRITE (7,2090)
        write (10,2100)
2050 FORMAT ('#_No._of Data_Points, No._of grams_ of_solid')
2060 FORMAT (I4,2X,F5.3)
2070 FORMAT ('Data_for temp_set ',I3,5X,'Temp(K): ',f7.2)
2080 FORMAT ('#_Data_for temp_set ',I3,5X,'Temp(K): ',f7.2)
2090 FORMAT (/3X,'#',6X,'Eq_conc',7X,'Exp_Ads',9X,'Calc_Ads',12X,
  *      'Err',15X,'Per')
2100 FORMAT ('#',3X,'Eq_conc',6X,'Exp_Ads',8X,'Calc_Ads',10X,
  *      'Err',17X,'Per')

      DO 2150 l=1,N(k)
        HCAL=GE(k) * CAL(k,l,ip,P,B,NS,fixedn)
        PER = DABS(100.0*DIF(k,l)/HH(k,l))
        if (B(k,l).lt.1e-9) then
          WRITE (7,2110) l,B(k,l),H(k,l),HCAL,DIF(k,l),PER
          WRITE (10,2120) B(k,l),H(k,l),HCAL,DIF(k,l),PER
        else
          WRITE (7,2130) l,B(k,l),H(k,l),HCAL,DIF(k,l),PER
          WRITE (10,2140) B(k,l),H(k,l),HCAL,DIF(k,l),PER
        endif
2150 continue
2110 FORMAT (1X,I3,3X,e14.8,3X,E14.8,2(3X,E14.8),3X,F9.4)
2120 FORMAT (1X,e14.8,3X,E14.8,2(3X,E14.8),1X,F9.4)
2130 FORMAT (1X,I3,3X,F11.9,3X,E14.8,2(3X,E14.8),5X,F9.4)
2140 FORMAT (1X,F11.9,3X,E14.8,2(3X,E14.8),3X,F9.4)

      write (7,2160) k, square(k)

```

```

tot_sq = square(k) + tot_sq
write (7,*)
write (10,2170)
WRITE (10,2180) ns(k), temp(k)
2160 FORMAT (/3X,'The_sum_of_squares_for temp_set',l2,' is ',E14.8)
2170 FORMAT ('# number of sites above with: n1,K1, n2,K2...; Temp(K)')
2180 FORMAT (l2,F7.2)

```

```

DO 2240 IS=1,NS(k)
  if (fixedn.eq.0) then
    L1 = ip + 2*is - 2
  else
    L1 = 2*is - 1
  endif
  L2 = ip + 2*is - 1
  if (fixedn.eq.0) then
    WRITE (7,2200) IS,P(l1),SD(k,is,1),IS,P(l2),SD(k,is,2)
  else
    WRITE (7,2210) IS,P(l2),SD(k,is,2)
  endif
2200 FORMAT (2X,'n',l1,'_is ',E20.11,2X,' +/- ',2X,E15.5,2X,
* 'in_mole/g',
* /2X,'K',l1,'_is ',E20.11,2X,' +/- ',2X,E15.5)

```

```

2210 FORMAT (2X,'K',l1,'_is ',E20.11,2X,' +/- ',2X,E15.5)

```

```

  if (UPORDWN.LE.3) then
    IF ((ddown(l1).eq.0.0).and.(dup(l1).eq.0.0)) then
      write (10,2220) P(l1),0,0
    else
      WRITE (10,2230) P(l1),P(l1)*.01,P(l1)*.01
    endif
    IF ((ddown(l2).eq.0.0).and.(dup(l2).eq.0.0)) then
      write (10,2220) P(l2),0,0
    else
      WRITE (10,2230) P(l2),P(l2)*.01,P(l2)*.01
    endif
  else
    IF ((ddown(l1).eq.0.0).and.(dup(l1).eq.0.0)) then
      write (10,2220) P(l1),0,0
    else
      WRITE (10,2230) P(l1),P(l1)*1e-10,P(l1)*1e-10
    endif
    IF ((ddown(l2).eq.0.0).and.(dup(l2).eq.0.0)) then
      write (10,2220) P(l2),0,0
    else
      WRITE (10,2230) P(l2),P(l2)*1e-10,P(l2)*1e-10
    endif
  endif
2240 CONTINUE
2220 FORMAT (E21.15,15X,l1,25X,l1)
2230 FORMAT (E21.15,5X,E21.5,5X,E21.5)

```

```

  IF (NE(k).GT.0) WRITE (7,2250) GE(k)

```

```

2250 FORMAT(/3X,'Grams of_Solid_for_equilibrium_data_is ',

```

* F5.3,3X/)

ip = ip + 2*ns(k)

2260 continue

if (fixedn.ne.0) then

n_tot = 0.0

n_sd = 0.0

DO 2280 IS=1,maxns

L1 = 2*is - 1

WRITE (7,2270) IS,P(l1),SD(1,is,1)

n_tot = P(l1) + n_tot

n_sd = SD(1,is,1) + n_sd

2270 FORMAT (2X,'n',l1,'_is ',E20.11,2X,' +/- ',2X,

* E15.5,' in_mole/g')

2280 CONTINUE

write (7,*)

write (7,2300) n_tot, n_sd

2290 FORMAT (/)

2300 format (3X,'The_total n_is ',E16.10,' +/- ',3X,

* E11.5,' in_mole/g')

endif

write (7,2310) tot_sq

2310 format (/3X,'The_total sum_of_sq is_',E16.10)

if (calc_dim.eq.1) then

write (7,2290)

write (7,2320) AREA, MVL

write (7,*)

DO 2340 IS=1,maxns

L1 = 2*is - 1

WRITE (7,2330) IS,AREA*P(l1)*1000*6.023,

* AREA*SD(1,is,1)*1000*6.023

2340 CONTINUE

WRITE (7,2350) AREA*n_tot*1000*6.023, AREA*n_sd*1000*6.023

write (7,*)

DO 2370 IS=1,maxns

L1 = 2*is - 1

WRITE (7,2360) IS,MVL*P(l1), MVL*SD(1,is,1)

2370 CONTINUE

WRITE (7,2380) MVL*n_tot, MVL*n_sd

endif

2320 FORMAT (' The_AREA_per_molc_is ',F7.3,' The_MVL_is ',F7.3)

2330 FORMAT (2X,'n',l1,'_area_is ',7X,F10.3,2X,' +/- ',2X,

* F10.4,' in_meters^2/g')

2350 FORMAT (2X,'Total_area_is ',4X,F10.3,2X,' +/- ',2X,

* F10.4,' in_meters^2/g')

2360 FORMAT (2X,'n',l1,'_pore_vol_is ',3X,F10.7,2X,' +/- ',2X,

* F10.7,' in_mL/g')

2380 FORMAT (2X,'Total_pore_vol_is ',F10.7,2X,' +/- ',2X,

* F10.7,' in_mL/g')

write (7,*)

write (7,2400)

```

2400 FORMAT (/,' Temp:',4X,'Temp_#',3X,'K',12X,'K',14X,
*          'SD(K)')

ip = 1

do 2560 k=1, nt
do 2550 is=1,maxns
  L2 = ip + 2*is - 1
  sx(IS) = 0
  sx2(IS) = 0
  sxy(IS) = 0
  sy(IS) = 0
  wgt(k,IS) = 0
  t_wgt(IS) = 0
  write (7,2500) temp(k),k,IS,P(L2),SD(k,IS,2)
2550 continue
  ip = ip + 2*ns(k)
2560 continue
2500 FORMAT (f7.2,4X,i2,6X,i1,4X,f16.9,1X,f16.9)

  if (WEIGHT.eq.0) write (7,2570)
2570 format (/,' Temp:',4X,'Temp_#',3X,'K',7X,'1/Temp',11X,'ln(K)',8X,
*          'Weight(K)')
  if (WEIGHT.eq.1) write (7,2580)
2580 format (/,' Temp:',4X,'Temp_#',3X,'K',7X,'1/Temp',11X,'ln(K)',8X,
*          'Weight(K)',8X,'Wgt_Factor')

ip = 1

if (WEIGHT.eq.0) then
do 2670 k=1, nt
  DO 2650 IS=1,maxns
    L2 = ip + 2*is - 1
    sx(IS) = 1/temp(k) + sx(IS)
    sx2(IS) = (1/temp(k))**2 + sx2(IS)
    sy(IS) = LOG(P(L2)) + sy(IS)
    sxy(IS) = 1/temp(k)*LOG(P(L2)) + sxy(IS)
    write (7,2600) temp(k),k,IS,1/temp(k),LOG(P(L2)),
*          P(L2)/SD(k,IS,2)
2650 continue
  ip = ip + 2*ns(k)
2670 continue
endif
2600 format (F7.2,4X,i2,6X,i1,4X,f11.8,2X,f14.7,2X,f14.7)

if (WEIGHT.eq.1) then
do 2700 k=1, nt
  DO 2690 IS=1,maxns
    L2 = ip + 2*is - 1
    wgt(k,IS) = P(L2)/SD(k,IS,2)
    t_wgt(IS) = t_wgt(IS) + wgt(k,IS)
2690 continue
  ip = ip + 2*ns(k)
2700 continue
endif

```



```

if (WEIGHT.eq.1) then
do 2710 IS=1,maxns
  t_wgt(IS) = t_wgt(IS)/nt
2710 continue
endif

if (WEIGHT.eq.1) then
ip = 1
do 2770 k=1, nt
  DO 2750 IS=1,maxns
    L2 = ip + 2*is - 1
    sx(IS) = (wgt(k,IS)/t_wgt(IS))*(1/temp(k)) + sx(IS)
    sx2(IS) = (wgt(k,IS)/t_wgt(IS))*(1/temp(k))**2 + sx2(IS)
    sy(IS) = (wgt(k,IS)/t_wgt(IS))*LOG(P(L2)) + sy(IS)
    sxy(IS) = (wgt(k,IS)/t_wgt(IS))*1/temp(k)*LOG(P(L2)) + sxy(IS)
    write (7,2730) temp(k),k,IS,1/temp(k),LOG(P(L2)),
      * P(L2)/SD(k,IS,2),(wgt(k,IS)/t_wgt(IS))
2750 continue
  ip = ip + 2*ns(k)
2770 continue
endif
2730 format (F7.2,4X,I2,6X,I1,4X,f11.8,2X,f14.7,2X,f14.7,2X,f14.7)

if (nt.eq.1) then
goto 5010
else
write (7,*)
if (WEIGHT.eq.0) write (7,2790)
if (WEIGHT.eq.1) write (7,2800)
2790 FORMAT (' These_are_the unweighted_regression_parameters')
2800 FORMAT (' These_are_the weighted_regression_parameters')

do 2830 IS=1, maxns
  slope(IS) = (nt*sxy(IS)-sx(IS)*sy(IS))/(nt*sx2(IS)-sx(IS)**2)
  yinter(IS) = (sx2(IS)*sy(IS)-sxy(IS)*sx(IS))
    * /(nt*sx2(IS)-sx(IS)**2)
2830 continue

  DO 2840 IS=1,maxns
    sd_y(IS) = 0
2840 continue
  ip = 1
  do 2860 k=1, nt
    DO 2850 IS=1,maxns
      L2 = ip + 2*is - 1
      dy(k,IS) = LOG(P(L2)) - (slope(IS)*1/temp(k)+yinter(IS))
      sd_y(IS) = dy(k,IS)**2 + sd_y(IS)
2850 continue
    ip = ip + 2*ns(k)
2860 continue

  IS=1
  D = sx2(IS)*nt-sx(IS)**2

if (nt.gt.2) then

```

```

DO 2880 IS=1,maxns
  sd_m(IS) = sqrt((sd_y(IS)/(nt-2))*nt/D)*1.987/1000
  sd_b(IS) = sqrt((sd_y(IS)/(nt-2))*sx2(IS)/D)*1.987
  write (7,2820) IS,slope(IS)*1.987/1000,sd_m(IS),
*      IS,-yinter(IS)*1.987,sd_b(IS)
2880  continue
endif

if (nt.le.2) then
  DO 2890 IS=1,maxns
    sd_m(IS) = sqrt(((sd_y(IS)/(nt-1))*nt/D)**2)*1.987/1000
    sd_b(IS) = sqrt(((sd_y(IS)/(nt-1))*sx2(IS)/D)**2)*1.987
    write (7,2820) IS,slope(IS)*1.987/1000,sd_m(IS),
*      IS,-yinter(IS)*1.987,sd_b(IS)
2890  continue
endif
2820 FORMAT ('-dH',I1,',',F10.4,' +/- ',F8.5,' kCal/mole',3X,
* '-dS',I1,',',F10.4,' +/- ',F8.5,' Cal/(mol*K)')

ip = 1

DO 2940 IS=1,maxns
  sx(IS) = sx(IS)/nt
  sy(IS) = sy(IS)/nt
  rt(IS) = 0
  rbx(IS) = 0
  rby(IS) = 0
2940  continue
do 2970 k=1, nt
  DO 2950 IS=1,maxns
    L2 = ip + 2*is - 1
    rt(IS) = (1/temp(k) - sx(IS))*(LOG(P(L2)) - sy(IS)) + rt(IS)
    rbx(IS) = (1/temp(k) - sx(IS))**2 + rbx(IS)
    rby(IS) = (LOG(P(L2)) - sy(IS))**2 + rby(IS)
2950  continue
  ip = ip + 2*ns(k)
2970  continue

do 2990 IS=1,maxns
  r(IS) = rt(IS)/SQRT(rbx(IS)*rby(IS))
  write (7,2980) IS, r(IS)**2
2990  continue
2980 FORMAT ('R^2(',I1,')= ',f7.5)

5010 endif
CLOSE (7)
close (10)
5000 continue
close (9)
STOP

END

```

double precision FUNCTION FUNK(H,P,B,N,nt,NS,fixedn)

implicit none

integer MAXNTEMP,MAXNPOINT,MAXNSITE

parameter (MAXNTEMP=5)

parameter (MAXNSITE=5)

parameter (MAXNPOINT=200)

double precision H(MAXNTEMP,MAXNPOINT),P(MAXNTEMP*2*MAXNSITE)

double precision B(MAXNTEMP,MAXNPOINT),f,b2

integer nt,n(MAXNTEMP),ns(MAXNTEMP),i,k,is,ip,n_tot,fixedn

integer l1,l2

FUNK = 0.0

n_tot = 0

B2 = 0.0

ip = 1

do 20 k=1,nt

DO 10 l=1,N(k)

F=0.0

DO 15 IS=0,NS(k)-1

if (fixedn.eq.0) then

l1 = ip + 2*is

else

l1 = 1 + 2*is

endif

l2 = ip + 2*is + 1

B2 = P(l1)*P(l2)*B(k,l)/(1.0+P(l2)*B(k,l))

f = f + b2

15 CONTINUE

FUNK=FUNK+(H(k,l)-F)**2

10 CONTINUE

ip = ip + 2*ns(k)

n_tot = n_tot + n(k)

20 continue

FUNK=SQRT(FUNK/(n_tot-1))

RETURN

END

double precision FUNCTION CAL(k,l,ip,P,B,NS,fixedn)

implicit none

```
integer MAXNTEMP,MAXNPOINT,MAXNSITE
parameter (MAXNTEMP=5)
parameter (MAXNSITE=5)
parameter (MAXNPOINT=200)
```

```
double precision P(MAXNTEMP*2*MAXNSITE),B(MAXNTEMP,MAXNPOINT),b3
integer is,i,ns(MAXNTEMP),k,ip,fixedn,l1,l2
```

```
CAL = 0.0
B3 = 0.0
```

```
DO 10 IS=1,NS(k)
```

```
  if (fixedn.eq.0) then
    l1 = ip + 2*is - 2
  else
    l1 = 2*is - 1
  endif
```

```
  l2 = ip + 2*is - 1
  B3 = P(l1)*P(l2)*B(k,l)/(1.0+P(l2)*B(k,l))
  CAL = CAL + B3
```

```
10 CONTINUE
```

```
RETURN
END
```

```
SUBROUTINE SIMPLEX(nt,EP,NP,N,KX,T,Ddown,dup,H,B,NS,fixedn,count,
*m,br)
implicit none
```

```
integer MAXNTEMP,MAXNSITE
parameter (MAXNTEMP=5)
parameter (MAXNSITE=5)
double precision RI(MAXNTEMP*2*MAXNSITE),T(MAXNTEMP*2*MAXNSITE)
double precision TT(MAXNTEMP*2*MAXNSITE)
double precision S(MAXNTEMP*2*MAXNSITE,MAXNTEMP*2*MAXNSITE + 1)
double precision H(MAXNTEMP,MAXNSITE),B(MAXNTEMP,MAXNSITE)
double precision Ddown(MAXNTEMP*2*MAXNSITE)
double precision dup(MAXNTEMP*2*MAXNSITE)
double precision ep,br,wr,f,rt,r
integer np,n(MAXNTEMP),ns(MAXNTEMP),kx,ki,jw,jb,i,j,nv,nt
integer fixedn, count, m
```

```
CALL PARMAT(nt,NP,S,T,RI,Ddown,dup,B,H,N,NS,fixedn)
```

```
NV = NP+1
```

```
IF (RI(1).EQ.0.0) then
  GO TO 110
endif
```

```
KI = 0
```

BR = 0.0

20 WR = RI(1)

BR = WR

JW = 1

JB = 1

DO 30 I = 2,NV

IF (RI(I).GE.WR) then

WR = RI(I)

JW = I

endif

IF (RI(I).LT.BR) then

BR = RI(I)

JB = I

endif

30 CONTINUE

if (KI.eq.500) print 131, BR, KI, count-m

if (KI.eq.1000) print 131, BR, KI, count-m

if (KI.eq.2000) print 131, BR, KI, count-m

if (KI.eq.3000) print 131, BR, KI, count-m

if (KI.eq.4000) print 131, BR, KI, count-m

if (KI.eq.5000) print 131, BR, KI, count-m

if (KI.eq.6000) print 131, BR, KI, count-m

if (KI.eq.7000) print 131, BR, KI, count-m

if (KI.eq.8000) print 131, BR, KI, count-m

if (KI.eq.9000) print 131, BR, KI, count-m

if (KI.eq.10000) print 131, BR, KI, count-m

if (KI.eq.15000) print 131, BR, KI, count-m

if (KI.eq.20000) print 131, BR, KI, count-m

if (KI.eq.25000) print 131, BR, KI, count-m

if (KI.eq.30000) print 131, BR, KI, count-m

if (KI.eq.35000) print 131, BR, KI, count-m

if (KI.eq.45000) print 131, BR, KI, count-m

if (KI.eq.50000) print 131, BR, KI, count-m

if (KI.eq.55000) print 131, BR, KI, count-m

if (KI.eq.KX) print 131, BR, KI, count-m

IF (KI.GE.KX) then

GO TO 110

endif

IF (BR.LT.EP) then

print *, 'Best Test within acceptable limits.'

GO TO 110

endif

KI = KI+1

F = 1.0

CALL VERTEX(nt,S,T,JW,NP,F,H,B,R,N,NS,fixedn)

```

IF (R.GT.BR) GO TO 40

RT = R

DO 50 I = 1,NP
  TT(I) = T(I)
50 CONTINUE

F = 2.0
CALL VERTEX(nt,S,T,JW,NP,F,H,B,R,N,NS,fixedn)

IF (R.GT.RT) GO TO 60

90 DO 70 I = 1,NP
  S(I,JW) = T(I)
70 CONTINUE

RI(JW) = R

GO TO 20

60 R = RT

DO 80 I = 1,NP
  T(I) = TT(I)
80 CONTINUE

GO TO 90

40 IF (R.LE.WR) GO TO 90

F = -0.5
CALL VERTEX(nt,S,T,JW,NP,F,H,B,R,N,NS,fixedn)

IF (R.LE.WR) GO TO 90

DO 100 I = 1,NP

  DO 100 J = 1,NV

    IF (J.NE.JB) S(I,J) = (S(I,JB)+S(I,J))/2

100 CONTINUE

GO TO 20

110 IF (KI.GE.KX) WRITE (6,120)
  IF (KI.LT.KX) WRITE (6,130)

110 IF (BR.GT.EP) then
  print *, ' Best test improves less than acceptable limits.'
  print 31,br,ep
31  format(' Best test=','E21.15,' Acceptable limit=','E8.2)
  endif

120 FORMAT (/5X,'Maximum Number of Loops (KX) Exceeded')

```

```
130 FORMAT (/5X,'Convergence Reached, Best Residual will not improve'
  *' in this count.',/)
```

```
131 FORMAT ('BR = ',E25.17,3X,'Loops = ',i11,2X,'Count = ',i2)
```

```
RETURN
END
```

```
SUBROUTINE PARMAT(nt,NP,S,T,RI,d down,dup,B,H,N,NS,fixedn)
implicit none
```

```
integer MAXNTEMP,MAXNPOINT,MAXNSITE
parameter (MAXNTEMP=5)
parameter (MAXNSITE=5)
parameter (MAXNPOINT=200)
```

```
double precision T(MAXNTEMP*2*MAXNSITE)
double precision S(MAXNTEMP*2*MAXNSITE,MAXNTEMP*2*MAXNSITE+1)
double precision RI(MAXNTEMP*2*MAXNSITE)
double precision Ddown(MAXNTEMP*2*MAXNSITE)
double precision dup(MAXNTEMP*2*MAXNSITE),B(MAXNTEMP,MAXNPOINT)
double precision H(MAXNTEMP,MAXNPOINT)
integer nv,np,i,j,n(MAXNTEMP),ns(MAXNTEMP),nt,fixedn
double precision FUNK
```

```
NV=NP+1
```

```
DO 30 I=1,NP
```

```
DO 30 J=1,NV
```

```
IF (I.GE.J) then
  S(I,J) = T(I)+dup(I)
else
  S(I,J) = T(I)-d down(I)
```

```
  if (S(i,j) .LT. 0.0) then
    S(i,j) = T(i) * 0.1
  endif
```

```
endif
```

```
30 CONTINUE
```

```
DO 40 I=1,NV
```

```
DO 50 J=1,NP
  T(J)=S(J,I)
```

```
50 CONTINUE
```

```
RI(I) = FUNK(H,T,B,N,nt,NS,fixedn)
40 CONTINUE
```

```
RETURN
```

```
END
```

SUBROUTINE VERTEX(nt,S,T,JW,NP,F,H,B,R,N,NS,fixedn)
implicit none

integer MAXNTEMP,MAXNPOINT,MAXNSITE

parameter (MAXNTEMP=5)

parameter (MAXNSITE=5)

parameter (MAXNPOINT=200)

double precision T(MAXNTEMP*2*MAXNSITE)

double precision S(MAXNTEMP*2*MAXNSITE,MAXNTEMP*2*MAXNSITE+1)

double precision C(MAXNTEMP*2*MAXNSITE),B(MAXNTEMP,MAXNPOINT)

double precision H(MAXNTEMP,MAXNPOINT)

double precision f,r,su

integer np,n(MAXNTEMP),ns(MAXNTEMP),nv,i,j,jw,nt,fixedn

double precision FUNK

SAVE

NV = NP + 1

DO 10 I = 1,NP

SU = 0.0

IF (F.NE.1.0) GO TO 30

DO 20 J = 1,NV

IF (J.NE.JW) SU = SU + S(I,J)

20 CONTINUE

C(I) = SU / NP

30 T(I) = C(I) * (1.0 + F) - F * S(I,JW)

if (T(I) .LT. 0.0) then

T(I) = 1.0d+1

endif

10 CONTINUE

R = FUNK(H,T,B,N,nt,NS,fixedn)

RETURN

END

subroutine getline(u)

implicit none

integer u

character*78 buf

10 read (u,'(A)') buf

if (buf(1:1).eq. '#') then

print *, buf

goto 10

endif

backspace(u)

RETURN
END

Input File Glossary and Example

An input line preceded by a pound sign (#) is ignored by the program and is used as a comment line.

CONVERGE: is the criterion for program convergence. The program will terminate when this value is reached.

INNER LOOPS: is the number of calculations the program will run before exiting. A small number is best as local minima are sometimes found and the only way of getting out of the local is to start again.

FIXEDN: a value of zero (0) results in the program using independent n_i -sets for each data set. A value of one (1) results in the program using a single n_i -set for the combined data set (all temperature sets).

UP-DOWN: sets the bound for the next input file.

OUTER LOOPS: is the number of times that the program will read in the new input file (created after CONVERGE or # INNER LOOPS is reached) before terminating.

A-V: a value of zero (0) results in areas and volumes not being calculated. A value of one (1) results in the calculation of surface areas and pore volumes based on the AREA and MV values.

WEIGHT: a value of zero (0) results in an unweighted linear regression of $\ln K_i$ versus T^{-1} . A value of one (1) uses a weighting factor of K^2/σ^2_K in a linear regression of $\ln K_i$ versus T^{-1} .

AREA: is the molecular area for the adsorptive used in \AA^2 .

MV: is the molar volume of the adsorptive used in $\text{mL}\cdot\text{mole}^{-1}$.

SETS: is the total number of data sets used.

POINTS: is the number of points in the data set

GRAMS SOL: is the number of grams of solid that the adsorption data is based. The data from the ASAP 2000 is based on one gram of solid.

EQ PRESS: is the equilibrium pressure in atmospheres.

MOLS ADS: is the number of moles adsorbed at the associated pressure.

PROCESSES: is the number of processes to be used to fit the data.

TEMP: is the temperature that the data set was collected in Kelvin.

There cannot be any blank lines in the data set or the program will terminate. The program will also terminate if one of the parameters does not agree with what is read, for example, 12 data points are expected and only 10 are included.

```
# N2 / A572 (-93°C, -43°C, & 0°C)
# 3 PROCESS FIT
# CONVERGE / # INNER LOOPS / FIXEDN
1E-13 25000 1
# UP-DOWN / # OUTER LOOPS / A-V / WEIGHT
2      5      1      1
# AREA / MV
15.27 25.02
## SETS
3
#-93°C
# POINTS      GRAMS SOL
12      1
# EQ PRESS      MOLS ADS
6.3371E-03      2.8399E-04
3.1718E-02      8.4942E-04
6.2951E-02      1.2648E-03
1.2705E-01      1.8251E-03
1.9319E-01      2.2311E-03
2.6239E-01      2.5648E-03
3.9229E-01      3.0478E-03
5.2274E-01      3.4238E-03
6.5346E-01      3.7316E-03
7.8703E-01      3.9981E-03
9.1965E-01      4.2277E-03
9.9096E-01      4.3385E-03
# PROCESSES / TEMP
3      180.15
#n1
0.000463      0      0
#K1
101      0      0
#n2
0.00179      0      0
#K2
10      0      0
#n3
0.00534      0      0
#K3
0.8      0      0
#-43°C
# POINTS      GRAMS SOL
12      1
# EQ PRESS      MOLS ADS
6.5405E-03      2.6564E-05
3.2874E-02      1.2248E-04
6.6625E-02      2.2958E-04
1.3195E-01      4.0504E-04
```

1.9687E-01	5.5408E-04
2.5886E-01	6.7924E-04
3.9474E-01	9.1756E-04
5.2648E-01	1.1139E-03
6.5148E-01	1.2778E-03
7.8859E-01	1.4404E-03
9.2094E-01	1.5825E-03
9.9232E-01	1.6538E-03

PROCESSES / TEMP

3 193.15

#n1

0 0 0

#K1

35 0 0

#n2

0 0 0

#K2

4 0 0

#n3

0 0 0

#K3

0.4 0 0

0°C

POINTS GRAMS SOL

9 1

EQ PRESS MOLS ADS

1.2704E-01 1.1048E-04

1.9475E-01 1.6449E-04

2.6137E-01 2.1485E-04

3.9487E-01 3.1036E-04

5.2280E-01 3.9553E-04

6.5481E-01 4.7765E-04

7.8627E-01 5.5481E-04

9.1808E-01 6.2803E-04

9.9313E-01 6.6855E-04

PROCESSES / TEMP

3 213.15

#n1

0 0 0

#K1

10 0 0

#n2

0 0 0

#K2

1.4 0 0

#n3

0 0 0

#K3

0.2 0 0

LIST OF REFERENCES

1. Ruthven, D. M. *Principles of Adsorption and Adsorption Processes*; John Wiley and Sons: New York, 1984.
2. Tabor, D. *Gases, Liquids, and Solids and Other States of Matter*; Cambridge University Press: Cambridge, 1991.
3. Rouquerol, J.; Avnir, D.; Fairbridge, C. W.; Everett, D. H.; Haynes, J. H.; Pernicone, N.; Ramsey, J. D. F.; Sing, K. S. W.; Unger, K. K. *Pure & Appl. Chem.* **1994**, *66*, 1739.
4. Sing, K. S. W.; Everett, D. H.; Haul, R. A. W.; Moscou, L.; Pierotti, R. A.; Rouquerol, J.; Siemieniowska, T. *Pure & Appl. Chem.* **1984**, *57*, 643.
5. Chen, S. G.; Yang, R. T. *Langmuir* **1993**, *9*, 3259.
6. Everett, D. H. *Langmuir* **1993**, *9*, 2586.
7. Choma, J.; Jaroniec, M. *Langmuir* **1997**, *13*, 1026.
8. Dubinin, M. M.; Stoeckli, H. F. *J. Colloid Interface Sci.* **1980**, *75*, 35.
9. Giona, M.; Giustiniani, M. *Langmuir* **1997**, *13*, 1138.
10. Everett, D. H.; Powl, J. C. *J. Chem. Soc., Faraday Trans. I* **1976**, *72*, 619.
11. Langmuir, I. *J. Am. Chem. Soc.* **1918**, *40*, 1361.
12. Mooi, J.; Pierce, C.; Nelson Smith, R. *J. Am. Chem. Soc.* **1953**, *57*, 657.
13. Steele, W. *Chem. Rev.* **1993**, *93*, 2355.
14. Dubinin, M. M. *Carbon* **1987**, *25*, 593.
15. Van Slooten, R.; Bojan, M. J.; Steele, W. A. *Langmuir* **1994**, *10*, 542.
16. Yang, R. T.; Baksh, M. S. A. *AIChE Journal* **1991**, *37*, 679.
17. Rodriguez, N. M.; Chambers, A.; Baker, R. T. K. *Langmuir* **1995**, *11*, 3862.
18. Cracknell, R. F.; Gordon, P.; Gubbins, K. E. *J. Phys. Chem.* **1993**, *97*, 494.
19. Bandosz, T. J.; Jagiello, J.; Putyera, K.; Schwarz, J. A. *Chem. Mater.* **1996**, *8*, 2023.

20. Faust, S. D.; Aly, O. M. *Adsorption Processes for Water Treatment*; Butterworth Publishers: Stoneham, MA, 1987.
21. Grunewald, G. C.; Drago, R. S. *J. Mol. Cat.* **1990**, *58*, 227.
22. Grunewald, G. C.; Drago, R. S.; Clark, J. L.; Livesey, A. B. *J. Mol. Cat.* **1990**, *60*, 239.
23. Grunewald, G. C.; Drago, R. S. *J. Am. Chem. Soc.* **1991**, *113*, 1636.
24. Stevens, M. G.; Foley, H. C. *J. Chem. Soc., Chem. Commun.* **1997**, 519.
25. Yang, R. T.; Chen, Y. D.; Peck, J. D.; Chen, N. *Ind. Eng. Chem. Res.* **1996**, *35*, 3093.
26. Kane, M. S.; Kao, L. C.; Mariwala, R.; Hilsher, D. F.; Foley, H. C. *Ind. Eng. Chem. Res.* **1996**, *35*, 3319.
27. Nishide, H.; Suzuki, A.; Tsuchida, E. *Bull. Chem. Soc. Jpn.* **1997**, *70*, 2317.
28. Mathais, P. M.; Kumar, R.; Moyer, D. J.; Schork, J. M.; Sirinivasan, S. R.; Auvil, S. R.; Talu, O. *Ind. Eng. Chem. Res.* **1996**, *35*, 2477.
29. Jagtoyen, M.; Derbyshire, F.; Brubaker, N.; Fei, Y. Q.; Kimber, G.; Matheny, M.; Burchell, T. *Mat. Res. Soc. Symp. Proc.* **1994**, *344*, 77.
30. Kane, M. S.; Goellner, J. F.; Foley, H. C.; DiFrancesco, R.; Billinge, S. J. L.; Allard, L. F. *Chem. Mater.* **1996**, *8*, 2159.
31. Foley, H. C. *Microporous Mater.* **1995**, *4*, 407.
32. Gierak, A. *Mater. Chem. Phys.* **1995**, *41*, 28.
33. Acharya, M.; Raich, B. A.; Foley, H. C.; Harold, M. P.; Lerov, J. J. *Ind. Eng. Chem. Res.* **1997**, *36*, 2924.
34. Bandosz, T. J.; Jagiello, J.; Putyera, K.; Schwarz, J. A. *Langmuir* **1995**, *11*, 3964.
35. Bandosz, T. J.; Jagiello, J.; Putyera, K.; Schwarz, J. A. *Chem. Mater.* **1996**, *8*, 2023.
36. Oda, H.; Tateishi, D.; Esumi, K.; Honda, H. *Carbon* **1994**, *32*, 355.
37. Kruk, M.; Jaroniec, M.; Berezinski, Y. *J. Colloid Interface Sci.* **1996**, *182*, 282.
38. Lafyatis, D. S.; Tung, J.; Foley, H. C. *Ind. Eng. Chem. Res.* **1991**, *30*, 865.
39. Putyera, K.; Jagiello, J.; Bandosz, T. J.; Schwarz, J. A. *Carbon* **1995**, *33*, 1047.
40. Gonzales-Serrano, E.; Cordero, T.; Rodriguez-Mirasol; Rodriguez, J. J. *Ind. Eng. Chem. Res.* **1997**, *36*, 4832.

41. Jagtoyen, M.; Derbyshire, F. *Carbon* **1993**, *31*, 1185.
42. Bansal, N.; Foley, H. C.; Lafyatis, D. S.; Dybowski, C. *Catal. Today* **1992**, *14*, 305.
43. Jin Suh, O.; Park, T. J.; Ihm, S. K.; Ryoo, R. *J. Phys. Chem.* **1991**, *95*, 3767.
44. Wang, F. C. Y.; Gerhart, B.; Smith, P. B. *Anal. Chem.* **1995**, *67*, 3536.
45. Jaroniec, M.; Gilpin, R. K.; Ramle, J.; Choma, J. *Thermochim. Acta* **1996**, *272*, 65.
46. Jaroniec, M.; Lu, X.; Madey, R. *J. Phys. Chem.* **1990**, *94*, 5917.
47. Hontoria-Lucas, C.; Lopez-Peinado, A. J.; Lopez-Gonzalez, J. D. D.; Rojas-Cervantes, M. L.; Martin-Arando, R. M. *Carbon* **1995**, *33*, 1585.
48. Carrott, P. J. M.; Sing, K. S. W. *J. Chromatogr.* **1987**, *406*, 139.
49. Sing, K. S. W. *Carbon* **1989**, *27*, 5.
50. Stoeckli, H. F. *Carbon* **1990**, *28*, 1.
51. Barrett, E. P.; Joyner, L. G.; Halenda, P. P. *J. Am. Chem. Soc.* **1951**, *73*, 373.
52. Amarasekera, G.; Scarlett, M. J.; Mainwaring, D. E. *J. Phys. Chem.* **1996**, *100*, 7580.
53. Hobson, J. P.; Armstrong, R. A. *J. Phys. Chem.* **1963**, *67*, 2000.
54. Jagiello, J.; Bandoz, T. J.; Putyera, K.; Schwarz, J. A. *J. Chem. Soc. Faraday Trans.* **1995**, *91*, 2929.
55. Jagiello, J.; Bandoz, T. J.; Schwarz, J. A. *Langmuir* **1996**, *12*, 2837.
56. Jaroniec, M.; Choma, J. *Mater. Chem. Phys.* **1986**, *15*, 521.
57. Meyer, E. F.; Mulvihill, G.; Feil, J. *Langmuir* **1993**, *9*, 3239.
58. Jaroniec, M.; Lu, X.; Madey, R.; Choma, J. *Carbon* **1990**, *28*, 737.
59. Brunauer, S.; Emmett, P. H.; Teller, E. *J. Am. Chem. Soc.* **1938**, *60*, 309.
60. Harkins, W. D.; Jura, G. *J. Am. Chem. Soc.* **1944**, *66*, 1366.
61. Horvath, G.; Kawazoe, K. *J. Chem. Eng. Japan* **1983**, *16*, 470.
62. Jaroniec, M.; Choma, J.; Lu, X. *Chem. Eng. Sci.* **1991**, *46*, 3299.
63. Lastoskie, C.; Gubbins, K. E.; Quirke, N. *J. Phys. Chem.* **1993**, *97*, 4786.
64. Mariwala, R.; Foley, H. C. *Ind. Eng. Chem. Res.* **1994**, *33*, 2314.
65. Giona, M.; Giustiniani, M. *Ind. Eng. Chem. Res.* **1995**, *34*, 3848.

66. Ehrburger-Dolle, F. *Langmuir* **1997**, *13*, 1189.
67. Adamson, A. W.; Ling, I. *Adv. Chem. Ser.* **1961**, *33*, 51.
68. Aharoni, C.; Romm, F. *Langmuir* **1995**, *11*, 1744.
69. Aranovich, G. L.; Donohue, M. D. *Carbon* **1995**, *33*, 1369.
70. Bragoli, P. B. J.; Almond, D. P.; McEnaney, B. *Carbon* **1988**, *26*, 109.
71. Dubinin, M. M. *Carbon* **1988**, *26*, 97.
72. Rudzinski, W.; Everett, D. H. *Adsorption of Gases on Heterogeneous Surfaces*; Academic Press: London, 1992.
73. Seri-Levy, A.; Avnir, D. *Langmuir* **1993**, *9*, 2523.
74. Tovbin, Y. K. *Langmuir* **1997**, *13*, 979.
75. Shigeta, T.; Yoneya, J.; Nitta, T. *Mol. Simul.* **1996**, *16*, 291.
76. Chen, S. G.; Yang, R. T. *Langmuir* **1994**, *10*, 4244.
77. Adamson, A. W. *Colloids Surf. A* **1996**, *118*, 193.
78. Graham, D. J. *Phys. Chem.* **1953**, *57*, 665.
79. Halsey, G. J. *Chem. Phys.* **1948**, *16*, 931.
80. Jaroniec, M.; Madey, R. *J. Phys. Chem.* **1989**, *93*, 5225.
81. Carrott, P. J. M.; Roberts, R. A.; Sing, K. S. W. *Chem. Ind.* **1987**, *24*, 855.
82. Suzuki, T.; Kaneko, K.; Setoyama, N.; Maddox, M.; Gubbins, K. *Carbon* **1996**, *34*, 909.
83. Balbuena, P. B.; Gubbins, K. E. *Stud. Surf. Sci. Catal* **1994**, *87*, 41.
84. Drago, R. S.; Burns, D. S.; Lafrenz, T. J. *J. Phys. Chem.* **1996**, *100*, 1718.
85. Drago, R. S.; McGilvray, J. M.; Kassel, W. S. *The Microreport* **1996**, *7*, 1.
86. Drago, R. S.; Kassel, W. S.; Burns, D. S.; McGilvray, J. M.; Showalter, S. K.; Lafrenz, T. J. *J. Phys. Chem. B* **1997**, *101*, 7548.
87. Kassel, W. S.; Drago, R. S. *Microporous Mater.* **1997**, *12*, 189.
88. Saito, A.; Foley, H. C. *AIChE Journal* **1991**, *37*, 429.
89. Person, W. B. *J. Am. Chem. Soc.* **1965**, *87*, 167.
90. Webster, C. E.; Drago, R. S.; Zerner, M. C. *J. Am. Chem. Soc.* **1998**, *120*, 5509.
91. Redlich, O.; Kwong, J. N. S. *On the Thermodynamics of Solutions* **1948**, 233.

92. Deming, S. N.; Morgan, S. L. *Anal. Chem.* **1973**, *45*, 278A.
93. Leggett, D. J. *J. Chem. Ed.* **1983**, *60*, 707.
94. Routh, M. W.; Swartz, P. A.; Denton, M. B. *Anal. Chem.* **1977**, *49*, 1422.
95. McClellan, A. L.; Harnsberger, H. F. *J. Colloid Interface Sci.* **1967**, *23*, 577.
96. Drago, R. S.; Dias, S. C.; McGilvray, J. M.; Mateus, A. L. M. L. *J. Phys. Chem. B* **1998**, *102*, 1508.
97. Chen, W. N.; Guthrie, J. T.; Lin, L. *Dyes and Pigments* **1992**, *19*, 129.
98. Huggahalli, M.; Fair, J. R. *Ind. Eng. Chem Res.* **1996**, *35*, 2071.
99. Jagiello, J.; Schwarz, J. A. *Langmuir* **1993**, *9*, 2513.
100. Bakaev, V. A.; Steele, W. A. *Langmuir* **1992**, *8*, 148.
101. Bakaev, V. A.; Steele, W. A. *J. Chem. Phys.* **1993**, *98*, 9922.
102. Riccardo, J. L.; Steele, W. A.; Ramirez Cuesta, A. J.; Zgrablich, G. *Langmuir* **1997**, *13*, 1064.
103. LumWan, J. A.; White, L. R. *J. Chem. Soc. Faraday Trans.* **1991**, *87*, 3051.
104. Sircar, S.; Myers, A. L. *Surf. Sci.* **1988**, *205*, 353.
105. Villieras, F.; Michot, L. J.; Bardot, F.; Cases, J. M.; Francois, M.; Rudzinski, W. *Langmuir* **1997**, *13*, 1104.
106. Heuchel, M.; Jaroniec, M.; Gilpin, R. K.; Brauer, P.; Szombathely, M. V. *Langmuir* **1993**, *9*, 2537.
107. Jaroniec, M.; Gadkaree, K. P.; Choma, J. *Colloids Surf. A* **1996**, *118*, 203.
108. Jaroniec, M.; Kruk, M.; Oliver, J. *Langmuir* **1997**, *13*, 1031.
109. Aranovich, G. L.; Donohue, M. D. *J. Chem. Phys.* **1996**, *104*, 3851.
110. Lastoskie, C.; Gubbins, K. E.; Quirke, N. *Langmuir* **1993**, *9*, 2693.
111. Lastoskie, C. M.; Quirke, N.; Gubbins, K. E. *Stud. Surf. Sci. Catal* **1997**, *104*, 745.
112. Baksh, M. S. A.; Yang, R. T. *AIChE Journal* **1992**, *38*, 1357.
113. Steele, W. A. *J. Colloid Interface Sci.* **1980**, *75*, 13.
114. Aranovich, G. L.; Donohue, M. D. *J. Chem. Phys.* **1996**, *105*, 7059.
115. Kaneko, K.; Suzuki, T.; Kakei, K. *Langmuir* **1989**, *5*, 879.

116. Kakei, K.; Ozeki, S.; Suzuki, T.; Kaneko, K. *J. Chem. Soc., Faraday Trans.* **1990**, *86*, 371.

BIOGRAPHICAL SKETCH

William Scott Kassel was born in Fairbanks, Alaska, on November 11, 1967, to David A. and Verlee M. Kassel. After graduating from Dakota High School in 1986, he attended the University of Illinois to pursue a degree in electrical engineering. He soon decided his passions did not lie with circuit diagrams and chips so he decided to take some time off. During that period away from the U of I, he discovered a deep interest in chemistry. He then returned to the University of Illinois and graduated with a degree in chemistry in the fall of 1991. During his last semester at the U of I, while trying to decide what to do next, he met Dr. Jim House who convinced him to move an hour away from Urbana and pursue a Master's degree at Illinois State University. While at ISU, he worked with Jim exploring sonochemistry, had a taste of industrial chemistry working in the Quality Assurance Lab at Caterpillar, Inc., in Pontiac, IL, and had the opportunity to teach a chemistry course at University High School in Normal, IL. The experience teaching at U-High and ISU left him wanting more and after receiving his Master's degree in August of 1994, he moved to Gainesville, FL, to work with another man who would make a great impression on his life, Russ Drago. At the University of Florida, he worked on problems in catalysis and adsorption science.

I certify that I have read this study and that in my opinion it conforms to acceptable standards of scholarly presentation and is fully adequate, in scope and quality, as a dissertation for the degree of Doctor of Philosophy.



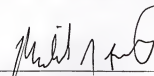
David E. Richardson, Chairman
Professor of Chemistry

I certify that I have read this study and that in my opinion it conforms to acceptable standards of scholarly presentation and is fully adequate, in scope and quality, as a dissertation for the degree of Doctor of Philosophy.



Daniel R. Talham
Associate Professor of Chemistry

I certify that I have read this study and that in my opinion it conforms to acceptable standards of scholarly presentation and is fully adequate, in scope and quality, as a dissertation for the degree of Doctor of Philosophy.



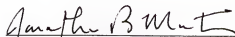
Michael J. Scott
Assistant Professor of Chemistry

I certify that I have read this study and that in my opinion it conforms to acceptable standards of scholarly presentation and is fully adequate, in scope and quality, as a dissertation for the degree of Doctor of Philosophy.



C. Russell Bowers
Assistant Professor of Chemistry

I certify that I have read this study and that in my opinion it conforms to acceptable standards of scholarly presentation and is fully adequate, in scope and quality, as a dissertation for the degree of Doctor of Philosophy.

A handwritten signature in dark ink, appearing to read "Jonathan B. Martin", is written over a horizontal line.

Jonathan B. Martin

Assistant Professor of Geology

This dissertation was submitted to the Graduate Faculty of the Department of Chemistry in the College of Liberal Arts and Sciences and to the Graduate School and was accepted as partial fulfillment of the requirements for the degree of Doctor of Philosophy.

August 1998

Dean, Graduate School